การวัดและการพัฒนาแบบจำลองทางคณิตศาสตร์สำหรับการเกาะตัวแบบแห้งของ โอโซนและซัลเฟอร์ไดออกไซด์

นาย สฤษดิ์ โชติชาครพันธุ์

วิทยานิพนธ์นี้เป็นส่วนหนึ่งของการศึกษาตามหลักสูตรวิศวกรรมศาสตรมหาบัณฑิต
สาขาวิชา วิศวกรรมเคมี ภาควิชา วิศวกรรมเคมี
คณะวิศวกรรมศาสตร์ จุฬาลงกรณ์มหาวิทยาลัย
ปีการศึกษา 2544
ISBN 974-03-0946-1

MEASUREMENT AND DEVELOPMENT OF MATHEMATICAL MODEL FOR DRY DEPOSITION OF OZONE AND SULFUR DIOXIDE

Mr. Sarit Chotchakornpant

A Thesis Submitted in Partial Fulfillment of the Requirements
for the Degree of Master of Engineering in Chemical Engineering
Department of Chemical Engineering
Faculty of Engineering
Chulalongkorn University
Academic Year 2001

ISBN 974-03-0946-1

Thesis Title	MEASUREMENT AND DEVELOPMENT OF MATHEMATICAL MODEL FOR DRY DEPOSITION OF OZONE AND SULFUR DIOXIDE
By	Mr. Sarit Chotchakornpant
Field of Study	Chemical Engineering
Thesis Advisor	Assistant Professor Prasert Pavasant, Ph.D.

Accepted by the Faculty of Engineering, Chulalongkorn University in Partial Fulfillment of the Requirements for the Master's Degree

…….Dean of Faculty of Engineering
(Professor Somsak Panyakeow, D.Eng.)

THESIS COMMITTEE

…….Chairman
(Professor Wiwut Tanthapanichakoon, Ph.D.)

…….Thesis Advisor
(Assistant Professor Prasert Pavasant, Ph.D.)

……..Thesis Co-Advisor
(Professor Masatoshi Aoki, Ph.D.)

…….Member
(Assistant Professor Vichitra Chongvisal, Ph.D.)

…….Member
(Sangchan Limjirakan, D.Sc.)

สฤษดิ์ โชติชาครพันธุ์:
การวัดและการพัฒนาแบบจำลองทางคณิตศาสตร์สำหรับการเกาะตัวแบบแห้งของโอโซนและซัลเฟอร์ไดออกไซด์ (MEASUREMENT AND DEVELOPMENT OF MATHEMAICAL MODEL FOR DRY DEPOSITION OF OZONE AND SULFUR DIOXIDE) อาจารย์ที่ปรึกษาวิทยานิพนธ์: ผู้ช่วยศาสตราจารย์ ดร. ประเสริฐ ภวสันต์, 130 หน้า. ISBN 974-03-0946-1

งานวิจัยนี้ศึกษาเกี่ยวกับการวัดและการพัฒนาแบบจำลองทางคณิตศาสตร์สำหรับการเกาะตัวแบบแห้งของโอโซนและซัลเฟอร์ไดออกไซด์ โดยทำการเก็บตัวอย่างในประเทศญี่ปุ่น ซึ่งแบ่งพื้นที่ศึกษาออกเป็น 3 พื้นที่ได้แก่ (ก) เขตพื้นที่เกษตรกรรม (ข) เขตพื้นที่ป่าสนและ (ค) เขตชุมชนเมืองโดยในเขตพื้นที่เกษตรกรรมพบว่าความเร็วในการเกาะตัวแบบแห้งของทั้งสองก๊าซนี้จะมีค่ามากในบริเวณไร่ถั่วเหลือง และมีค่าน้อยกว่าในบริเวณไร่ข้าวสาลี ทั้งนี้เนื่องจากถั่วเหลืองเป็นพืชที่ให้ค่าปริมาณพื้นที่ใบไม้ต่อพื้นที่การเพาะปลูกสูงกว่าข้าวสาลีและความเร็วในการเกาะตัวจะแปรผันเป็นเส้นตรงกับปริมาณพื้นที่ใบไม้ต่อพื้นที่การเพาะปลูก (leaf area index) นอกจากนี้ยังพบว่าค่าความเร็วในการเกาะตัวแบบแห้งจะไม่ขึ้นอยู่กับความเร็วลมและอุณหภูมิของสภาพอากาศในบริเวณแหล่งเพาะปลูก แต่จะขึ้นอยู่กับปริมาณพลังงานแสงอาทิตย์ (solar radiation) โดยมีความสัมพันธ์แบบลอกกาลิทึมและขึ้นอยู่กับความสามารถในการเคลื่อนที่ของก๊าซภายใต้ชั้นของต้นไม้ (canopy conductance) โดยมีความสัมพันธ์เป็นเส้นตรง ซึ่งความเร็วในการเกาะตัวของก๊าซมลพิษเหล่านี้สามารถอธิบายได้ดีโดยใช้แบบจำลองทางคณิตศาสตร์แบบเอมพิริคัล (Empirical Model) ที่มีตัวแปรต้นเป็นสภาวะทางอุตุนิยมวิทยา และปริมาณพื้นที่ใบไม้ต่อพื้นที่ผิวดิน และมีค่าความผิดพลาดในช่วง 30-40% ซึ่งเป็นค่าที่น้อยกว่าการใช้แบบจำลองของ Wesely ซึ่งมีค่าความผิดพลาดระหว่าง 90-150% ซึ่งแม้ว่าจะทำการปรับเปลี่ยนค่าสัมประสิทธิ์ของค่าความต้านทานต่าง ๆ ในแบบจำลองของ Wesely (modified Wesely model) แล้วความผิดพลาดก็ยังมีค่าอยู่ในช่วง 30-80% ซึ่งมากกว่าค่าความผิดพลาดจากแบบจำลองแบบเอมพิริคัล

การศึกษาในเขตพื้นที่ป่าสนพบว่ากลไกการเกิดปฏิกิริยาเคมีและชีวเคมีที่ซับซ้อนภายในป่าสนทำให้ไม่สามารถสร้างความสัมพันธ์แบบเอมพิริคัลระหว่างตัวแปรทางด้านอุตุนิยมวิทยากับความเร็วในการเกาะตัวของก๊าซมลพิษได้ โดยในบางครั้งพบว่าปฏิกิริยาเหล่านี้ก่อให้เกิดการปลดปล่อยก๊าซมลพิษแทนที่การเกาะตัวแบบแห้ง และสำหรับในช่วงฤดูร้อนที่ไม่มีความผันแปรสภาพบรรยากาศมากนักเท่านั้นที่พบว่าสามารถสร้างความสัมพันธ์ทางคณิตศาสตร์กับความสามารถในการเคลื่อนที่ของก๊าซโอโซนภายใต้ชั้นของต้นไม้มีลักษณะในรูปเชิงเส้นได้และเมื่อใช้แบบจำลองทางคณิตศาสตร์ของWeselyสำหรับการเกาะตัวแบบแห้งของโอโซนพบว่าจะให้ค่าความผิดพลาดสูงถึงประมาณ50-350% แต่เมื่อมีการปรับเปลี่ยนค่าสัมประสิทธิ์ของค่าความต้านทานต่างๆในแบบจำลองของWeselyพบว่าสามารถหาค่าสัมประสิทธิ์ของค่าความต้านทานที่เหมาะสมในช่วงเดือนมิถุนายนและกรกฎาคม (ฤดูร้อน) ได้ และมีค่าความผิดพลาดต่ำในช่วง40-50%ซึ่งสามารถนำไปใช้ในพื้นที่จริงได้ แต่สำหรับก๊าซซัลเฟอร์ไดออกไซด์จะไม่สามารถสร้างแบบจำลองทางคณิตศาสตร์ที่ใช้ในการอธิบายการเกาะตัวแบบแห้งได้เลย

เขตพื้นที่เมืองเป็นการศึกษาเฉพาะในส่วนของการเกาะตัวแบบแห้งของโอโซนเท่านั้นพบว่าไม่สามารถสร้างความสัมพันธ์ทางคณิตศาสตร์ในรูปใดๆระหว่างค่าความเร็วของการเกาะตัวแบบแห้งกับตัวแปรทางอุตุนิยมวิทยาได้ซึ่งทำให้ไม่สามารถสร้างแบบจำลองทางคณิตศาสตร์แบบเอมพิริคัลส่วนการประมาณค่าความเร็วของการเกาะตัวแบบแห้งโดยใช้แบบจำลองของWeselyที่มีการปรับค่าสัมประสิทธิ์ของค่าความต้านทานที่เหมาะสมจะทำให้สามารถประมาณค่าความเร็วในการเกาะตัวแบบแห้งในช่วงฤดูร้อนได้

ภาควิชา วิศวกรรมเคมี	ลายมือชื่อนิสิต…….....….
สาขาวิชา วิศวกรรมเคมี	ลายมือชื่ออาจารย์ที่ปรึกษา…….....……....
ปีการศึกษา 2544	ลายมือชื่ออาจารย์ที่ปรึกษาร่วม.....…….....….

4270586221 : MAJOR CHEMICAL ENGINEERING

KEY WORD: DRY DEPOSITION VELOCITY / OZONE / SULFUR DIOXIDE / LEAF AREA INDEX / SOLAR RADIATION / CANOPY CONDUCTANCE

SARIT CHOTCHAKORNPANT: MEASUREMENT AND DEVELOPMENT OF MATHEMATICAL MODEL FOR DRY DEPOSITION OF OZONE AND SULFUR DIOXIDE. THESIS ADVISOR: ASSISTANT PROFESSOR PRASERT PAVASANT, Ph.D. 130 PP. ISBN 974-03-0946-1

The aims of this work were to conduct an experiment for the measurement of dry deposition velocity of ozone and sulfur dioxide, and to develop a corresponding mathematical model for this process. Three areas in Japan with different types of land uses were selected as modeled study: (i) agricultural area, (ii) pine forest and (iii) city (urban) area. In agricultural area, the dry deposition velocities of both ozone and sulfur dioxide in bean fields were higher than in wheat fields. This was because the dry deposition velocity was found to depend linearly on Leaf Area Index (*LAI*), and LAI was larger in the bean than in the wheat cropping areas. In addition, measurement revealed that dry deposition velocity was independent of wind speed and air temperature, but depended on solar radiation and canopy conductance. The relationship between dry deposition velocity and solar radiation was best described by a logarithmic function, whilst a linear function was for the dependency of dry deposition velocity and canopy conductance. The empirical model was found to give good estimates of dry deposition velocity with approximately 30 to 40% deviation from measurement compared with 90-150% from the Wesely model. A modified Wesely model (with correlation coefficient) was found to give a slightly better results than the Wesely model (with 30-80% error), but still could not give the same level of accuracy as the empirical model.

The complicated mechanisms of chemical and biochemical reactions were believed to be the main factors that prevented accurate measurement of dry deposition velocity in the pine forest. In this area, some pollutants could emit to atmosphere instead of deposit onto the earth surface. This caused a variation in the ground-level concentrations of pollutants and made the measurement of the dry deposition velocity difficult. However, the relationship between dry deposition velocity and canopy conductance in certain periods of summer time, where weather conditions were relatively stable, could still be established. The associated errors from the Wesely model in predicting ozone deposition velocity was found to be quite high, 50-350%. The introduction of correlation coefficients into the Wesely model could bring the error down to 40-50% in summer period (June-July). In the case of sulfur dioxide, it was not possible to establish any dry deposition velocity model.

The study in the city area focused only on dry deposition velocity of ozone. No mathematical relationships between the dry deposition velocity and meteorological factors in any form could be formulated. Therefore the empirical model could not be established. The modified Wesely model with appropriate correlation coefficients were found to give good estimates of dry deposition velocity during summer season.

Department	Chemical Engineering	Student's signature……
Field of study	Chemical Engineering	Advisor's signature……
Academic year	2001	Co-Advisor's signature……

ACKNOWLEDGEMENTS

I would like to express my sincere gratitude to Assistant Professor Prasert Pavasant, my advisor, for his valuable suggestions, guidance, warm encouragement and generous supervision throughout my master program. In addition, this thesis could not have been completed without the helping hands from Professor Masatoshi Aoki, my co-advisor, for his efforts in my work, many valuable suggestions and knowledge during researching in Japan. I would also like to thank Assistant Professor Vichitra Chongvisal and Dr. Sangchan Limjirakan for giving me the best opportunity to conduct my experiment in Japan. I am grateful to Professor Wiwut Tanthapanichakoon, chairman of thesis committee for many valuable suggestions.

My work could not have been carried out without the help of my best friends, Miss Sakazume Suzuka, Miss Suzuki Haruko, Mr. Kenichi Takano, Mr. Nozoe Susumu, and Mr. Zhang Shangxun. I would like to express my deep appreciation to them and also to all of my Japanese friends who have helped me in many ways i.e. data analysis and instruction to use instrument. I cannot forget to express my thankfulness to my lovely friends, Mr. Vichian Suksoir, Mr. Sontaya Krichnavaruk, Mr. Kunawut Boonyanopakun, Mr. Chaiyanun Tangtong, Miss Ratchat Chantawongvuti, Miss Thanathorn Worapongsathorn, Miss Patchara Pupa, Miss Narumon Charoentra and Miss Pornthip Wongsuchoto, for their encouragement during my study. Moreover, special thanks should be made for all members in the Environmental and Biochemical Engineering Research Laboratories for the many nice times. Of course, I would like to say special thanks to Miss Sirarat Kongwuttiti for being so supportive during my research.

Most of all, I would like to express my sincere indebtedness to my parents and everyone in my family for their inspiration and worthy supports at all times.

CONTENTS

PAGE

LIST OF TABLES

TABLE **PAGE**

LIST OF FIGURES

FIGURE **PAGE**

Chapter 1

Introduction

1.1 Rationale of the study

Air pollution means the situation where the atmosphere has enough quantity of undesirable materials, which produces harmful effects to the environment such as human health, vegetation, buildings, wildlifes, etc. There are varieties of sources of air pollutants: the most common of which are human activities such as transportation, construction, industries, etc.

It was not until mid 1940s that air pollution problems disclosed their devastating effects and taken into serious consideration. However, the problem was only treated locally and temporally because it was believed that pollutants had short lifetime and were not spread or settled far from the point of source. To date, the knowledge of air pollution becomes more aware of and there have been evidences that the air pollution had long life and could transport a long distance, even between countries (Nevers, 1995). The consequences of air pollutants may well be grouped into “direct” and “indirect” types. The direct type comes primarily from the toxicity of the pollutants themselves, which have a potential capability to attack the targets once the targets are exposed to the pollutants. For instance, the presence of ozone on the earth’s lower atmosphere can result in a serious health damage (Patrick, 1994). Sometimes pollutants in the gaseous form do not present their damaging power but they change forms or phases and, in a new form or phase, the damage is visible. This kind of consequence is treated as indirect effect. The example of this indirect effect is acid rain, which is a result of sulfur dioxide in a gaseous form being absorbed by the moisture in the atmosphere and changing from gas to an acidic solution (acid rain). Another more recent aspect of indirect consequence of air pollutant is the destruction of the ozone layer due to the buildup of oxidizing agents particularly chlorinated

organic compounds such as CFCs in the upper atmosphere, which results in more UV radiation penetrating to the earth's surface.

Apart from the knowledge of how the pollutants attack their targets, one of the other most important facets is how fast they can come from the atmosphere to the targets which are mainly present on the earth's surface. The rate at which the pollutants take to travel from atmosphere to the earth's surface is called "deposition velocity". This velocity depends on several atmospheric and terrain parameters such as the stability of the atmosphere, wind speed, solar radiation, stomata, mesophyll, cuticle, terrain and soil types, etc.

The study of various aspects of air pollutants has always been cumbersome. This is due to difficulties in the measurement, which depends too much on the non-ideality and non-homogeneity of the atmospheric conditions. One of the challenging issues in the study of air pollution is the development of a mathematical model to predict the behavior of air pollutant in the atmosphere. Accurate models help save considerable time and efforts in the tedious process of measurement of the concentration of air pollutants. The development of the model can largely be divided into two major areas: (i) the distribution of air pollutant in the atmosphere and (ii) the deposition of air pollutants onto the earth's surface. Most of the previous reports concentrated on the development of the first type of the model, and a number of air dispersion models were proposed, for instance, Fixed-box, Gaussian plume, ISC3 (Industrial Source Complex) models etc. The deposition of air pollutants, on the other hand, is still not well understood. It is known that the deposition can take place in two forms, wet and dry. The wet deposition occurs when gaseous pollutants are absorbed by the moisture in the atmosphere and comes down to the earth's surface in the form of rain, fog and mist. On the contrary, dry deposition occurs by gravitational settling where the pollutants are absorbed directly to the ground and/or vegetation's surface.

Recently, dry deposition has been treated as a serious problem as it is already known that pollutants can travel long distance and the effect is obvious even if the targets are distanced away from emission sources. There were a few investigations

reporting the mechanism of the dry deposition which were based on the summation of the transport resistances of air pollutants from the atmosphere to the surface (as will be described in detail in the next chapter). It is also the aim of this study to carry out necessary experimental work that is needed to develop a mathematical model that can predict the dry deposition velocity of various gaseous pollutants.

1.2 Objectives of this work

The objective of this work was twofold. Firstly, it aimed to carry out an experimental work to collect data on the dry deposition of air pollutants. The measurement was based primarily on the Bowen ratio technique. The air pollutants of concern were SO_2 and O_3. Secondly, this work was set out to develop a mathematical model capable of describing the dry deposition of the target pollutants. This model was based on environmental parameters obtained from the experimental work.

1.3 Scope of this work

1. The air pollutants of concern were ozone and sulfur dioxide.

2. The measurement was performed in 3 different places:

2.1. Agricultural area: the reference site was selected in Saiwai-cho, Fuchu-shi, Tokyo, Japan. The location is 35^{o} 41′ N, 139^{o} 29′ E, and elevation is about 60 m above sea level, which the total area is about 100x150 m^2. The vegetations schedule in this area are:

- bean. (soybean, *Glycine max merrill*): July. - October 1999,
- corn. (*Zea mays L.*): July - October 2000 and
- wheat. (*Triticum aestivum*): January - May 2001.

2.2. Pine forest: the reference site was selected in Ohoshiba-Kougenn, Minami-Minowa Village, Kami-Ina Gun, Nagano Prefecture, Japan. The location is 35^{o} 52′ N, 137^{o} 58′ E, and elevation is about 60m above sea level and the total area is about

1600x1000m^2. The predominant plant species is red pine (*Pinus densiflora sieb. et zucc.*) and the period of this experiment is during May - September 2001.

2.3. City area: the reference site was selected above JA building (Japan Agriculture building), Tachikawa, Japan and the period of this experiment is during August - November 2000. The location is about 100 m south of Tachikawa.

3. All measurements of dry deposition velocity were based on the Bowen ratio technique.

Chapter 2

Theory and Literature Review

2.1 Backgrounds

2.1.1 Air pollutants

Air pollutants is defined as one or more contaminants or undesired materials in atmosphere that are present in adequate quantity and time to be injurious to human beings, plants, animal lives, or to damage properties and even interfere with the comfortable enjoyment of life. In 1990, the U.S. Environment Protection Agency (EPA) established the National Ambient Air Quality Standards (NAAQS) in order to study and set up a list of standard chemicals as hazardous air pollutants (EPA, 2000). These standards are summarized in Table 2.1.

A number of toxic gases are present in the atmosphere and all of them are equally important in the evaluation of their damaging effects. However, this work will only focus on the distribution of sulfur dioxide and ozone particularly their deposition mechanism. This is primarily due to the limitation on the availability of the real-time measurement equipment during the time of this work, which only allows the measurement of these two pollutants. However, this choice of pollutants is, in fact, appropriate, as the deposition of these two pollutants have direct and visible effects on the eco-systems: this will be described in detail later in this section. In addition, the results from this study will potentially be important as a case study for further investigation of the deposition of other gaseous pollutants.

The following subsections provide brief introduction to the characteristics of ozone and sulfur dioxide.

(i) OZONE: Ozone is a colorless gas, bp –111.9 C, toxic, very pungent, has a characteristic odor, and is able to oxidize all materials, both organic and inorganic. In the atmosphere, ozone can be classified roughly into 2 groups: good ozone and bad ozone. Good ozone occurs in the Earth's upper atmosphere, where its main task is to shield the earth's surface from the sun's ultraviolet rays. Bad ozone, which stays in the earth's lower atmosphere, nearer to ground surface, is an important toxic pollutant. This is because it possesses the oxidizing ability, which is destructive to most creators' respiratory systems, aggravated asthma, lung diseases, etc. Ozone is found in the natural atmosphere as a result of the action of solar radiation and electrical storm. Moreover, it can be considered as a secondary pollutant, which means that it is a result of an interaction between primary pollutants. For instance, NO and HC (hydrocarbon) in the atmosphere can undergo a photochemical oxidation, and this leads to the formation of ozone (Guicherit, 1978) (Eq. 2.1).

$$NO + HC + O_2 + \text{light} \longrightarrow NO_2 + O_3 \qquad (2.1)$$

(ii) SULFUR DIOXIDE: Sulfur dioxide is a colorless gas at ambient temperatures, bp –10 C, nonflammable but toxic, has a strong suffocating odor, and can be soluble in water and organic solvents. The sulfur dioxide produced by burning of fuels containing sulfur is an important toxic pollutant in the atmosphere due to its capability to attack human both directly e.g. respiratory system, skin, eyes, and lung, and indirectly through the acidification of rain and soil. The indirect effect is induced from the settling of the gas molecules onto the ground. This is because SO_2 can react with water in the ground resulting in soil acidification. This damages the natural equilibrium and lead to a shift of the balance of the eco-system, e.g. alteration of local species of flora and fauna. Main sources of sulfur dioxide emission are coal and oil industries, steel mills, refineries, metal smelting, and pulp and paper mills, where large quantity of fuel is needed as an energy source.

2.1.2 Pathways of air pollutants

The transportation pathways of pollutants from a source to a receptor can largely be described by two distinct mechanisms. A direct mechanism occurs when pollutants travel through only one medium that intervenes between the source and the receptor. A direct pathway is shown in form of “dispersion”, which is the transport caused by concentration gradient, and “advection”, where pollutants transport from one location to another without a change in concentration. Chemical inhalation by living creators is a good example of the direct pathway. Industries can emit varieties of gaseous pollutants which can attack human beings or other creators through their respiratory systems. Toxic gases e.g. ozone, sulfur dioxide, phosgene, are all regarded as hazardous gaseous and can present their damaging capability directly. Cases where pollutants move passed more than one medium are categorized as an indirect mechanism and an indirect pathway is described by the deposition due to the settling of materials emitted from any sources to the earth’s surface. For instance, if a pollutant is released from a particular source, it can be transported through several layers of atmosphere (each of which has different resistances to the transport of air pollutants), deposited on the earth’s surface and absorbed into a soil or water. This leads to harmful consequences at receptors, e.g. human, animals or plants.

Since this work focuses mainly on the deposition of the pollutants onto the earth’s surface, only the indirect pathway will be considered thereafter.

2.1.3 Deposition of air pollutants

Deposition of pollutants can take place both in dry and wet forms. The wet deposition is the consequence of washout and rainout (Oden, 1976), which is the precipitation process of pollutant due to some specific interactions between the pollutant and airborne chemicals such as rain, fog and mist. Acid rain is a good example for the wet deposition of sulfur dioxide in the atmosphere. The dry deposition, on the other hand, is a consequence of settling by gravitation and absorption of molecules or particles.

Wet deposition depends significantly on the behavior of the atmosphere and the meteorological conditions, and there are still far too many unknown parameters that prevent a thorough study of its mechanism. Dry deposition, on the other hand, can be treated a little more simply as fewer parameters will be involved in the study. Despite so, the knowledge of dry deposition is still not well established.

2.1.4 Atmospheric boundary layer

It was pointed out that when a fluid flows over a surface the flow velocity decreases towards that surface as a consequence of the friction between the surface and the fluid, and of the viscous forces within the fluid. The zone adjacent to surface, where the mean velocity is reduced significantly below that of the free stream, is termed 'the boundary layer'. One common arbitrary definition of the boundary layer defines its limit as that streamline where the velocity reaches 99% of that in the free stream. The pattern of fluid movement within a boundary layer may be either laminar, where all the fluid movement is parallel to the surface, or it may be turbulent. Fig 2.1 shows the boundary layer in an airstream flowing over rough canopy surface.

Experimentally it was found that, for a smooth plate, the transition from a laminar to turbulent boundary layers generally occurs when the value of a dimensionless group of terms called the Reynolds number exceeds a value between 10^4 and 10^5 (Monteith et al., 1995). The Reynolds number is a dimensionless group given by ud/v, where u is the free fluid velocity, d is a characteristic dimension of the objective and v is the kinematic viscosity.

The flux of mass transfer above the crop within the boundary layer can be described by the standard gradient-diffusion assumption where the flux is proportional to the transfer coefficient multiplied by the driving concentration gradient (Jones, et al., 1996):

$$J_i = -D_i(z)\,(\delta c_i/\delta z) = -K_i(z)\,(\delta c_i/\delta z) \qquad (2.2)$$

where J_i = mass transfer rate per unit area or flux density [kg $m^{-2}s^{-1}$]

D_i = molecular diffusion coefficient for laminar flow [$m^2\ s^{-1}$]

K_i = molecular eddy transfer coefficient for turbulent flow [$m^2\ s^{-1}$]

C = concentration [kg m^3]

z = height from the ground [m]

The depth of the boundary layer increases with distance or 'fetch' from the leading edge (or the starting point, A, in Fig 2.1). In general, it is assumed that measurements may be made with adequate precision when the height above the canopy was large enough, and often this height was set at about 0.01 × fetch (Monteith, et al., 1995). It is also found that measurement needs to be made well above the underlying canopy because the erratic turbulence structure near and within canopies leads to such great variability in *K* that Eq.2.2 has a small practical value in this zone. Usually, micrometeorological studies of fluxes through the crop boundary layer require large areas of homogeneous vegetation, the size of which depends on the height above the canopy at which sensor are placed.

2.1.5 Influences of physical and meteorological factors on dry deposition velocity

Factors that have significant effects on the dry deposition velocity can largely be grouped into 2 categories, i.e. physical and meteorological factors. Physical factors represent the characteristics of plants such as leaf area and the rate of photosynthesis. The later factors include ambient temperature, wind speed, sunlight intensity, etc. which can have both direct and indirect effects on the changes of mass and energy between the different atmospheric layers.

1. Physical factors:

(i) Leaf Area Index (*LAI*): LAI represents an overall area of leaves within one unit area. The rate of change of LAI demonstrates the physical growth of plant, and generally, LAI becomes higher when plants grow, and lower when plants die. LAI is generally employed to indicate the quantity of stomata of each plant because almost all of stomata are in the plants' leaves, and stomata changes accordingly with the

growth of the plant. Since plants exchange gas, including gaseous pollutants, with the atmosphere through stomata, the quantity of stomata can impose strong influence on the rate of pollutant deposition. Fig. 2.2 shows a mechanism of the uptake of gases in stomata and absorption of gas at the leaf surface. Once the gas molecules are inside the stomata cavity, they may enter and react with intercellular fluids or transport across cell membranes depending on the reactivity and solubility of the gas molecules. Stomatal closure and opening are primarily controlled by light intensity, temperature, humidity and leaf water potential. The effect of light intensity, temperature and humidity will be discussed in the meteorological factors section. The leaf water potential was the ability of leaf in absorbing water. This ability depends on plant types which causes a different level of stomata opening. For example, desert plants have a high capacity in water absorbing, which means that stomata is narrowly open to keep the water in the leaf. On the other hand, but plants in the jungle absorb less water, therefore its stomata is more widely open. The level of stomata opening has an effect on the flux of gas. When stomata is narrowly open, the gas flux through the stomata is small and the gas absorbing activity in plant decreases accordingly. In contrast, wide open stomata helps increase the plant absorbing activity and allows higher gas exchange rate.

(ii) Net photosynthesis (P_n): Photosynthesis is the metabolism used in transforming carbon dioxide to various structures of plants, such as, trunk, leaf, root, and even products. Generally a high uptake rate of carbon dioxide is needed during the productive stage of the plant. Net photosynthesis, hence, indicates the overall capability of plants in absorption (deposition) and release (emission) of CO_2 and other gases from/to the atmosphere.

2. Meteorological factors:

(i) Solar radiation (I): Solar radiation is the energy flux from sun light (short wave radiation) and emission (long wave) from cloud, sky and star into 1 m^2 area. Solar radiation provides the main energy to the earth, with much of this energy being converted to heat and driving other processes such as mass, heat and momentum transfers between resistance layers i.e. aerodynamic, quasi-laminar and canopy

resistances. Moreover, solar radiation has effects on the rates of photosynthesis and transpiration of plants. Generally, when the intensity of light is high, the stomata will be wide open due to an increase in the net photosynthesis of plants. Conversely, a decrease in light intensity reduces the photosynthesis, and the stomata shrinks. This phenomenon directly influences the plant's ability in absorbing ozone and sulfur dioxide from the atmosphere.

(ii) Wind speed (*ws*): The increases in wind speed decrease the boundary layer resistance. When the flow regime in the boundary layer changes from laminar to turbulent by increasing wind speed, the mass transfer becomes more rapid because of eddies. In this case the boundary layer conductance increases because *D*, the molecular diffusion coefficient, is replaced by a larger eddy transfer coefficient, *K* (see Eq. 2.2), therefore, the flux of pollutant also increases.

(iii) Ambient temperature (*T*): The effect of ambient air temperature on dry deposition velocity is two-fold. Firstly, the number of molecular diffusion coefficient and eddy transfer coefficient depend on temperature, which is usually expressed by a power law, e.g. $D(T) = D(0)\{T/T(0)\}^n$ = where $D(0)$ is the coefficient at a base temperature $T(0)$ [*K*] and *n* is an index between 1.5-2.0. The value of the diffusion coefficients of air at various temperatures were calculated by Chapman-Eskog (Monteith et al., 1995). It can be observed that when temperature increases, the diffusion coefficient also increases. The second effect of ambient temperature on dry deposition velocity is on the relative humidity (*RH*) in the air. Fundamentally, RH can effectively control the closing and opening of stomata such that small opening stomata is obtained in dry condition (low *RH*) and large opening in wet condition (high *RH*).

(iv) Canopy conductance (g_c): The canopy conductance is the ability of gas in transfer between air and plant inside canopy. The canopy conductance parameter is very important because it includes the effects of stomata, mesophyll, cuticle, soil, water surfaces and stone & other materials inside canopy. The canopy conductance

can be estimated from Penman-Monteith equation (Monteith et al., 1995) as shown in Eq. 2.3

$$g_c = [\ \frac{\Delta(R_n-G)+\rho c_p\{e_s(T(z))-e(z)\}/r_a}{\lambda_E}\ -\ \Delta]\ r_a/\gamma - r_a \qquad (2.3)$$

where Δ = rate of change of saturation vapour pressure with temperature

$= \delta\ e_s(T)/\delta T$ [mb $^oC^{-1}$]

R_n = net radiation flux [W/m^2]

G = ground heat flux [W/m^2]

ρ = air density [g.cm^{-3}]

$c_p = C_P$: heat capacity of air [cal.g^{-1}.$^oC^{-1}$]

$e(z)$ = partial pressure of vapor at height Z [mb]

r_a = aerodynamic resistance [s/m]

λ_E = latent heat flux [W/m^2]

γ = psychrometer constant [mb $^oC^{-1}$] ($=c_p p/\lambda E$)

P = air pressure [mb]

2.1.6 Conventional models for dry deposition of pollutants

The dry deposition velocity can generally be formulated in terms of the summation of the reciprocals of the transportation resistances:

$$V_d = 1/\ (r_a + r_b + r_c) \qquad (2.4)$$

The various resistances in this model represent the ability of the various atmospheric layers to retard the movement of the pollutants. Generally the atmosphere that influences the deposition rate of air pollutants can be divided into 3 layers (Fig. 2.3), each of which has different magnitudes of resistances depending on various parameters as described below:

(i) The aerodynamic resistance (R_a): this is the top layer resistance above the canopy that mass or energy transfers with turbulent pattern. This resistance is a

function of wind speed, surface properties and atmospheric stability, which is shown in Eq. 2.5 (Monteith et al., 1995).

$$Ra = \frac{[ln\ \{(Z-d)/Z_o\}]^2}{\kappa^2\, u(z)} \qquad (2.5)$$

$\log Z_o = 0.977 \log h - 0.883$

$\log d = 0.9793 \log h - 0.1536$

Z = height of measurement [m]

$u(z)$ = wind speed [m/s)]

d = zero plane displacement [m]

Z_o = roughness length [m]

κ = karman's constant ≈ 0.4

h = height of plant (m)

(ii) The quasi-laminar boundary layer resistance (R_b): this is a buffered, thin layer, staying in between the aerodynamic and the canopy stomata resistances. The differential properties of the two upper and lower atmospheric layers e.g. temperature, density, stability etc. significantly affect the magnitude of this resistance, which is calculated by Eq. 2.6 (Hicks et al., 1987).

$$Rb = \frac{5}{u_*}(\nu/D)^{2/3} = \frac{5\, Sc^{2/3}}{u_*} = \frac{2\,(Sc/Pr)^{2/3}}{\kappa u_*} \qquad (2.6)$$

u_* = friction velocity [m/s]

$$\left(u(z) = \frac{u_*}{\kappa} \ln (z-d)/z_o \right)$$

ν = kinematic viscosity of air (cm^2/s) ≈ 0.151 cm^2/s (at 20 ^oC)

D = molecular diffusivity of species (cm^2/s) ≈ $D_{\text{water vapour in air}}$ ≈0.242 cm^2/s (at 20 ^oC)

The value of Sc/Pr are shown in table 2.2 (Hicks et al., 1987)

(iii) The lowest and most complex layer is the canopy resistance (R_c), which includes the effects of stomata, mesophyll, cuticle, soil, water surfaces and stone & other materials. The estimation of this resistance varies between different types of models, e.g. Baldochi model, ADOM model, Wesely model etc. This will be described further in the Literature Review Section. In this work, the Wesely model will be chosen as a modeled study as it is the simplest with respect to the experimental data requirement of the model and the ease of applying the model.

The canopy conductance from the Wesely model (Wesely, M.L. 1989) is calculated from:

$$r_c = \left(\frac{1}{r_{st} + r_m} + \frac{1}{r_{lu}} + \frac{1}{r_{dc} + r_{cl}} + \frac{1}{r_{ac} + r_{gs}} \right)^{-1} \qquad (2.7)$$

where r_{st} = leaf stomatal resistance

r_m = mesophyll resistance

r_{lu} = the leaf cuticular resistance

r_{dc} = resistance to transfer by bouyant convection

r_{cl} = resistance to uptake by leaves, twigs and other exposed surfaces

r_{ac} = transfer resistance for processes that depend only on canopy height and resistance for uptake by the soil, leaf litter

r_{gs} = ground surface resistance

Note Details for the calculations of all resistances in Eq. 2.7 were provided in Appendix A.

2.1.7 Measurement of dry deposition velocity

Dry deposition velocity can be measured using either direct or indirect methods. In the direct method, an explicit measurement is made to determine the deposition flux of material onto a surface, either by collecting material deposited on the surface itself or by measuring the vertical flux in the air near the surface. The accepted and

accurate theory of direct method is called “Eddy Correlation”. (Wesely et al., 1982) In this method, the vertical fluctuations of the wind speed ($w'(t)$) and concentration ($C'(t)$) fields are measured directly by high-speed instruments for both wind speed and pollutant concentrations. Then, the flux of dry deposition velocity is calculated by

$$F = w'(t)\, C'(t) \qquad (2.8)$$

However, this needs a real-time analyzer of gas concentration that is able to capture and analyze the data every 0.2 second or less. In practice, such analyzer with real-time speed is still unavailable, therefore, the Eddy accumulation theory is still in the process of development.

In the case of indirect method, the dry deposition is determined by measuring the vertical gradient of the depositing substance and using-transport theory to calculate the associated deposition flux. The most practised indirect theory is the Bowen ratio technique because it is easy to apply in fieldwork. This technique, invented in 1981 by Bowen (Sienfeld et al., 1996), involves 2 steps: (i) finding turbulent gaseous transfer coefficient and (ii) using Fick’s law theory in calculating the dry deposition velocity.

(i) Turbulent gaseous transfer coefficient

The turbulent gaseous transfer coefficient between measurement positions 1 and 2 (in Fig. 2.5) ($\vartheta_{1\text{-}2}$) is calculated from the summation of heat flux (Eq. 2.9) (see Fig. 2.4).

$$R_n = H + \lambda_E + G \qquad (2.9)$$

where R_n : net radiation flux [W/m^2]

G : soil heat flux [W/m^2]

H : sensible heat flux [W/m^2] $= \vartheta_h \times \rho \times c_p \times \Delta T \qquad (2.10)$

$= \vartheta_h \times \rho \times c_p \times (T_1 - T_2)$

λ_E : latent heat flux [W/m^2] $= \vartheta_{H20} \times \frac{0.622}{P} \times \rho_a \times l \times (e_1 - e_2) \qquad (2.11)$

l : heat of vaporization [cal.g^{-1}] (ex: at 30 ^{o}C, l = 579 cal.g^{-1})

P : air pressure [mb]

e_1, e_2 : partial pressure of vapor at height Z_1 and Z_2 [mb]

C_P : heat capacity of air [cal.g^{-1}.^{o}C^{-1}] (ex: C_P = 0.24 cal.g^{-1}.^{o}C^{-1})

T_1, T_2 : air temperature at height Z_1 and Z_2 [^{o}C]

ρ_a : air density [g.cm^{-3}] (ex: at 30 ^{o}C, ρ_a = 1.145 $\times 10^{-3}$ g.cm^{-3})

(1 cal.cm^{-2}.min^{-1}: 698 W.m^{-2})

$\vartheta_{1\text{-}2}$: gaseous turbulent transfer coefficient [cm.s^{-1}]

ϑ_h : heat transfer coefficient [cm.s^{-1}]

ϑ_{H2O} : vapor transfer coefficient [cm.s^{-1}]

The Bowen ratio technique assumes that the transfer coefficients between positions 1 and 2 for heat and water vapor in the turbulent boundary layer above the crop layer are equal to the turbulent gaseous transfer coefficient ($\vartheta_{1\text{-}2} = \vartheta_h = \vartheta_{H20}$). Then, Eq.(2.8) can be rearranged by the following formula:

$$\vartheta_{1\text{-}2} = (R_n - G)/ \{(\rho_a . l . \frac{0.622}{P} . (e_1\text{-}e_2)) + (C_p . \rho_a . (T_1\text{-}T_2))\} \qquad (2.12)$$

Note that the turbulent gaseous transfer coefficient ($\vartheta_{1\text{-}2}$) can only be calculated during the day time. At the night time, R_n equals zero due to no light and although the summary of heat tranfer (G, H and λ_E) in system is not zero, the assumtion that is $\vartheta_{1\text{-}2} = \vartheta_h = \vartheta_{H20}$ is not correct. Consequently, all data analysis in this experiment were selected only in daytime.

(ii) Fick's law

Fick's law states that the dry deposition flux can be calculated from the product between the concentration gradient of pollutant ($\partial C/\partial z$) and the diffusivity (D) as shown in following formula:

$$F = D (\partial C/\partial z)$$

However, the measurement of ∂C in real field was difficult, therefore, it was assumed that the value of ∂C was C_1–C_2 at two points (see Fig. 2.5). And the turbulent gaseous transfer coefficient between two points was the molecular diffusivity at difference of two points, $D / (Z_1 - Z_2)$. Consequently, Fick's Law can be rearranged in following fomula:

$$F = \vartheta_{1\text{-}2} \times (C_1 - C_2) \qquad (2.13)$$
$$= V_d \times C_{avg}$$

where

C_1, C_2 : gaseous concentration at height Z_1 and Z_2 [μg.cm^{-3}]

V_d : dry deposition velocity [cm.s^{-1}]

$C_{avg,1}$: averaged gaseous concentration every 30 min at height Z_1 [μg.cm $^{-3}$]

2.2 Literature Review

Investigation on the dry deposition of air pollutants began as early as in 1977 when Wesely et al. (1977) reported the relationship and effect of atmospheric factors on the quantity of aerodynamic resistance (R_a) and quasi-laminar resistance (R_b). These parameters included friction velocity, roughness length, stability correction parameter, molecular thermal diffusivities. From that point onwards, the atmospheric pathways of pollutants were considered to have some sort of resistances to the transport of air pollutants. A number of studies have then contributed to the investigation of these various resistances. Baldocchi et al.(1987) studied and described necessary factors that had effects on the stomata resistance parameter, (R_{st}), and arranged it as a function of conductance (g) of photosynthetically active radiation (PAR), air temperature (T), leaf water potential (Ψ) and vapor pressure deficit (ω). This work was concluded from the experiment where SO_2, O_3 and NO_2 were deposited on soybeans, spruce and oak.

Several researchers developed the deposition velocity model with the influence of natural factors. Baldocchi et al.(1988) investigated and exhibited a one dimensional, multi-layer model to estimate sulfur dioxide deposition in a deciduous forest. The main idea of this model was to have several sets of leaf resistances (R_l) connected in series. Each set of the leaf resistances consisted of a quasi-laminar (R_b) and a canopy resistances (R_c), where R_c was derived from a complex interaction between several other resistances such as those from stomata (R_s), mesophill (R_m), and cuticle (R_{cut}) (see Fig. 2.6 for graphical diagram of this model). In their work, the aerodynamic and quasi-laminar resistances were derived based on the formulation of Hick et al. (1977), whereas the stomata resistance was based on the formulation of Baldocchi et al.(1987).

A year later, Wesely (1989) proposed a new method for calculating the stomata resistance (as a part of canopy resistance) and the model was later referred to as “W-model”. The principle of this model was based on the uncertainty and inequality of the quantity of solar radiations from the sun and from the earth’s surface

(reflection) which led to a scattering of pollutants in the canopies. The canopy layer was separated into 2 layers, upper and lower, each of which was exposed to solar radiation at different density. This was because the lower layer would be more exposed to the reflection of the solar radiation from the earth's surface. The resistance of this model was then formulated in terms of solar radiation. The canopy resistance (R_c) was thought to comprise a series of leaf cuticle resistance and the parallel of 3 series i.e. (i).R_s and R_{meso}, (ii).R_{dc} and R_{cl}, and (iii).R_{ac} and R_{gs}. Detail of these resistances and the schematic diagram of this model is illustrated in Fig 2.7. Gao et al.(1995) investigated and further developed this model to include the effect of an increase or decrease of the solar radiation due to the reflection of each sub-resistance inside the canopy. The quantity of solar radiation, from the sun or reflecting ground, was collected by satellite for using in the models and compared with data of dry ozone deposition velocity on tallgrass areas in the Kansas city in 1987.

Padro et al. (1991,1995) described the ADOM, Acid Deposition and Oxidant Model, which was formulated by Pleim et al.(1984) and Venkatram et al.(1988).This model assumed that the canopy resistance of atmosphere was a bulk parameter; however, R_c of this model was calculated from the leaf area index (*LAI*) instead of integrating a vertical distribution of leaf density in canopy. The R_c consisted of stomata and mesophyll resistances in series which was in parallel to the resistance exerted by the dry cuticle, wet cuticles, ground water and other resistances as shown in Fig 2.8. This model was verified by the ozone deposition data collected in Ontario, Canada during several summer periods, e.g. a deciduous forest (1991), a vineyard (1994), a cotton field and a senescent grass field (1994).

Subsequently, Zhang et al. (1996) investigated the multi-layer model proposed by Baldocchi et al.,1988 and the single-layer in ADOM (Padro et al. 1995), and compared the results with the observed O_3 dry deposition velocities in a deciduous forest in Ontario, Canada in the summer of 1988 and winter of 1990, and a cotton field and a vineyard in California for the summer of 1991. It was shown that ADOM and multi-layer models gave a better prediction than the W-model in deciduous forest over summer; however, the W-model was a better choice in the winter. And in the

summer, the multi-layer was a better model for night prediction in vineyards, but the two models (ADOM and multi-layer) predicted similar results for the cotton fields. Similarly, Brook et al. (1999) demonstrated the use of deposition models using the multi-layer (Baldocchi et al. 1988) and ADOM (Padro et al. 1995). It was found that the multi-layer model was suitable for the tall canopy cases whilst the ADOM was more suitable for short grass. Table 2.3 summarizes the formulas used to estimate the resistance of the various atmospheric layers.

Literature revealed that, although several deposition mechanisms have been proposed, the prediction of the rate of dry deposition of air pollutants are still subjective to varieties of factors, e.g. temperature, moisture, wind direction and velocity, the terrain type. It implies, in one sense, that the mechanism might depend on the topography. Hence, it is important that local measurement is performed to provide necessary information needed to develop a mechanism that is suitable for a particular area. The objective of this work is to investigate and find the appropriate factors in various terrain types, e.g. pine forest, cropland and city area, in Japan.

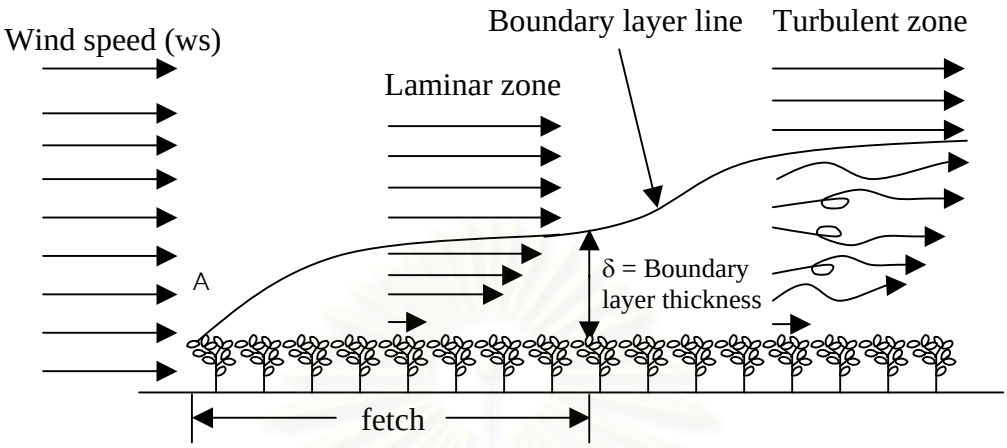

Figure 2.1 Diagrammatic representation of boundary layer and fetch

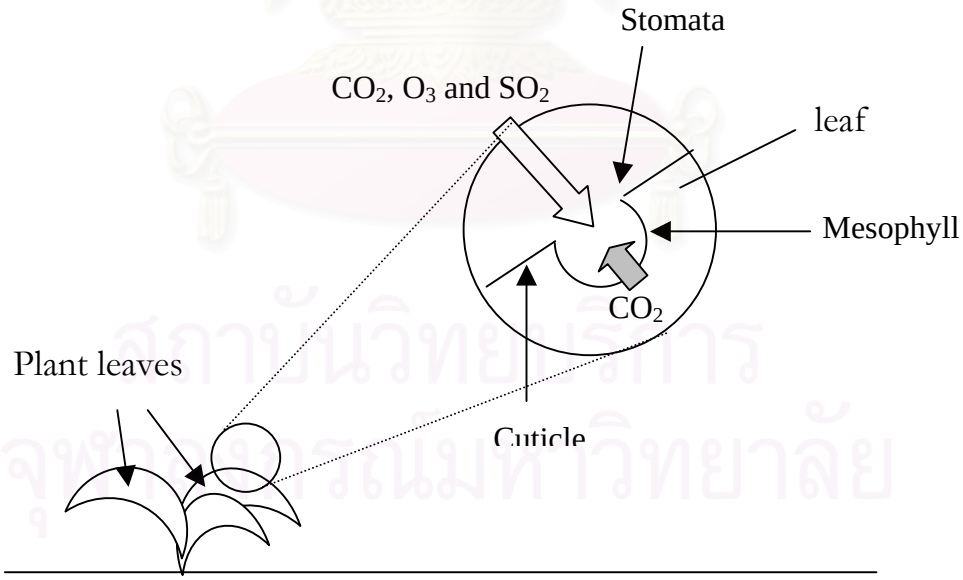

Figure 2.2 Gaseous transfer at the stomata of plants' leaves

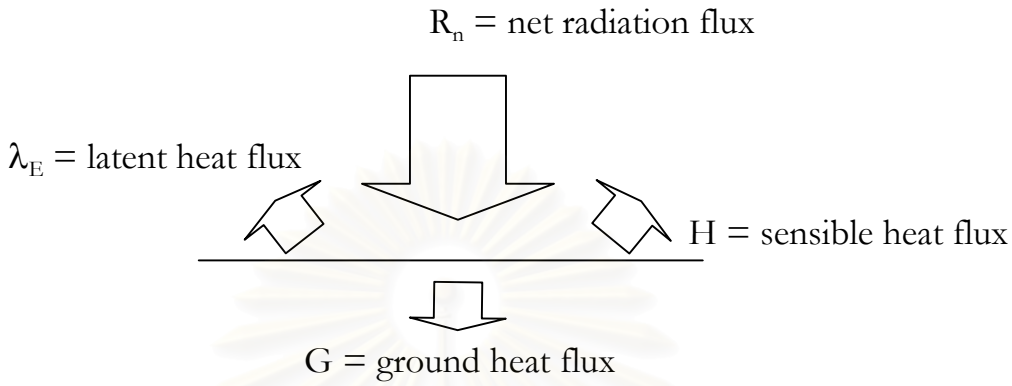

Figure 2.4 Diagrammatic representation of heat flux at ground surface

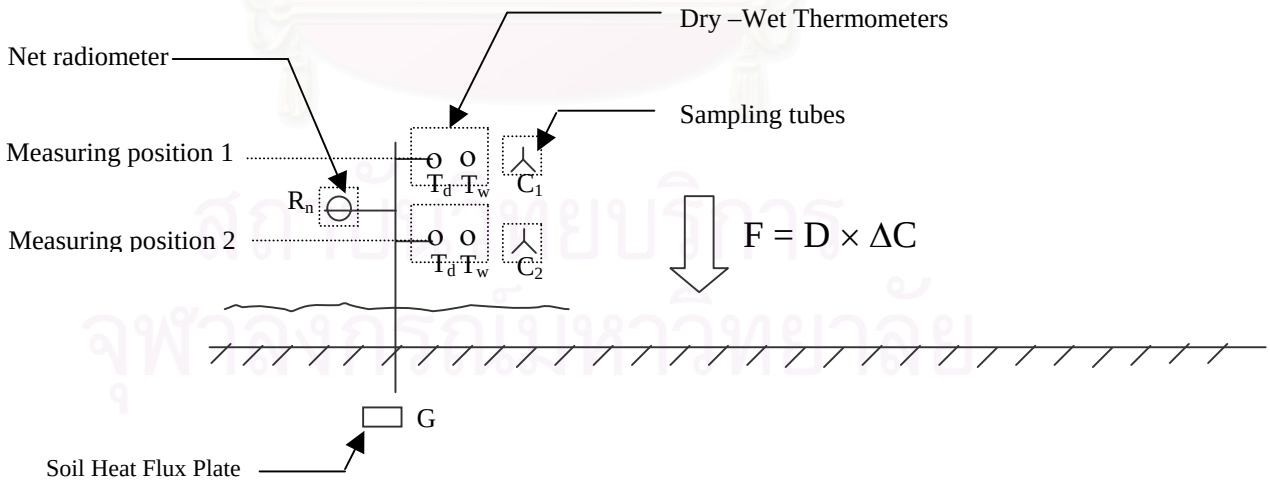

Figure 2.5 Bowen ratio technique and Fick's law measurement

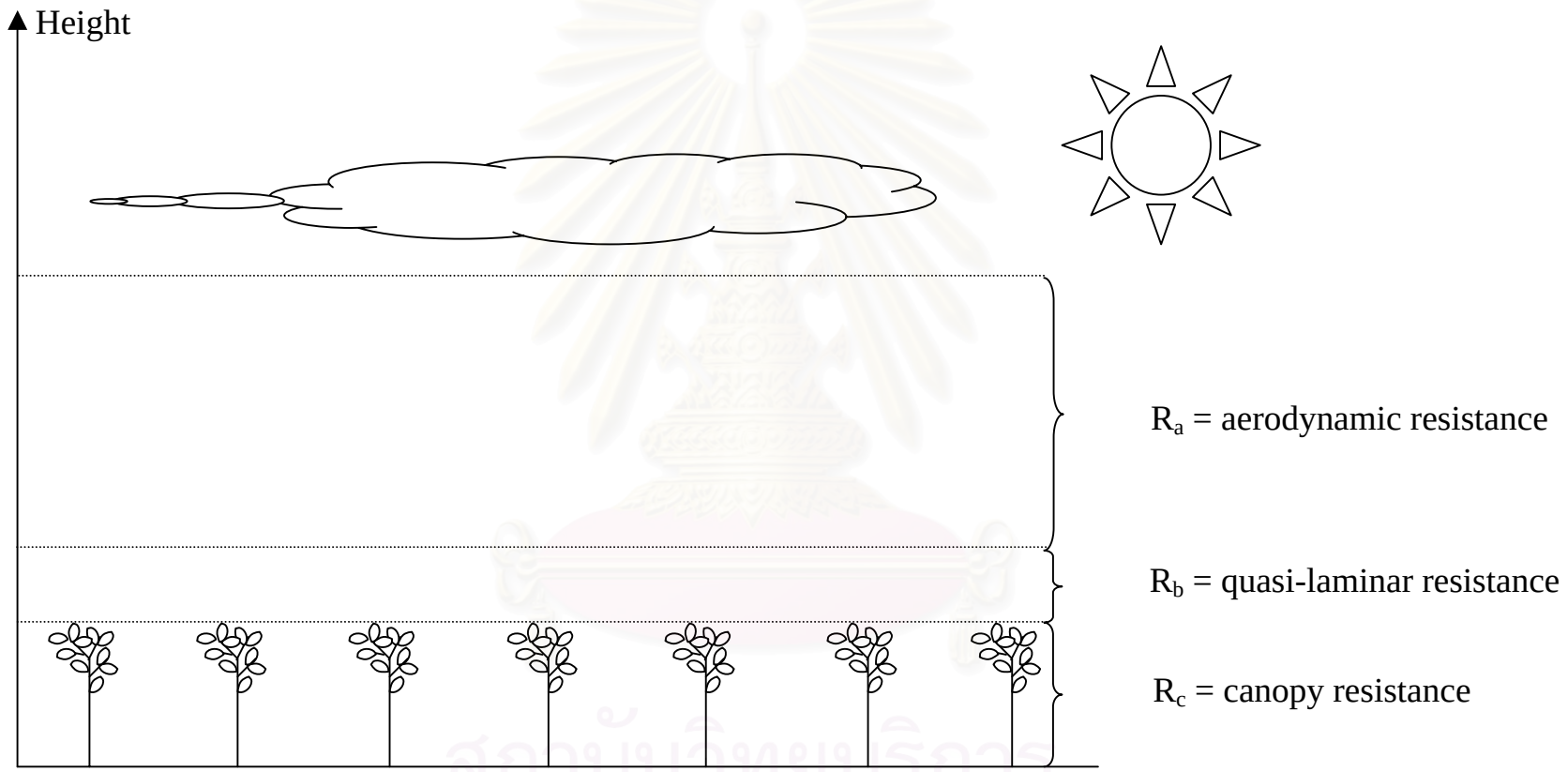

Figure 2.3 Schematic representation of various atmosphere resistances above the canopy

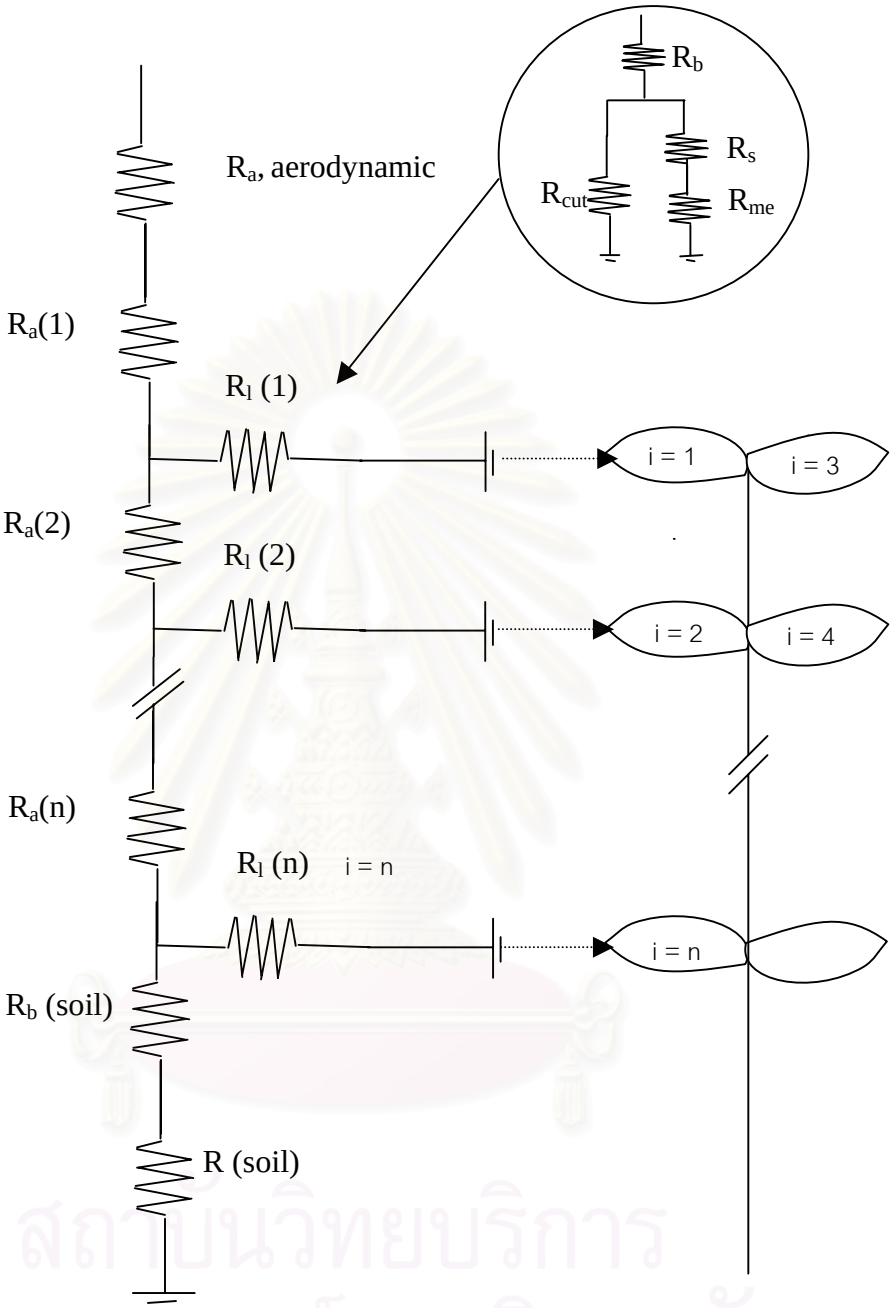

Figure 2.6 Schematic pathway of multi-layers resistances at vegetation areas, R_a represent aerodynamic, R_l for leaf resistance, R_b for diffusive each boundary layer, R_s for stomata, R_{meso} for mesophyll, R_{cut} for cuticular, R_{soil} for soil resistances Baldocchi et al.(1988)

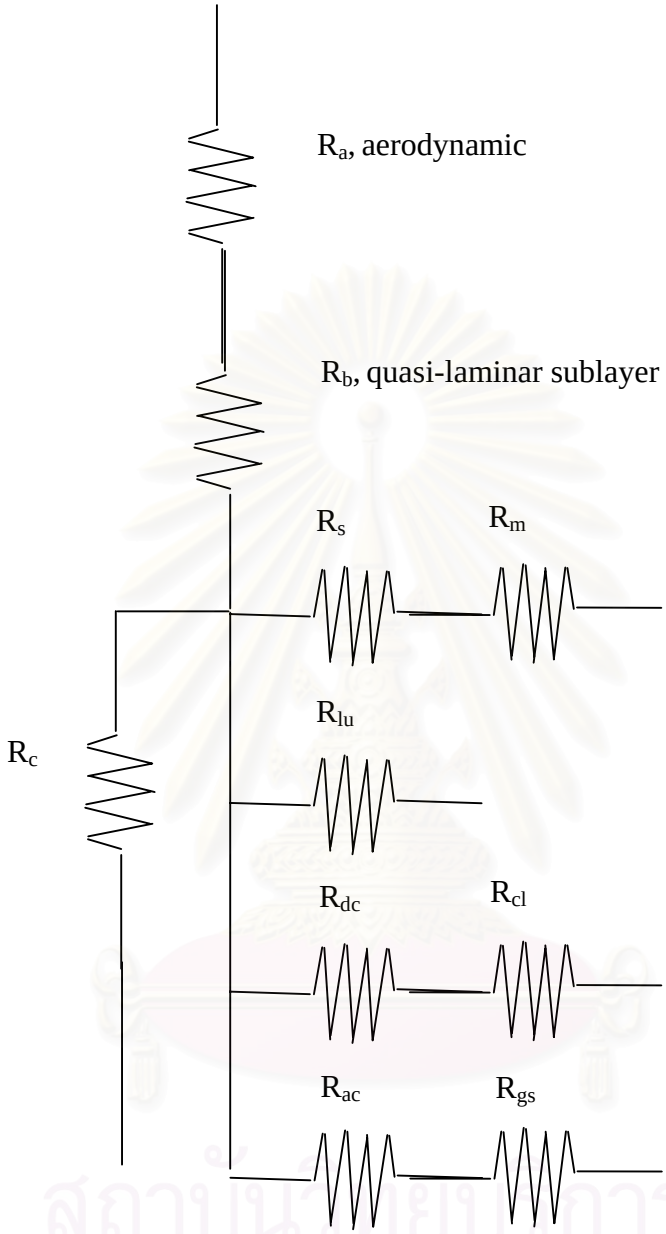

Figure 2.7 Schematic pathway of the resistances described in Wesely (1989), R_s represents surface bulk resistance component for leaf stomata, R_m for leaf mesophyll resistance, R_{lu} for leaf cuticles in healthy vegetation and otherwise the outer surfaces in the upper canopy, R_{dc} for a gas-phase transfer affected by buoyant convection in canopies, R_{cl} for leaves, twig, bark, or other exposed surfaces in the lower canopy, R_{ac} for transfer that depends only on canopy height and density and R_{gs} for the soil, leaf litter etc., at the ground.

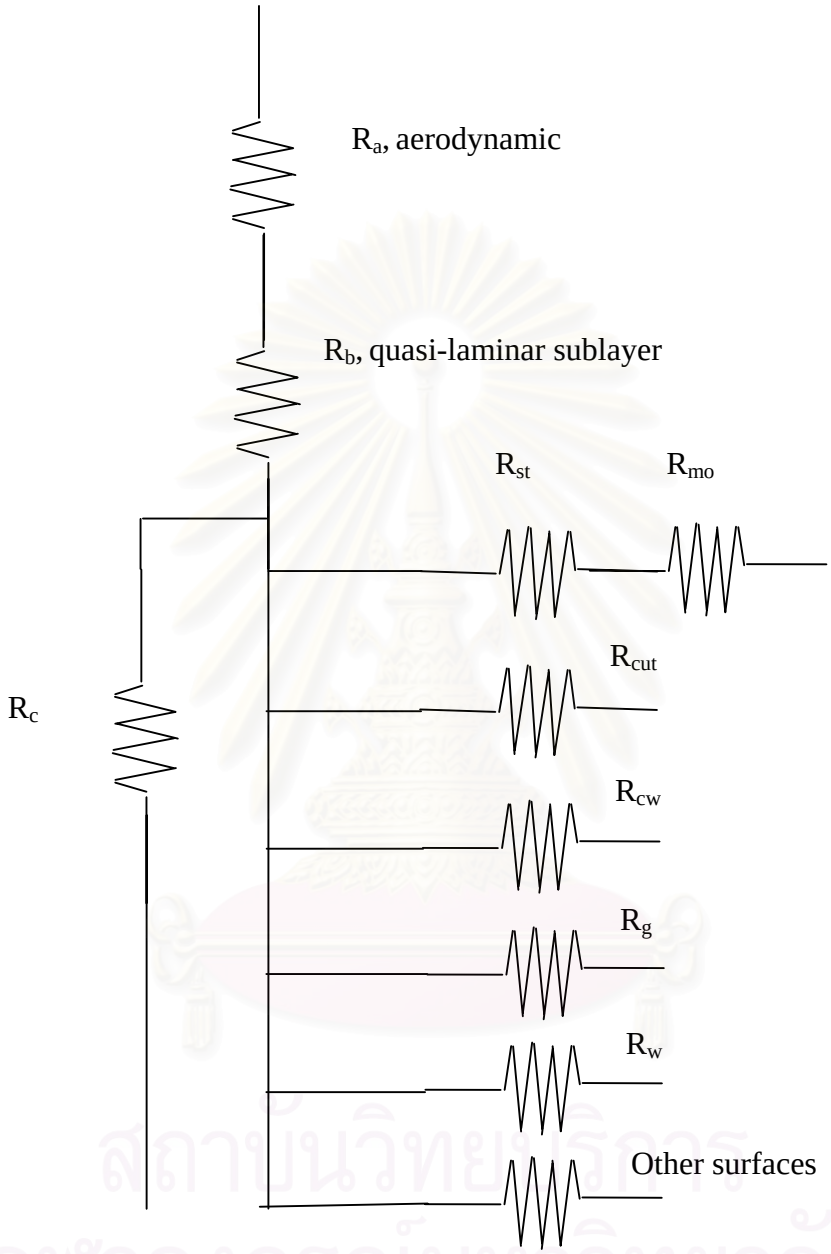

Figure 2.8 Schematic pathway resistance of ADOM, R_{st} represents for canopy stomatal, R_{cut} for dry cuticle resistance, R_{cw} for wet cuticles, R_{mo} for mesophyll, R_g for ground and R_w for open water resistance. Prado et al.(1991,1995)

Table 2.1 Common air pollutants and their permitted ambient concentrations.

Pollutant	Standard value*	**
Carbon monoxide (CO)		
8-hour average	10 mg/m^3 (9 ppm)	10.26 mg/m^3
1-hour average	40 mg/m^3 (35 ppm)	30 mg/m^3
Nitrogen dioxide (NO_2)		
annual arithmetic mean	100$\mu g/m^3$ (0.053 ppm)	320 $\mu g/m^3$
1-hour average		
Ozone (O_3)		
8-hour average	157 mg/m^3 (0.08 ppm)	100 mg/m^3
1-hour average	235 mg/m^3 (0.12 ppm)	200 mg/m^3
Lead (Pb)		
quarterly average	1.5 $\mu g/m^3$	
Particulates< 10 micrometers (PM-10)		
annual arithmetic mean	50 $\mu m/m^3$	
24-hour average	150 $\mu m/m^3$	120 $\mu g/m^3$
Particulates< 2.5 micrometers (PM-2.5)		
annual arithmetic mean	15 $\mu m/m^3$	
24-hour average	65 $\mu m/m^3$	
Sulfur dioxide (SO_2)		
annual arithmetic mean	80 $\mu g/m^3$ (0.03 ppm)	
24-hour average	365 $\mu g/m^3$ (0.14 ppm)	300 $\mu g/m^3$
3-hour average	1300 $\mu g/m^3$ (0.50 ppm)	

* The United States of America data's emission standard (EPA, 2000)

** Thailand's emission standard (PDC, 2002)

Table 2.2 Mathematical representations of resistances used in calculation of deposition velocity

Name		Model
Wesely et al.	(1977)	$R_a = (ku_*)^{-1}[ln(z/z_0) - \Psi_c]$
		$R_b = B^{-1}/u_* = \frac{ln(z_o/z_{oc})}{kB^{-1}} = \frac{ln(z_o/z_{oc})}{ku_*}$
	(1989)	$R_c = [1/(R_s + R_m) + 1/R_{lu} + 1/(R_{dc} + R_{cl}) + 1/(R_{ac} + R_{gs})]^{-1}$
		$R_s = R_i\{1 + [200(G + 0.1)^{-1}]^2\}\{400T_s(40 - T_s)]^{-1}\}$
Baldocchi et al.	(1987)	$R_s = g(PAR)g(T)g(D)g(\Psi)D_v/D_i$
		$1/R_l(z) = 1/[R_s s(z) + R_b(z)] + 2/[R_{cut} + R_b(z)]$
		$R_{ss}(z) = R_s(z) + R_{meso}$
	(1988)	$F(z) = -K_s(z)ds(z)/dz$
ADOM		$1/R_c = LAI/R_s + LAI(1-CWC)/R_{cut} + LAI\ \ CWC/R_{cw} + 1/R_g$

where k = the von Karman constant (about 0.41)

u_* = the friction velocity [m sec^{-1}]

z = height [m]

z_{oc} = capture length [m]

Ψ_c = stability correction parameter

B^{-1} = surface transfer function

$= \frac{2(\kappa/D_c)^{2/3}}{k}$ (Brutsaert, 1975)

D_c = diffusion coefficient [m^2 sec^{-1}]

κ = thermal conductivity [W m^{-2} K^{-1}]

G = solar radiation [W m^{-2}]

$g(PAR)$ = photosynthetically active radiation [W m^{-2}]

$g(T)$ = air temperature [^oC]

$g(\Psi)$ = leaf water potential [Mpa]

$g(D)$ = vapor pressure [Pa]

T_s = surface air temperature [^oC]

$F(z)$ = fluxes of pollutant [mol $m^{-2}sec^{-1}$]

$K_s(z)$ = the eddy exchange coefficient at height [m^2 sec^{-1}]

$s(z)$ = concentration of pollutant [mol m^{-3}]

LAI = Leaf Area Index

CWC = Fraction of water area in air

Table 2.3 The value of Sc/Pr of gas (Erisman, 1995)

Component	$(Sc/Pr)^{2/3}$
SO_2	1.44
NO_2	1.30
HNO_3	1.44
H_2O	0.96
O_3	1.30

Chapter 3

Methodology

3.1 Experimental apparatus

The diagrams of the experiment setups for agricultural areas, pine forest, and city area are illustrated in Figs. 3.1, 3.2 and 3.3, respectively. The detail of apparatus is as follows:

3.1.1 Anemometer (R.M. Young company, Model 05103-16B): An anemometer or wind vane is the wind monitor device installing at the top of the measuring tower. It measures both wind speed and direction in horizontal plane (radian from north, clock-wise). The propeller and vertical shaft in the anemometer are made of stainless steel. The rotation of this properller produces an AC sinodal wave signal, which is sent to the recorder every ten seconds.

3.1.2 Dry-wet bulb thermometers: Two sets of dry-wet bulb thermometers with a minimum detection limit of 0.01^{o}C are installed at 2 measuring positions along the height of the measuring tower.

1. For agriculture area, the lower set is 15 cm above canopy and the upper is 2 m from the lower level.
2. For pine forest, the lower and upper are 17 and 21m from ground level.
3. For city area, the lower and upper are 32 and 39m from ground level.

The wet-bulb thermometer is covered with moisturized cloth (Fig.3.4). The results from both dry and wet bulb thermometers, recorded every 10 seconds, are used to calculate the vapor pressure from Eq. 3.1.

$$e_i = e_s - (0.5 \times \frac{1013}{P} \times (T_d - T_w)) \qquad (3.1)$$

where e_i : vapor pressure at position i (mbar), i = 1, 2 (see Fig. 3.1)

e_s : vapor pressure at T_w [mbar]

T_d : dry bulb temperature [^oC]

T_w : wet bulb temperature [^oC]

P : ambient pressure [mbar]

Note that 1013 mbar is equal to 760 mmHg.

$e_s(T_w)$: saturated vapor pressure at T_w [mbar] (Monteith et al. 1995)

3.1.3 Net radiometer (Eko Co. Ltd, model MS-40): The net radiometer is an instrument used to measure net all-wave heat flux from incoming (sun) and outgoing(ground) radiation. The receiving surface of a net radiometer is a black plate with temperature sensors attached both at upper and lower surfaces (Fig. 3.5). This allows the measurement of the temperature difference across the plate which is, in turn, translated into a voltage output. The net radiation readings from the net radiometer are the difference between the total incoming and outgoing radiation fluxes which are proportional to this voltage output from the temperature sensors.

3.1.4 Soil heat flux plates: The soil heat flux plates are made from circle metal with dimenstion of 7 cm (diameter) and 5 mm (thickness). These plates are buried 1-2 cm below the ground level. Fig. 3.5 shows soil heat flux plate with temperature sensors attached at the upper and lower surfaces. The soil heat flux is then calculated from:

$$Q = K \times (\Delta T) \qquad (3.2)$$

K = conductance coefficient of metal [W m^{-2} sec^{-1}]

$\Delta T = T_{top} - T_{bottom}$ difference between temperature at top and bottom surfaces of the plate [^oC]

3.1.5 O_3 analyzer : (Thermo Environmetal Instruments Inc., Model 49C for pine forest. Dasibi Inc., Model DY-1500 for agriculture area, and Monitor Labs Inc., Model

ML9810 for city area): Ozone concentration is measured via an automated procedure based on the chemiluminescent measurement principal. In an short, ambient air sample containing ozone is mixed with ethylene in a reaction chamber and formaldehyde is then formed. This formaldehyde is electronically excited at the detection section of the analyzer during which a light at ~435 nm is emitted. Intensity of this emitted light is proportional to the ozone concentration.

3.1.6 SO_2 analyzer (Thermo Environmetal Instruments Inc., Model 43C for pine forest and Model 43S for agriculture area): The measurement of sulfur dioxide concentration is based on the Pulsed Fluorescent Method. Sulfur dioxide molecules are energized by an ultraviolet pulsed light source. Loss of excess energy results in a fluorescent light emission that is specific to SO_2. The intensity of the emitted light is proportional to the concentration of SO_2 in the sample.

3.1.7 Air Sampling & Computing System: Fig. 3.7 shows a schematic diagram for the air sampling and computing system. The procedure begins with air samples being collected through the sampling tubes at positions 1 or 2 depending on the position of the switching valve. The volume of the gas sample is controlled at a fixed value before entering the analyzer. The output from the analyzer is derected towards the micro-computer to compute simultaneously the pollutant concentration at position 1 and the difference in concentrations between the two positions. The recorder, thereafter, receives and digitally stores these signals. Fig. 3.8 demonstrates the outputs from the analyzer which can be read at the recorder.

3.1.8 Recorder (Eko Co. Ltd, SolacV for pine forest and Solac III for agricuture and city areas): Solac-V and III are digital recorders with 30-channels where the data can be stored at every 1 minute interval.

3.2 Determination of sampling positions

The ideal position of the measuring tower should be at the point where the boundary layer was fully developed. However, this experiment was performed in the laboratory plantation areas, which were limited by the availability of the land in the university. Hence, the tower was setup centrally in the experimental field to minimize effects that might result from the boundary layer. Table 3.1 summarizes the fetch distances and the thickness of boundary layers for each experiment. In the pine forest, the measuring position was selected as to minimize the effect of roads. In the city, however, it was difficult to identify boundary layer due to the uneven terrain, dynamic conditions, construction, household expanding, vehicle increase, industry developing, etc. The availability of the area with autherization in the city was also limiting. This did not allow the selection of the measuring point. Note that the sampling tower was only authorized at the top of JA building and this was assumed to be well inside of the canopy of Tachikawa city.

3.3 Measurement of dry deposition velocity

Measurement of dry deposition velocity (V_d) from three different areas could be performed through a 3 step procedure:

3.3.1 Determination of averaged turbulent gaseous transfer coefficient (m/s)

1. Dry and wet bulb temperatures at both positions 1 and 2 were measured every 30 seconds and the averaged temperature differences over the 30 minute interval were calculated as follows:
   a. $\Delta T_{(d\text{-}w)}$ = difference in dry and wet bulb temperatures at positions 1 and 2
   b. $\Delta T_{(d1\text{-}d2)}$ = difference in dry bulb temperature between positions 1 and 2
2. $\Delta T_{(d\text{-}w)}$ was used to calculate e_1 and e_2 using Eq. 3.1.

3. The value of e_1 and e_2 and $\Delta T_{(d1-d2)}$ were then used to calculate latent heat flux (λ_E) from Eq.2.11 and sensible heat flux (H) from Eq.2.10
4. The net radiation (R_n) and ground heat flux (G) were measured by the net radiometer and the soil heat flux plate, respectively, every 30 seconds and were averaged for a 30 minute time interval.
5. The 30 min-average values of R_n, G, λ_E, and H were used to calculate ϑ_{1-2} using Eq.2.12

3.3.2 Calculations of average C and ΔC

The examples of measurement are

1. In the first 3 minutes (t_0 to t_1 in Fig 3.7), the air sampling & computing system drew a sampling gas from the sampling tube at position 1 to analyzer (Fig.3.6), afterwhich the analyzer sent the results back to the air sampling & computing system. The computing system discarded the results during the first two and a half minutes and only averaged those of the last 30 seconds. This is because the first 2 and a half minutes was considered as a lack time that the recorder needed to adjust between the two readings (from the end of tube to analyzer). This reading, although, was calculated from the last 30 seconds of the interval, was considered as an average C_1 of this 3 minute interval.
2. In the second three muniute interval (t_1 to t_2 in Fig 3.7), the machine switched to draw gas from the position 2 (and automaticaly closed the sampling tube at position 1) and passed it to analyzer. The same procedure as that for the calculation of C_1 was performed for this three minute interval, but this time for average C_2. Then the air sampling & computing system automatically calculated ΔC which was equal to C_1-C_2 and the values of C_1 and ΔC during this 3 minute interval was sent to the recorder.

3. The procedures in 1 and 2 were repeated and the resulting evolutions of C_1 and ΔC were recorded in the recorder. An example of the results is shown in Fig. 3.8. At every 30 minute interval, the program automatically calculated the average C_1 and ΔC for further calculation.

3.3.3 Calculation of dry deposition velocity, V_d

The dry deposition verlocity was simply calculated from Eq.2.13 using information on $\vartheta_{1\text{-}2}$, C_1 and ΔC obtained above.

During field experiment, once the experiment was setup, the data collection and calculation would be performed by the computerized system (Visual basic for Excel, Microsoft) where each record was stored for at most one day.

3.4 Data analysis

There are inaccuracies in data from the recorder due to several reasons such as night data, data during rainy or gusty days, etc. These data should not be included in the consideration of dry deposition velocity. Criteria for the selection of data for further analysis were:

1. The magnitude of R_n must be higher than G, H, and λ_E.
2. The value of $\vartheta_{1\text{-}2}$ must be higher than 0.
3. There must be no rain or snow.
4. The trend of R_n, G, H, λ_E, $\vartheta_{1\text{-}2}$ and ΔC should be smooth (gradual increase or decrease, not dramatic). The example of bad data is shown in Fig 3.9.

3.5 Development of empirical model for V_d

In this work, pre-tests were performed to investigate the effect of various parameters on the dry deposition velocity. The preliminary results showed that the relationship between dry deposition velocity and some meteorological factors are linear. Hence, for the sake of simplicity, the development of dry deposition velocity was based on the multiple linear regression. The steps in developing the mathematical model for dry deposition velocity follow.

3.5.1 Multiple linear regression of dry deposition velocity

The least square method was employed to find the multiple linear regression equation that represented the relationship between meteorological factors and V_d. A general form of this equation is:

$$V_d = a_1 (ws) + a_2 (T) + a_3 (I) + a_4 (g_c) + a_5 \qquad (3.3)$$

where $a_{1\text{-}5}$ are constants obtained from the regression.The SPSS version 10.07 was employed as a means to estimate these constants. Steps involved in SPSS are:

1. Classify all data i.e. V_d, ws, T, I and g_c to each column of SPSS.
2. Use command:
   Analyzer → Regression→ Linear
3. Specify types of parameters in SPSS:
   V_d = independent parameter
   ws, T, I and g_c = dependent parameters

Finally, the coefficients and constant value of the multiple linear regression equation are shown in the ANOVA table.This table also shows the value of accuracy (r^2), deviation (δ) and confidence (α) of the multiple linear regression equation.

3.5.2 Influence of plant physical changes on dry deposition velocity

For the pine forest and city area, Eq. 3.3 provided the final correlation for the dry deposition velocity. This is because the constants in this equation were not affected by the physical factors of the plants in the area. In the pine forest, the number of trees and leaves were not significantly changed with time and the pine trees at the time of the study were already in the maturing stage. Hence, the physical condition was nearly stable and the effect of changes in physical properties of the plants on dry deposition velocity was assumed to be negligible. In the case of city, the percentage of natural green area was extremely small, therefore, it was not necessary to consider the physical change influence ot dry deposition velocity. Hence, $a_{1\text{-}5}$ in Eq. 3.3 for cases of pine forest and city area can be treated as an independent parameter.

In contrast, the physical changes in plant structure are relatively large and can have significant influence on dry deposition velocity in agriculture area. In first step, the net photosynthesis (P_n) was used to seperate the period of growth and death mechanisim. Next step, Leaf Area Index (*LAI*) was used as factor showing the plant growth influence on dry deposition velocity, therefore, *LAI* will be considered in function of $a_{1\text{-}5}$.

In this topic, only the consideration of the influence of *LAI* on a_1 will be given. The influence of *LAI* on other coefficient ($a_{2\text{-}5}$) can be performed in the same way. Steps in constructing the correlation include:

1. The relation between dry deposition velocity and meteorological factors in every stage of plant growth was investigated in the multiple linear regression equation (Eq.3.3) in order to find a_1 at every stage of physical plant growth.

2. The value of a_1 (from first step) are specified to be dependent parameter and averaged *LAI* of each stage of physical plant growth is independent parameter where the relationship between these two quantities are in quadratic form.

3. Finally, a new equation of coefficient of a_1 (and a_2 to a_5) in term of *LAI* can be formulated, which has the general form as follows.

$$a = b_1(LAI)^2 + b_2(LAI) + b_3 \qquad (3.4)$$

3.6 Deviation of model prediction from measurement data

The deviation of model prediction from measurement data was calculated in terms of Eq. 3.5(Chapra et al., 1998)

$$\text{Error} = \frac{|V_d \text{ from model} - V_d \text{ measurement}|}{(|V_d \text{ from model} + V_d \text{ measurement}|)/2} \qquad (3.5)$$

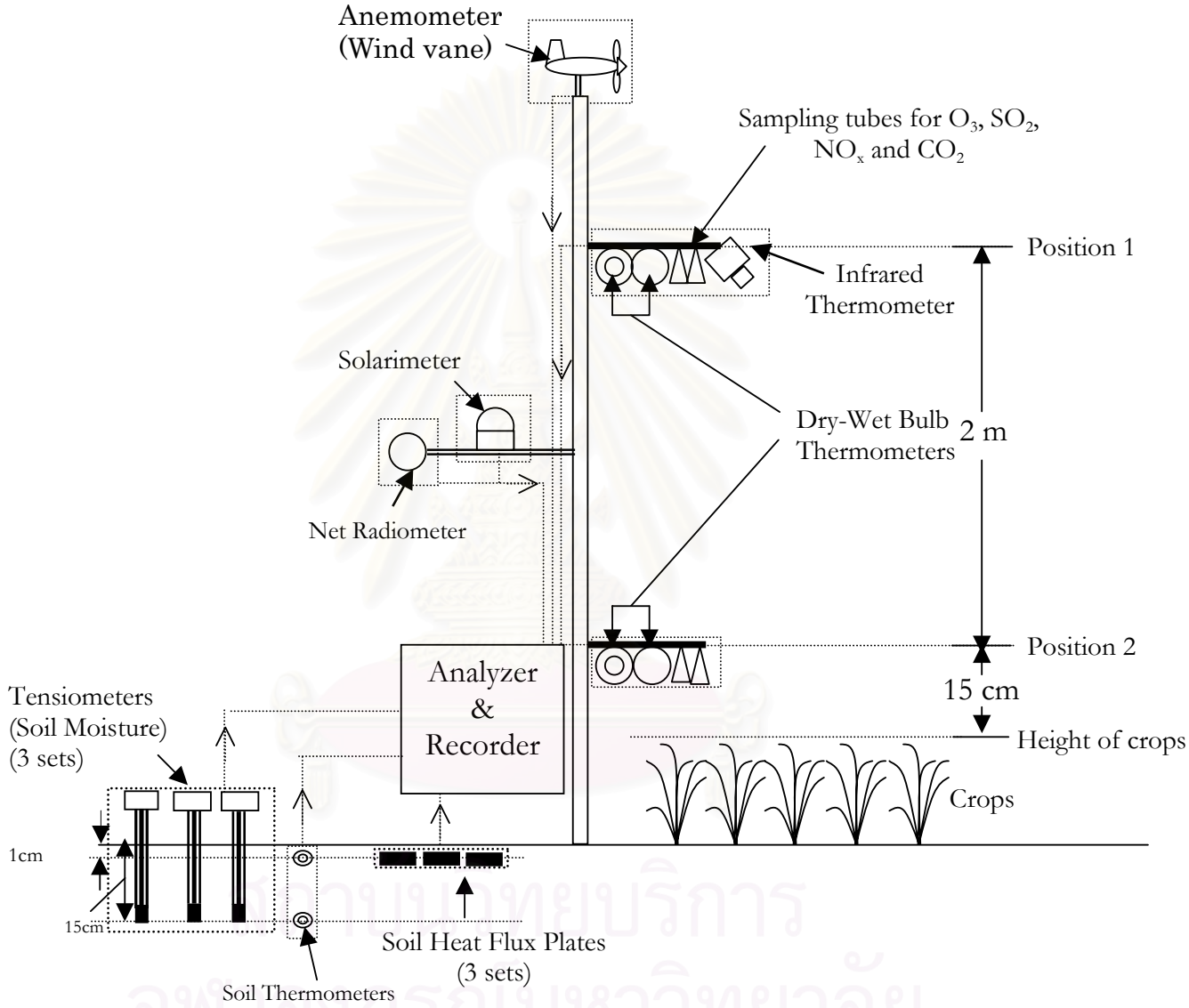

Figure 3.1 Experiment set up in agriculture area

(* Illustrations of equipments are provided in Appendix B)

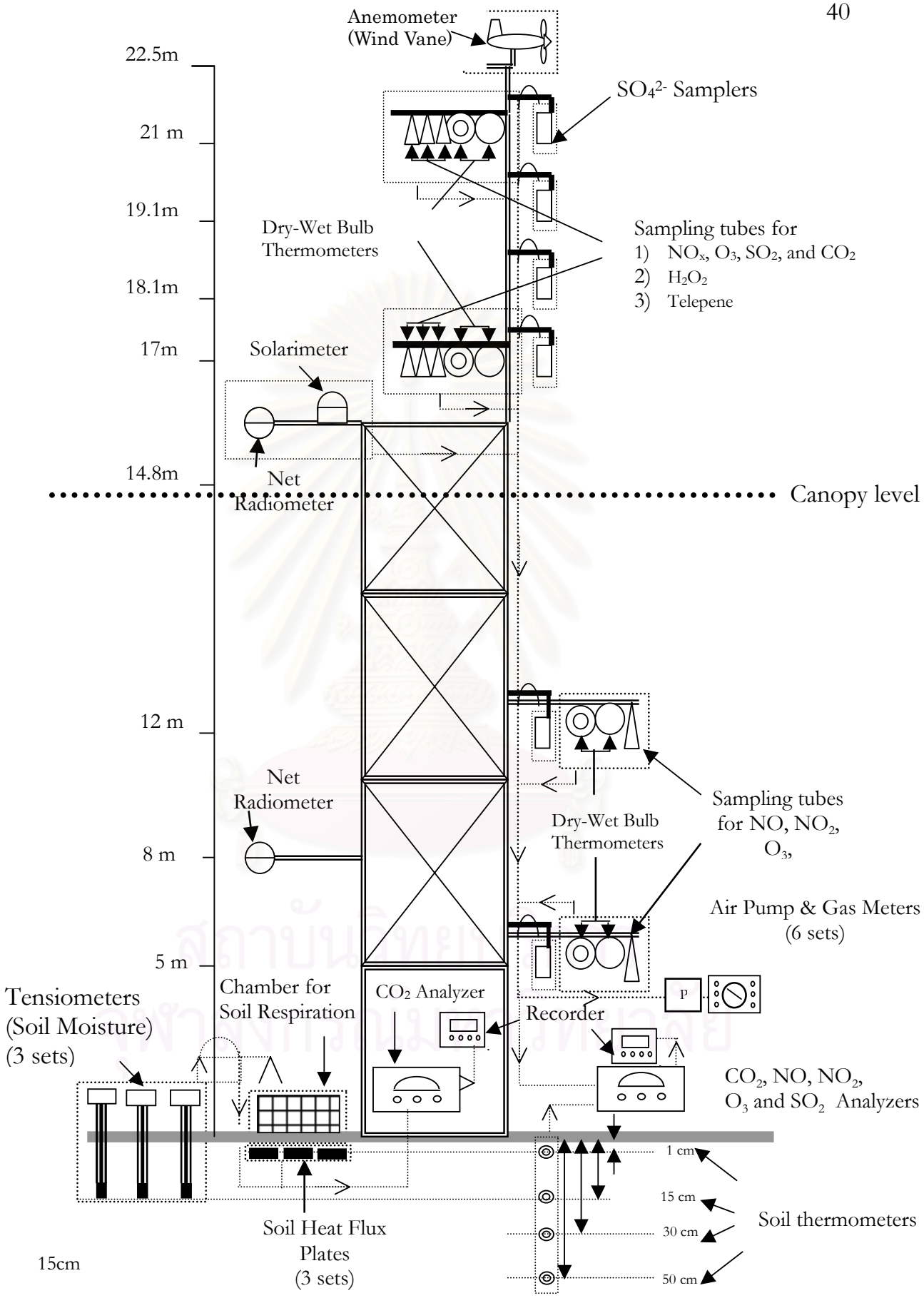

Figure 3.2 Experiment set up in pine forest

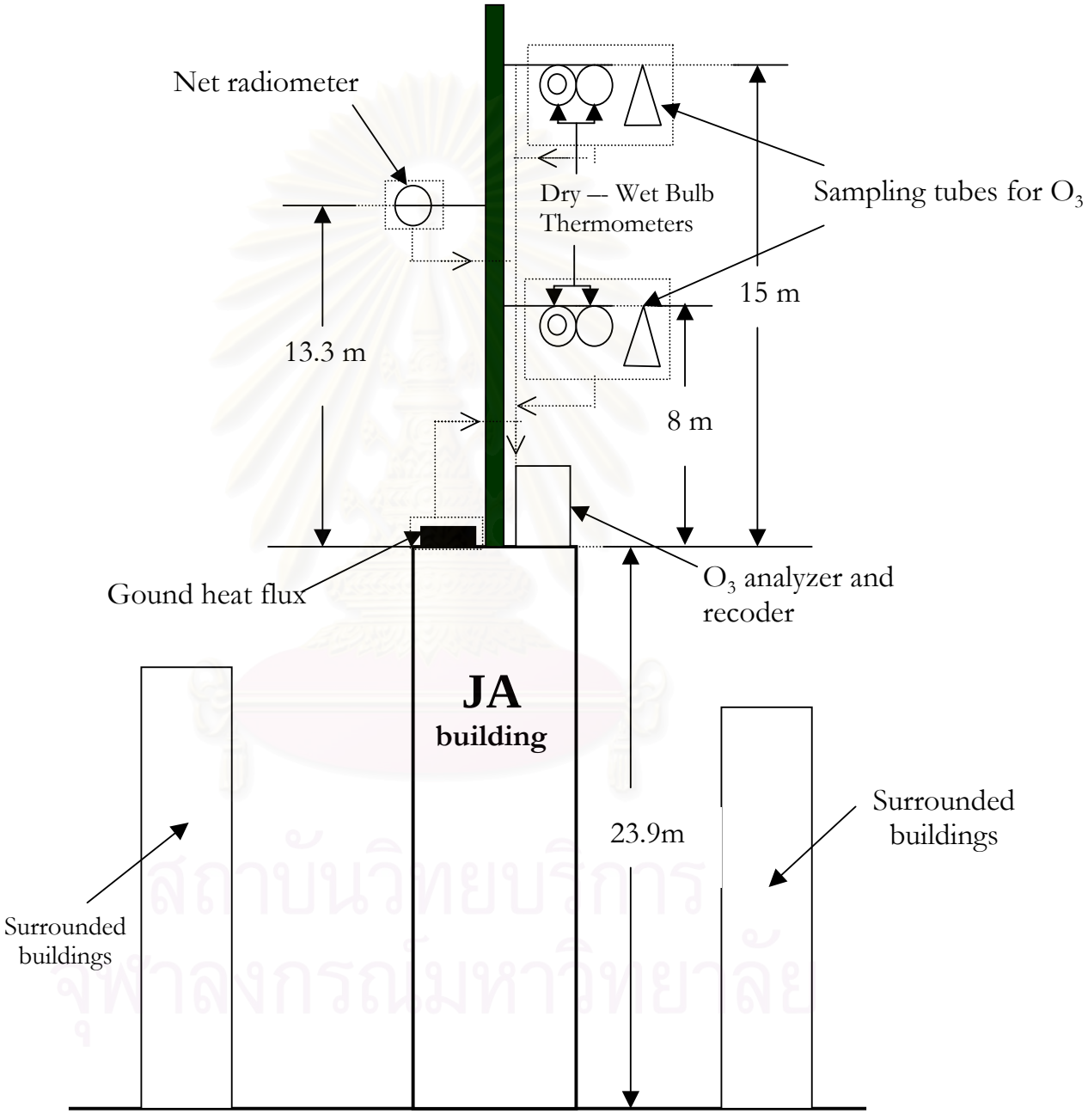

Figure 3.3 Experiment set up in city area

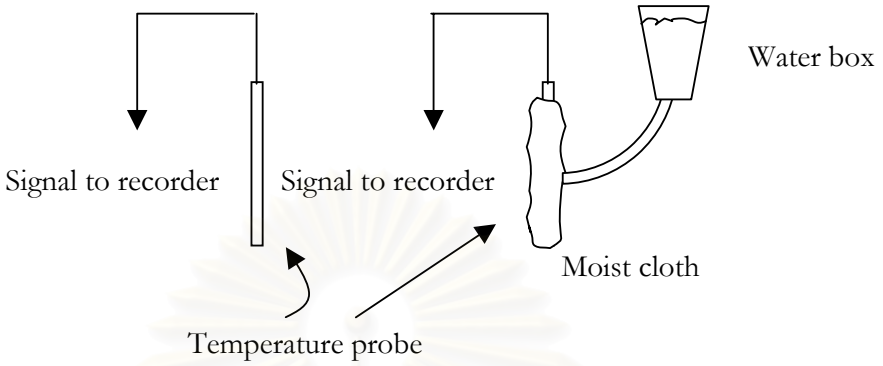

Figure 3.4 Dry and wet bulb tempertature sensors

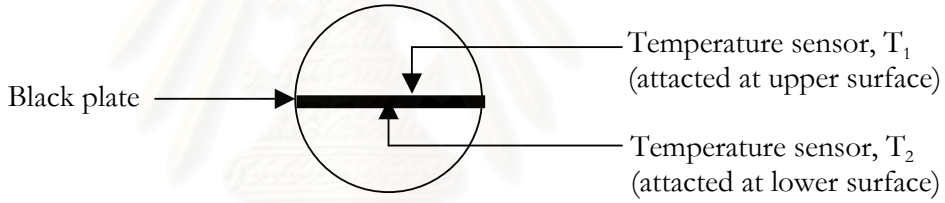

Figure 3.5 Net radiometer

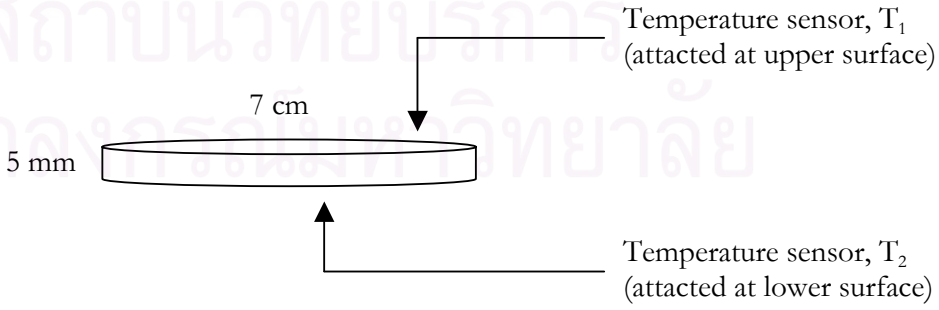

Figure 3.6 Dimension of heat flux plate

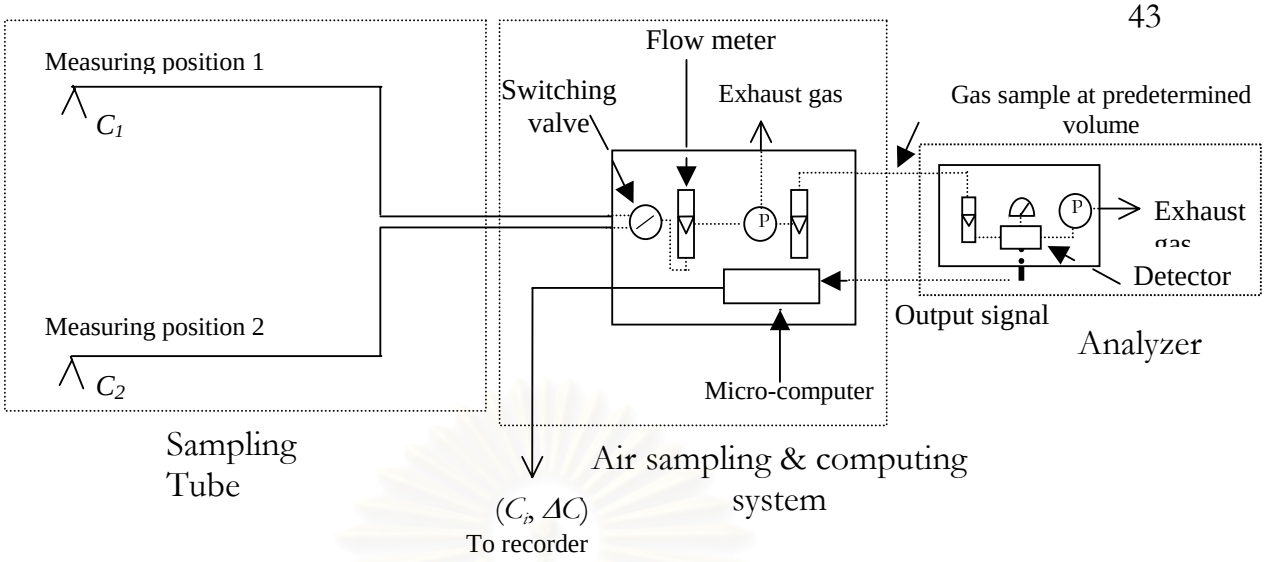

Figure 3.7 Schematic diagram of switching and computing components

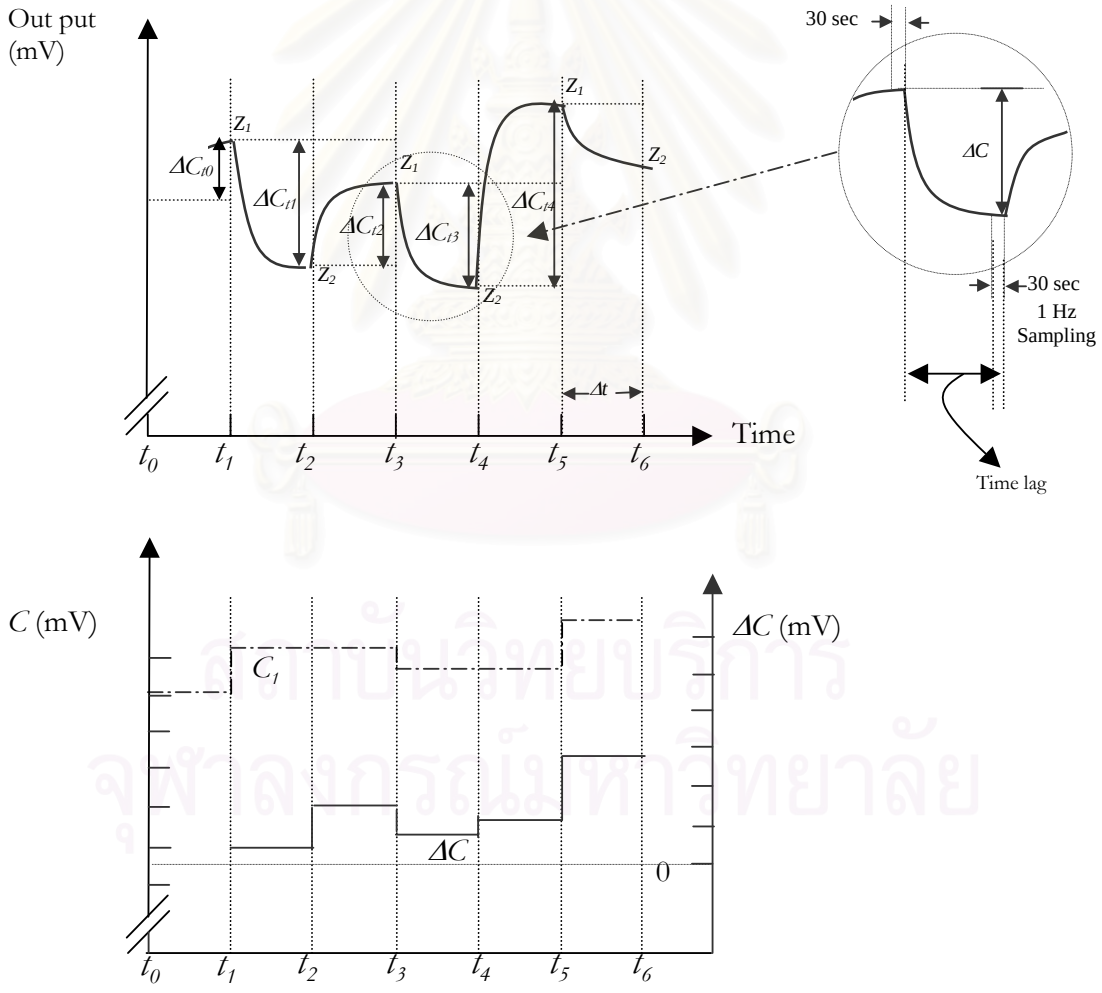

Figure 3.8 Signal from the switching and computing components

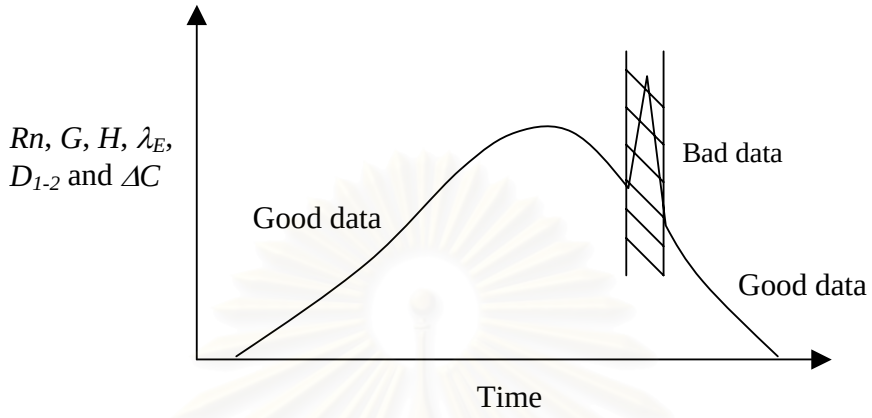

Figure 3.9 Characteristics of *Rn*, *G*, *H*, λ_E, $D_{1\text{-}2}$ and ΔC and time

Table 3.1 Boundary layer thickness and fetch distance in agriculture area, pine forest and city area of this experiment

	Boundary layer (m)	Fetch (m)
Agriculture area	2	200
Pine forest	5	500
City	-	-

Chapter 4

Results & Discussion

4.1 Agriculture area

4.1.1 Growth stages of vegetation

Fig.4.1.1 shows the growth rate of soya bean (bean), corn and wheat, which are represented in terms of the Leaf Area Index (*LAI*) over the various time periods of year. Generally, bean and corn are planted during summer time in Japan which starts from early August till late September. On the other hand, wheat season usually starts from winter (late December) to spring (early June). This figure illustrates that the three species of crops have similar growth characteristics, which can be classified with regards to plant growth into four stages including:

(i) First stage or initial stage where gradual increase in plant growth is observed. In this stage, plants began to structure themselves slowly. It will be shown later that the apparent specific rate of photosynthesis (photosynthetic rate per unit leaf area index) in this stage was the highest.

(ii) Second stage or productive stage, with a sharp increase in plant growth. In this stage, rapid formation of plant structure was observed. Although the overall rate of photosynthesis at this stage was higher than that in the first stage, the later section will demonstrate that the apparent specific rate of photosynthesis was, however, lower than the first stage.

(iii) Third stage or maturing stage, where plant growth became leveled off. During this stage, plants began to form their products.

(iv) Forth stage or senescent stage, with a sharp drop in growth rate. In this stage, the plants changed color from green to gray, which indicated that no more growth

took place and the number of chlorophyll and stomata decreased. Generally, the products were harvested soon after plants entered this stage.

In the following discussion, the behavior of dry deposition velocity in these four stages will be investigated.

4.1.2 Behavior of changes in V_d according to their growth

Figs. 4.1.2-4.1.3 show the averaged daily dry deposition velocities of ozone and sulfur dioxide (the value in this figure is an average of dry deposition velocity measured every 30 minutes daily from 8 am to 5 pm) over the cropping areas at various times of the year. It is mentioned here again that, due to the availability of the equipment, sulfur dioxide could only be measured for the cases of bean and wheat. All curves in these two figures show that the trajectories of the deposition velocities followed the trends of the LAI (in Fig. 4.1.1) quite closely. This is to say that the dry deposition velocities of both ozone and sulfur dioxide gradually increased in first stage of growth and sharply increased in the second stage. The maximum point was observed in the third stage followed by a dramatic fall in the forth stage.

This phenomenon took place due to both an abilily of each gas in depositing onto each surface and respiratory/photosynthesis activities of plants. Plants need to absorb necessary gases, e.g. N_2, CO_2, and etc, and transform them to constitute their structural integrity or products, and at the same time exhale metabolic gases out through a respiratory mechanism. The net uptake rate of gas in the stomata is usually called “net photosynthesis”. The intake of gases through stomata is by no means a selective process, which implies that plants have to absorb all gases from the air. Therefore, ozone and sulfur dioxide, if present in the atmosphere, also are absorbed along with other gas (positive deposition). The quantity of these gases being absorped into plants depends significantly on the photosynthetic activity of plants.

Fig.4.1.4 demonstrates the net photosynthesis at various growth stages of plants. This shows that the net photosynthesis increased monotonically over the first to third

stages. From previous discussion, it was known that all of these stages were growth associated, and therefore plants needed to absorb necessary gas to construct their structures and products. An increase in the net photosynthesis means that the inhalation rate of plants increased throughout these growth stages. However, as soon as the plants entered their senescent stage, the gas requirement declined as reflected in the drop in the photosynthetic rate. Hence, it was concluded that plant activities were classified into two mechanisms: growth (from first to third stages) and senescence (forth stage).

Figs 4.1.5-4.1.7 indicate the apparent specific rate of photosynthesis (with respect to one unit of LAI) in each growth stage of bean, corn and wheat, respectively. For bean and corn (Figs. 4.1.5-4.1.6), it was observed that this apparent specific rate of photosynthesis decreased continuously throughout the life of the plant. This indicated that as the plants grew, they needed less photosynthetic products per unit area of their leaves. It is noted that the net photosynthetic rate was much higher in the second and third stages of growth, although the apparent specific photosynthesis was lower. The reason for this will be discussed in the following paragraph. In addition, it was found that the net photosynthesis in the forth stage was not zero, even though decline in the growth rate was observed where the number of stomata and chlorophyll decreased. This small photosynthesis was thought to occur because there were still some chlorophyll and stomata which remained active.

Turning back to the point where the net photosynthesis in the second and third stages were higher than that in the first stage despite a lower apparent specific photosynthetic rate, it was worth noting that plants in the second and third stages had a large quantity of leaves. Hence, it was highly probable that some of the leaves were not exposed to sunlight at adequate intensity (due to shading effect) and therefore could not carry out photosynthesis at its maximum or high rate. In other words, only leaves at the top layers would be exposed to sunlight at high intensity and could carry out more photosynthesis than leaves underneath them. This was reflected in the low apparent specific photosynthetic rate.

In case of wheat (Fig 4.1.7), the result was not as clear as the others. The net apparent specific photosynthetic rate decreased dramatically in the first stage of growth and stayed rather constant at low level in the second stage. However, this net apparent specific photosynthetic rate rose again in the third stage (the maturing stage) to the level similar to the first stage before dropping slowly through the forth stage. The reasons behind this incidence were still unclear but one of the reasons might be because wheat was planted and grown during winter and spring seasons where a change in weather conditions between winter and spring was rather extreme (from warm to cold weather). Wheat, therefore, had to adjust its growth to the weather resulting in the hiccup in the apparent specific rate of photosynthesis. But bean and corn were planted only in summer where the effect of climate change was not extream.

This section demonstrates the existence of the growth and senescent mechanisms during the cropping period of various plants. To further develop a suitable model for dry deposition velocity, these two mechanisms must be evaluated separately. This research shall focus only on the growth mechanism because most of the plant activities took place during this phase, which could significantly affect the dry deposition of pollutants in a much greater extent than the senescent period. In addition, once the plants entered their senescent stage, more often, they would be subject to various human activities such as harvesting. This could seriously affect the plants metabolism and also their ability to absorb gaseous pollutants, and it was considered appropriate to discard this stage from further consideration in this work.

4.1.3 Effects of metorological factors on dry deposition velocity

The relation between dry deposition velocity and meteorological factors; wind speed, temperature, solar radiation and canopy conductance are shown in Figs. 4.1.8-4.1.11. It can be observed from these figures that the relationship pattern between meteorological factors and the dry deposition velocity for various different crops were similar and will be explained as follows:

Wind speed

The effect of wind speed on dry deposition velocities of ozone and sulfur dioxide was illustrated in Figs.4.1.8a and 4.1.8b, respectively. Large scatters of deposition velocities of both pollutants were observed and it was concluded that the effect of wind speed on the dry deposition velocity of both ozone and sulfur dioxide at all growth stages of the plants could not be generalized in a simple mathematical form.

Temperature

The effect of temperature on the dry deposition velocities of both pollutants was found to be similar to the effect of wind speed as illustrated in Figs.4.1.9a and 4.1.9b. In these figures, it was seen that the dry deposition velocity varied widely even with a very small range of temperature. Therefore it was concluded, again, that the effect from the change of temperature on V_d could not be characterized.

Solar radiation

Fig 4.1.10 illustrates how the dry deposition velocity was affected by solar radiation. It was found that the relationships between ozone and sulfur dioxide could be characterized in a form of logarithmic curves. At a low range of solar radiation intensity, the dry deposition velocity sharply increased with solar radiation. This was because the increase in solar radiation in this range caused plants stomata to open more widely. However, the stomata soon reached its maximum size and the net photosynthesis could no longer increase with the size of stomata. This meant that the uptake rate of pollutant through the stomata also reached its maximum. This was reflected in a response from the measurement where, at adequately high solar radiation, the dry deposition velocity reached a plateau.

Canopy conductance

The effect of canopy conductance to the dry deposition velocity was shown in Fig 4.1.11 where the following points can be summarized:

1) The canopy conductance increased as plants grew from first to third stages. This was due to the increase in the number of stomata in plants and also the activity of plants in developing their structures and products, which needed higher absorbtion of carbon from the atmosphere.

2) Linear relationship between the dry deposition velocity and canopy conductance could be formulated. This was because the increase in canony conductance would increase the transfer of molecules from air to plants inside the canopy. This increased the ability of gas in depositing inside the canopy.

From the aforementioned description, it was concluded that only solar radiation and canopy conductance had significant effects on the dry deposition velocity. These findings will be useful for the development of mathematical model to describe the characteristics of the dry deposition velocity of pollutants.

4.1.4 Development of an empirical model for the dry deposition velocity

As stated in Chapter 2, nitric oxide (NO) could undergo reaction with hydrocarbon (HC) from which ozone was produced. However, the volume of HC or volatile organic compounds (VOCs) released from the plants and from other sources in agricultural area was assumed to be extremely low (data from past records at the fieldwork at the Tokyo University of Agriculture and Technology, but no written evidence was available for reference at the time this thesis was written). To put it more simply, the amount of VOC released from the reaction between the measurement positions 1 and 2 in Fig. 3.1 will be assumed neglegible and will not be considered in the following discussion.

The relationships between dry deposition velocity, V_d, and light intensity, I, and canopy conductance, g_c, for each growth stage were correlated in a form of multiple linear regression equation (Eq.4.1). The SPSS program version 10.0.7 was employed as a tool for computing the values of coefficients and the result are summarized below (for the case of bean cropping).

$$V_d = a_1 \ln(I) + a_2 g_c + a_3 \qquad (4.1)$$

	a_1	a_2	a_3
1st stage	1.37	-0.29	-5.2
2nd stage	0.74	0.95	-2.67
3rd stage	0.25	1.45	-0.4

Note The complete set of these coefficients for all types of vegetations examined in this work was shown in Table 4.1.

These coefficients a_1, a_2 and a_3 were also dependent on LAI and it can be shown that the relationships between these parameters are quadratic in nature (see Figs 4.1.12-4.1.17), that is:

$$a = b_1(\mathrm{LAI})^2 + b_2(\mathrm{LAI}) + b_3 \qquad (4.2)$$

where

	b_1	b_2	b_3
a_1	0.1	-0.2	2
a_2	-0.1	0.8	-0.86
a_3	-0.05	1.3	-6.2

The complete list of these coefficients are available in Tables 4.2 and 4.3.

4.1.5 Estimates from the Wesely model and its associated error

Figs 4.1.18-4.1.22 show the prediction from the Wesely model compared with the actual dry deposition velocities of ozone and sulfur dioxide from first to third stages at every 30-minute period starting from 8 am to 5 pm. It was clear that the Wesely model consistently under-estimated the dry deposition velocity at all cases.

Fundamentally, the Wesely model assumes that the atmosphere above the ground which have effects on the dry deposition velocity comprises three layers, and each of these layers imposes a resistance to the movement of gas pollutants. These resistances

include: aerodynamic (the top layer), quasi-laminar (the middle layer), and the canopy (the lowest) resistances. Generally, the canopy resistance was found to be the greatest among the three, followed by the atmospheric resistance, and the quasi-laminar being the least.

An analysis was carried out to evaluate the appropriateness of the values for these resistances. Firstly, each of the resistances was made zero and the overall resistance was re-calculated. The results illustrated that, even when any of these three resistances was made zero, the Wesely model still under-estimated the deposition velocity. Further analysis was carried out in an attempt to find weighing factors or correlation coefficients for each of the resistances according to the following equation:

$$V_d = 1/ (\alpha r_a + \beta r_b + \gamma r_c) \qquad (4.3)$$

Hereafter Eq. 4.3 will be called the modified Wesely model. The values of α, β and γ for all types of vegetations were calculated subject to the objective of minimizing the error or difference between the prediction and measurement. The results are shown in the following tabulation.

		α	β	γ	%error	%error (α=β=γ=1)
O_3	- bean	0.02	0.01	0.33	33.60	124.37
	- corn	0.01	0.01	0.11	59.81	142.20
	- wheat	0.01	2.95	0.11	64.24	98.17
SO_2	- bean	0.33	0.01	0.22	44.07	120.43
	- wheat	0.01	0.01	0.41	80.91	115.50

In this tabulation, %error in the penultimate column represents the errors from the modified Wesely model (Eq. 4.3) which were obtained with the values of α, β, and γ in the same row. The last column is the errors from the conventional Wesely model with all coefficients equal to unity (α=β=γ=1). It is obvious that the modified Wesely model provided a significantly better prediction of V_d than the conventional model in

every case. These values of coefficients were not found, or at least not yet, to have physical meanings in the prediction of V_d. And in this work, these values were obtained from the simple optimization module provided in Excel, Microsoft Office 97. The fact that each of the coefficients found in the above tabulation did not hold the same value for different type of vegetation triggers some additional thoughts. These are:

1. Different type of vegetation influenced the atmospheric resistance differently. This might be logical for the canopy resistance which coverred the area of vegetations, but might not be so for the other top two atmospheric layers.
2. Patterns of meteorological conditions during one particular measurement differred from the others.

Although this is a very interesting and challenging topic which should be carried out to complete this piece of knowledge, the limitation in time disallows further experiment which, in some way, is out of scope of this work.

4.1.6 Comparison of errors between the Empirical and Wesely models

The results from the two models were compared along with the experimental data for verification purposes. The errors from the empirical, Wesely, and modified Wesely in estimating the dry deposition velocity from first to third growth-stages were compared in Table 4.4. It was clear that the error from the conventional Wesely model was highest in every case. In comparing these errors, the model that gave the lowest value of error is considered to be the most accurate one, which, in this case, was the empirical type.

Figs 4.1.23-4.1.27 show the comparative plots of dry deposition velocity from measurement and simulation during the growth stages (from first to third stages). It was clear that the empirical model provided a much better accurate prediction than the conventional Wesely model that constantly under-estimated the deposition velocity.

The modified Wesely model could significantly improve the accuracy of the conventional model, but the quality of the prediction was still not quite as good as that of the empirical model. It is noted that the modified Wesely model gave the best prediction for the case of ozone dry deposition in the bean cropping area. However, with our current knowledge of this model, this had very little meaning in terms of the overall model performance as it failed to provide the same level of accuracy for other cases.

4.1.7 Concluding remarks

The overall performance of the empirical model was found to be most appreciable among the three types of models investigated above. The Wesely model and its modified form, although included physical parameters in the consideration of dry deposition velocity, failed to accommodate the growth rate of plants into the calculation which might be the main reason for its inaccuracy. The empirical model, on the other hand, did not represent the logistic mechanism of how the atmosphere exerted resistances to the deposition of gaseous pollutant, but did cover various aspects of meteorological factors which might influence the deposition velocity. The growth of plant was also included in the model in terms of leaf area index (*LAI*) to represent any possible effect this might have on the deposition velocity.

However, the absolute error from empirical model was still high (> 30%) and the use of this model was only limited to the specific area. To apply this model for other area of interest, one needs to carry out experimental work to identify the effect of meteorological conditions on the deposition velocity which might be costly and time-consuming.

4.2 Pine Forest

4.2.1 Characteristics of dry deposition velocity

Ozone

The experiment carried out in the pine forest during May-September 2000 indicated that the hourly-average dry deposition velocity of ozone for each month was mostly positive (Fig 4.2.1). This meant that, on the usual basis, ozone was deposited onto the earth surface. Some negative deposition or emission was also evidenced, although in a much lesser extent. The dry deposition velocity of ozone was the highest in June. During summer time, i.e. June-September, the dry deposition velocities in the morning were higher than those in the afternoon. The situation was opposite in May where the morning deposition velocity was lower than the afternoon. The reason for this phenomenon will be discussed later in Section 4.2.3.

Sulfur dioxide

Fig 4.2.2 shows the hourly-average dry deposition velocity from the measurement in the pine forest during May-September 2000 which indicated that, most of the time, the deposition velocity was negative which implied that SO_2 was released or emitted from the forest. The maximum emission took place in May. Section 4.2.3 explains this finding.

4.2.2 Effects of meteorological factors on dry deposition velocity

Wind speed & Temperature

Fig 4.2.3 indicates that the effects of windspeed and temperature on the dry deposition velocity of ozone and sulfur dioxide were simply too complicated to be expressed in a general mathematical correlation. This result was similar to the results obtained from the study in agriculture areas.

Solar radiation

In contrast to the results obtained in the agricultural area, Fig 4.2.4 demonstrates a scattering relationship between solar radiation, *I*, and dry deposition velocity for both ozone and sulfur dioxide (where it was shown earlier in the agriculture case that this relationship exhibits logarithmic nature). The cause of this was believed to be the chemical reaction occurring inside the pine forest as will be illustrated later on.

Canopy conductance

The effect of canopy conductance, g_c, on the dry deposition velocity of ozone and sulfur dioxide was found to be rather complicated. In June and July, a linear relation between these two quantities could be formulated (Fig 4.2.4), but in other months, scattering data prevented a solid conclusion on the type of relationship between them. These complex phenomena might have been a result of the climate change in Japan. There were few occasions where considerable changes in climate were extreme, i.e. spring to summer in May, and summer to autumn in September. In addition, August was a typhoon month where the weather changed drastically all the time. And during these periods of changes, it was difficult to obtain good data. In June and July which was the mid of summer on the other hand, the climate was much more stable, and therefore it was easier to have good measurement of dry deposition velocity.

4.2.3 Possible mechanisms of gaseous emission and deposition in pine forests

One of the unique properties of pine trees was the ability to release hydrocarbon e.g. Volatile Organic Compound (VOC) in large amount (this was not found in agriculture area) (Smith, 1981, Isidorov, et al. 1985, and Lamb, et al. 1985). Consequently, the reaction between NO and HC must be considered as a significant source of ozone. Moreover, the soil in pine forest area also released dimethyl sulfide (DMS), hydrogen sulfide (H_2S) and oxide of nitrogen, e.g. NO, NO_2 (nitrogen dioxide), N_2O (nitrous oxide) which were produced from microbial activities in the soil itself. This phenomenon happened because this area was naturally accumulated

by plants remains, and far from human invasion, therefore, the soil was in good conditions for bacterial or microbial growth. Conversely, the soil in agriculture area was usually adjusted for farming which disturbed the microorganism, and hence, the quantity of gas released from agricultural soil was in a significantly lower extent.

The following subsections will attempt to provide possible mechanism, which affect the quantities of O_3 and SO_2 in the pine forest.

Ozone

Generally, ozone can be produced from the transformation of NO_2 to NO but in the case of pine forests, ozone can be produced by the reaction of hydrocarbon from pine tree with NO (Fig.4.2.5). Most of hydrocarbons (VOCs) released by pine trees were terpene such as α-pinene, campehene, myrcene, etc. Figs 4.2.6 and 4.2.7 show the amount and composition of terpene which was released by pine forest at various heights of the pine forest in the morning and afternoon of Sep 7, 2001. One of the important properties of terpene is its ability to undergo chemical reactions inside the canopy. There are 2 types of reactions which might affect ozone quantity:

1. Ozone produced by the terpene reaction:

   Under favorable conditions, e.g. enough radiation energy from the Sun, terpene can react with NO, O_2 and produce NO_2 (Hill, 1971) and O_3 (Peñuelas et al., 1999 and Lindskog et al., 1993). NO was commonly known to derive from NO_2 decomposition, anaerobic metabolism (William et al., 1991) and could also be transported in from remote areas such as industry, city, vehicles, volcano, etc.

   This reason might well explain the declination of the dry deposition velocity of ozone in afternoon. Generally, the afternoon temperature is higher than the morning since the heat from solar radiation is accumulated in the forest. This was reflected in the time-plot of temperature at the top of canopy in the pine forest in Fig 4.2.8 where it was shown that gradual increase in the temperature

in the pine forest was observed. This high temperature could accelerate chemical reaction between terpene and NO the inside canopy and resulted in the decrease of terpene concentration in afternoon (Figs.4.2.6 and 4.2.7), and the increase in ozone concentration inside canopy. This implied a reduction in the dry deposition velocity of ozone. In addition, there might be times that ozone was produced in large quantity and that the dry deposition velocity of ozone in the pine forest was sometimes found to be negative (positive emission to atmosphere, Fig 4.2.1). In May, the result was opposite where the morning deposition velocity was lower than the afternoon. These causes of phenomenon were still unknown but it might come from the changes in the terpene rate from pine trees during season change (spring to summer). However, the annual emission of terpene in pine trees was not measured, and hence, this phenonenon was still to be proven experimentally.

2. Ozone used in terpene reaction:

Fig 4.2.5 also illustrated that ozone could react with terpene, and resulted in hydrogen peroxide (H_2O_2) and methyl hydrogen peroxide (CH_3OOH, MHP) (William, H.S. 1981). These 2 gases affected the sulfur dioxide emission rate as will be discussed in the next part. However, the influence of this reaction to the quantity of ozone could still not be identified due to the lack of the measurement data of H_2O_2 and MHP.

Sulfur dioxide

Fig.4.2.5 shows the pathway of chemical reaction involved with the generation and reaction of sulfur dioxide inside the pine forest. This pathway could be divided into two steps. The first step is the generation of H_2S and DMS into the atmosphere by sulfate-consuming bacteria in the soil. (Freyney, 1997 and Henk et al., 2000) The next step was for the subsequent reaction (oxidation) of H_2S and DMS to sulfur dioxide.

After sulfur dioxide was produced, it followed the two pathways including:

1. Emission to the atmosphere (no further chemical reaction).

2. Reaction with H_2O to produce H_2SO_4 or with H_2O_2 and MHP to produce sulfate (William, H.S. 1981).

If sulfur dioxide followed the second pathway, the resulting sulfate would fall into the ground surface and became nutrients for bacteria (which completes the natural sulfur cycle). Statistically, this proposed mechanism was still not proven due to the lack of measurement information of H_2SO_4, H_2O_2 and MHP.

4.2.4 Development of an empirical model for the dry deposition velocity

Section 4.2.2 suggests that no relationships between meteorological factors and dry deposition velocity could be realised in the pine forest. This makes the development of multiple linear regression not possible by the least square method. Hence, it is concluded here that, over the scope of this work, no empirical models could accurately explain the behavior of dry deposition velocity in the pine forest. This was thought to be due to the highly complex interaction between various chemical components as explained in Section 4.2.3.

In the next section, the Wesley model and its modification will be investigated for their suitability in estimating deposition velocity in the pine forest.

4.2.5 The Wesely and the modified Wesely models

Prediction of dry deposition velocity of Ozone

Fig 4.2.9 illustrates that the conventional Wesely model could not provide an accurate prediction of deposition velocity of ozone where most of the simulation results were lower than the measurement in morning but in the afternoon, the predictions were over-estimated. The percentage of error varied from 50% to as large as 343%. Similar procedure as explained in Section 4.1.5 was applied here to develop

a modified Wesely model with correlation coefficient, α, β and γ, and the results are summarized as follows:

Month	α	β	γ	%error	%error (α=β=γ=1)	%error (α=β= 0.01, γ =0.8)
May	3.06	3.7	0.37	146.46	174	161.68
June	0.01	0.01	0.5	34.11	77	48.44
July	0.01	0.01	0.8	39.9	50.66	39.9
August	0.01	0.01	1.12	308.37	343.06	332.9
September	0.01	0.01	0.69	118.04	130.6	118.73

It can be seen that the modified Wesely model only gave a slightly better estimates of ozone dry deposition velocity. The percentage errors in the fifth and sixth columns represent the errors from the modified Wesely and conventional Wesely models, respectively. And the last column show the error from the modified Wesely model with the best common correlation coefficients, which, in this case, were found to be 0.01, 0.01 and 0.8 for α, β and γ, respectively. Although the errors in June and July were relatively low, the average errors in other months were quite high, and in some case, the error was still as large as some 300%. This large error might be due to the influence of weather changes between seasons, i.e. spring to summer in May, typhoon season in August and summer to autumn in September, which affected the quantity of VOC emission and its chemical reaction in the pine forest.

Sulfur dioxide

Fig 4.2.10 reveals that sulfur dioxide was actually being emitted from the pine forest, instead of being deposited onto the surface. This negative deposition was believed to be a result of the complex reactions taking place inside the pine forest. However, it was not explanable using the Wesely model.

4.2.6 Concluding remarks

The interactions between various parameters in the pine forest are extremely complex such that no simple correlation could be formulated to explain the dry deposition velocity. Results from this work indicated that the chosen measured parameters were not enough to explain this complexity. As a results, an empirical model could not be constructed. However, this work proposed some possible physical/chemical reactions that might have taken place in the pine forest without the attempt to prove it experimentally. Future research in this area should be directed to investigate this aspect further.

Nevertheless, despite the lack of consideration on the effect of chemical reactions in the system, the Wesely and modified Wesely models were found to provide some good estimates during some periods of the year where there was no extreme changes in atmospheric conditions.

4.3 City area

4.3.1 Experimental data on ozone dry deposition velocity and effects of meteorological factors

Fig 4.3.1 shows the time variation of the dry deposition velocity of ozone in Tachikawa. It can be seen that the dry deposition of ozone was highest in October and lowest in November, whilst the deposition rates in August and September were similar to each other. Investigation reveals high scattering data between the dry deposition velocity of ozone and the meteorological factors such as wind speed, temperature, and solar radiation which suggested independent relationship (Fig 4.3.2).

Hence, the least square method could not be applied to analyze the multiple linear regression between these quantities. Moreover, in city area, the quantity of pollutants could well be derived from various human activities, transportation, and industries, and this might significantly affect the dry deposition velocity and chemical reaction of pollutants in the air. Unfortunately, the in-dept investigation of this area was not possible during the time of this work due to the difficulties in obtaining data particularly emission rates from industries, transportation, etc.

4.3.2 Estimates of ozone dry deposition velocity from the Wesely and modified Wesely models

The simulation results from the conventional and modified Wesely models are shown in Fig 4.3.3. The conventional Wesely model consistently over-estimated the dry deposition velocity and the percentage of error varied from 60 to 190%. The modified Wesely model was carried out with the correlation coefficients reported in the following tabulations (see Sections 4.1.5 and 4.2.5 for details of this model):

Month	α	β	γ	%error	%error (α=β=γ=1)	%error (α=β= 0.01, γ=0.34)
August	0.01	0.01	0.34	30.46	100.29	30.46
September	0.01	0.01	0.30	49.12	180.29	50.1
October	0.01	0.01	0.41	53.43	182.51	54.23
November	4.45	5.3	0.01	42.25	61.54	181.32

It was clear that the modified provided a significantly better prediction of dry deposition velocity than the conventional model in every case. For city area, the appropriate, common, correlation coefficients were found to be 0.01, 0.01 and 0.34 for α, β and γ, respectively. However, the errors in November were still high about 180%, this large error might come from the change of the weather change during autumn to winter, and the changes in the human behavior in using more heaters, which might affect the deposition mechanisms of pollutants in the city area.

4.3.3 Causes of errors from the model predictions

The cause of scattering data in the city may come from

1. Diversity of land uses in the city area

The Wesely model does not provide a method to consider the fact that land uses in the city area was much more complicated than those in the agriculture or forests. For example, some areas are covered with high buildings, some with roads, parks, etc. It is very likely that this diversity in land uses will have significant influence on the ability in deposition velocity of pollutants.

2. Human Activity

Human activities in the city were also likely to affect the dry deposition velocity of pollutants. Examples include the uses of vehicles, heaters, and even human respiration. These mechanisms are believed to change the speed and direction of wind

and temperature around surface of city area, and also the dry deposition velocity. In addition, these human activities are highly unpredictable and it is a very difficult task to incorporate into a simple mathematical model.

4.3.4 Concluding remarks

Even though there are still unknown factors in the city area, the Wesely model was surprisingly found to give a relatively good estimate for dry deposition velocity. And with appropriate correlation coefficients, the modified Wesely model could rectify the accuracy of the model. The findings from this work suggest that these correlation coefficients be unique for one particular climatic condition.

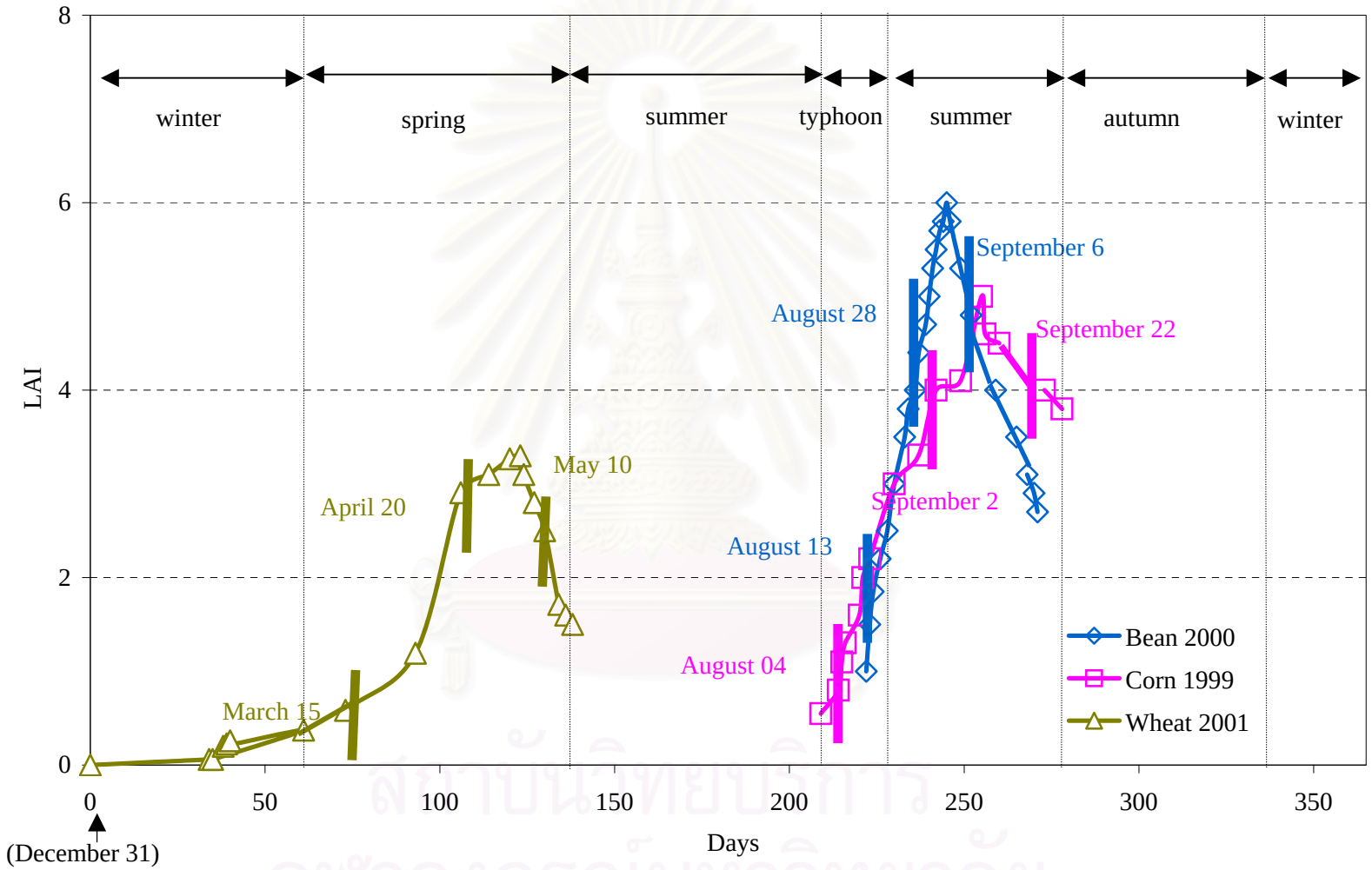

Figure 4.1.1 Changes in LAI over various time periods

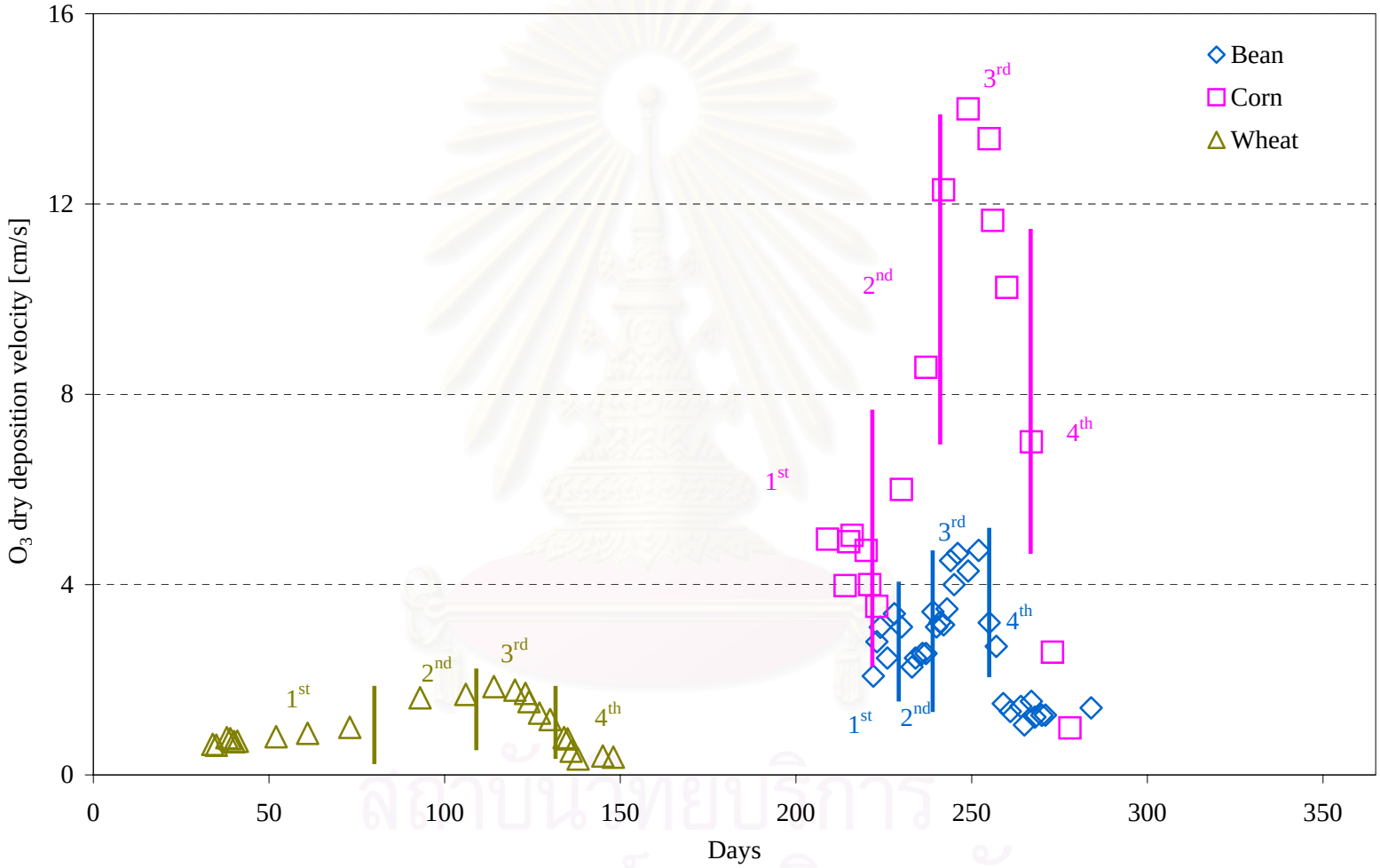

Figure 4.1.2 Dry deposition velocity of O_3 at various time periods

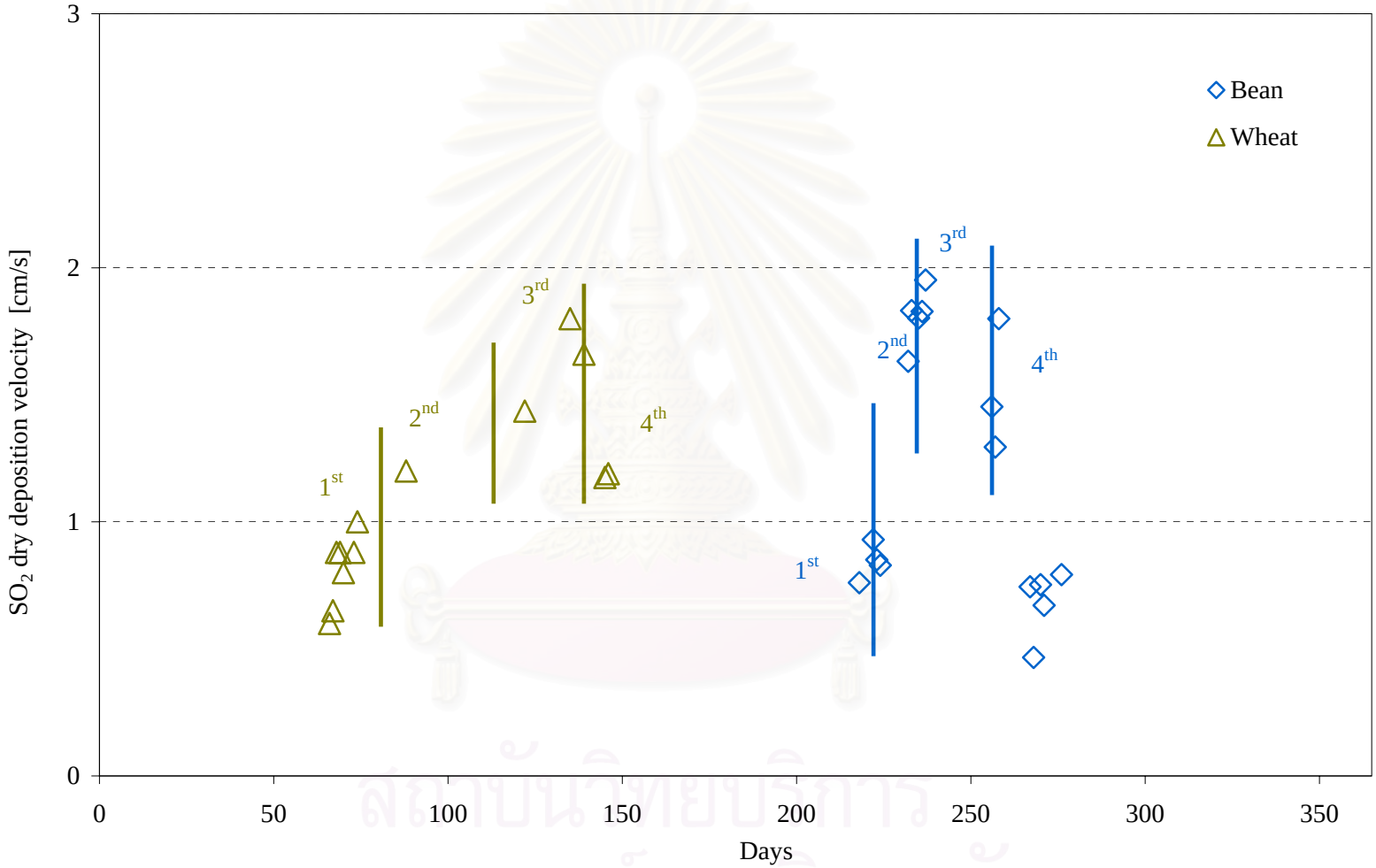

Figure 4.1.3 Dry deposition velocity of SO_2 at various time periods

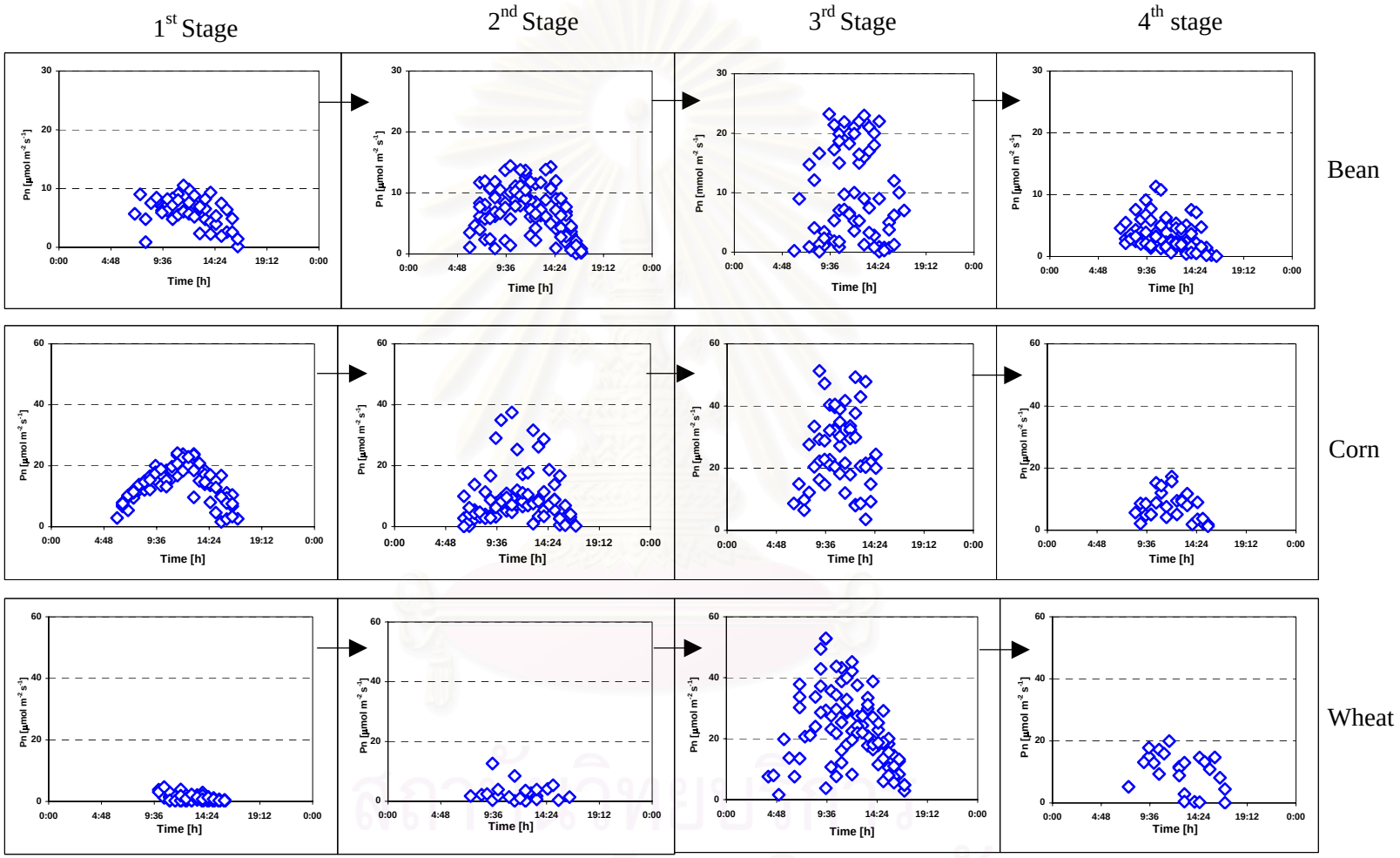

Figure 4.1.4 Net photosynthetic activity at various growth stages of bean, corn and wheat

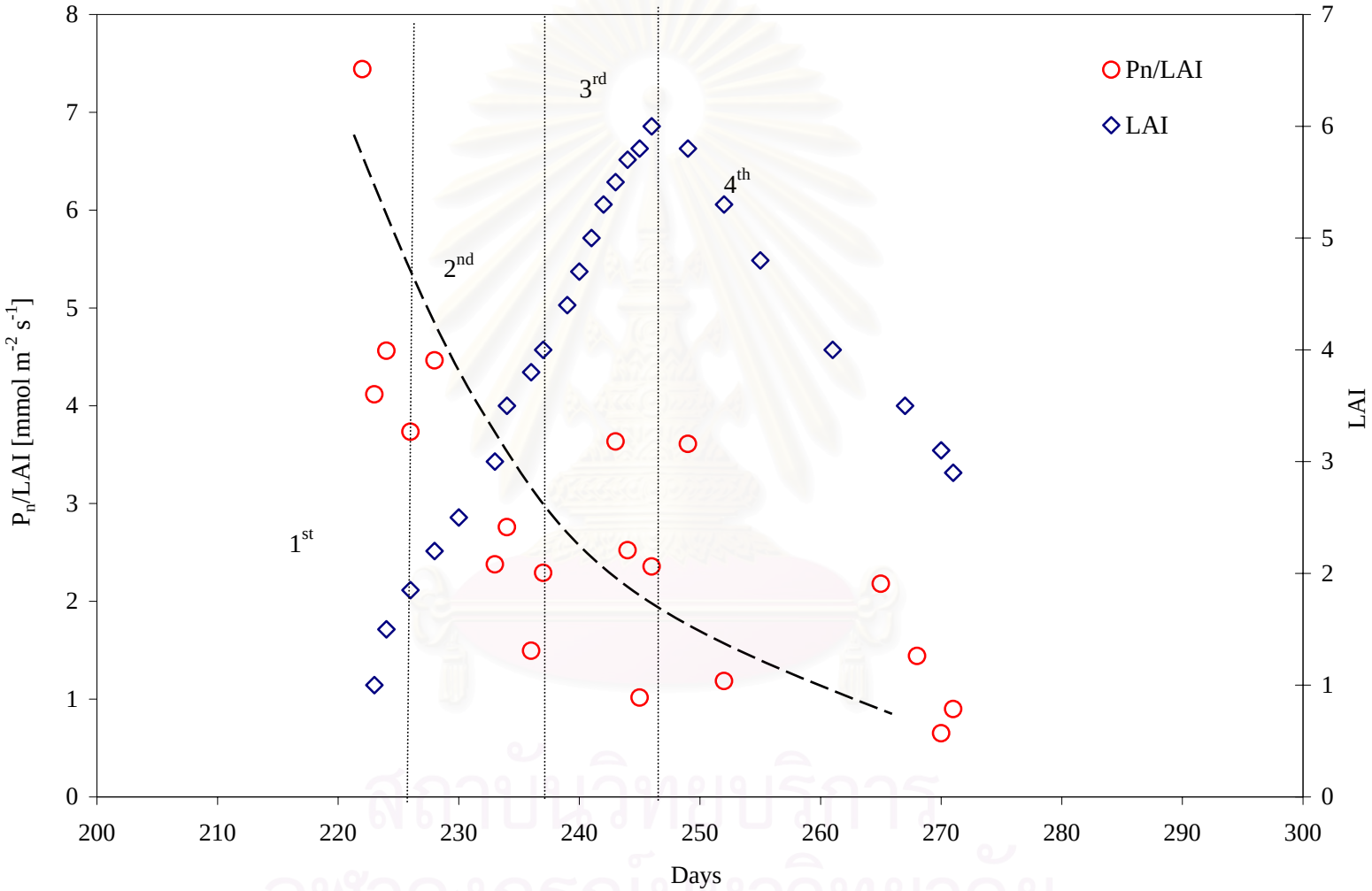

Figure 4.1.5 Net apparent specific photosynthetic activity of Bean

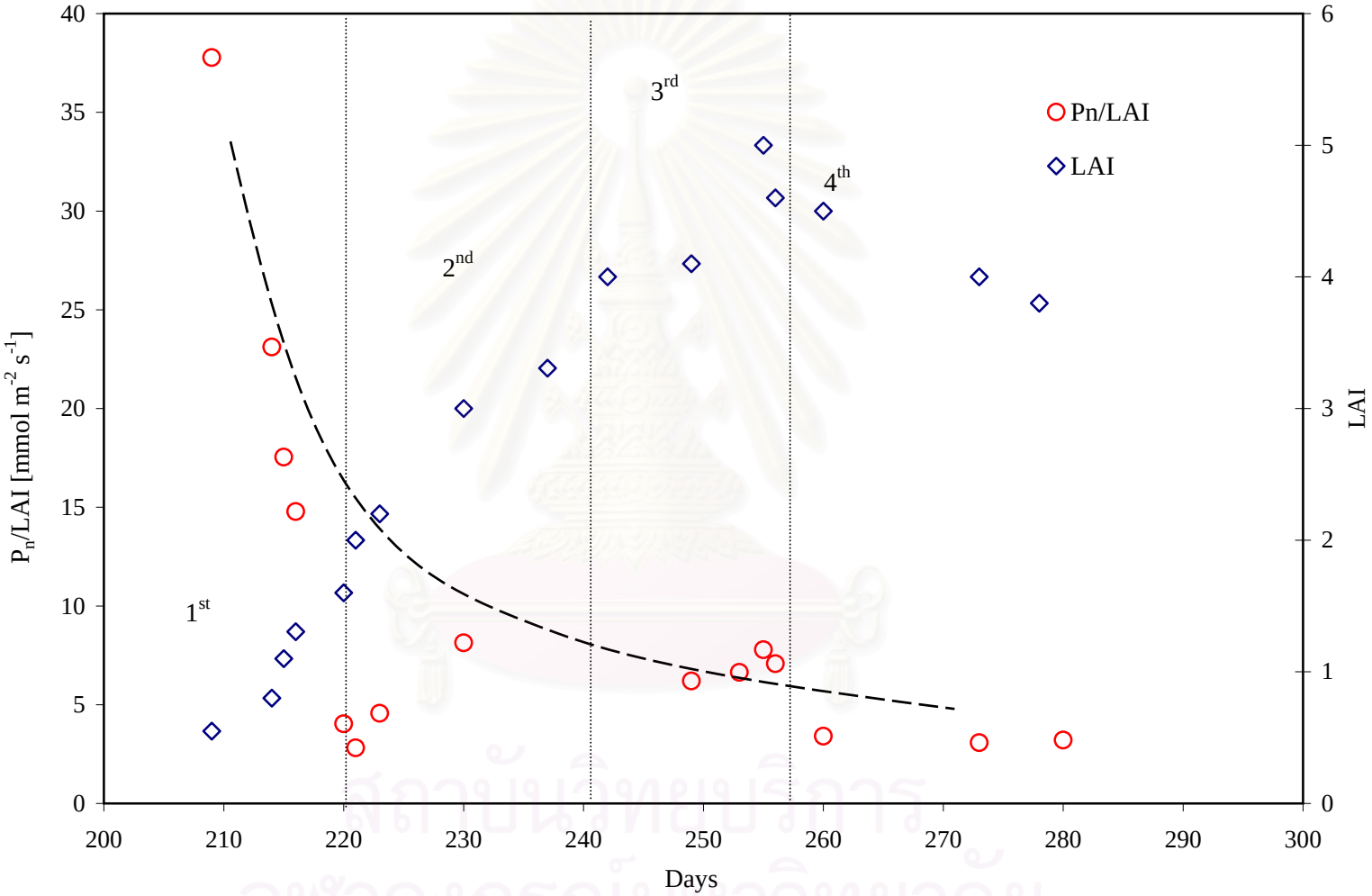

Figure 4.1.6 Net apparent specific photosynthetic activity of Corn

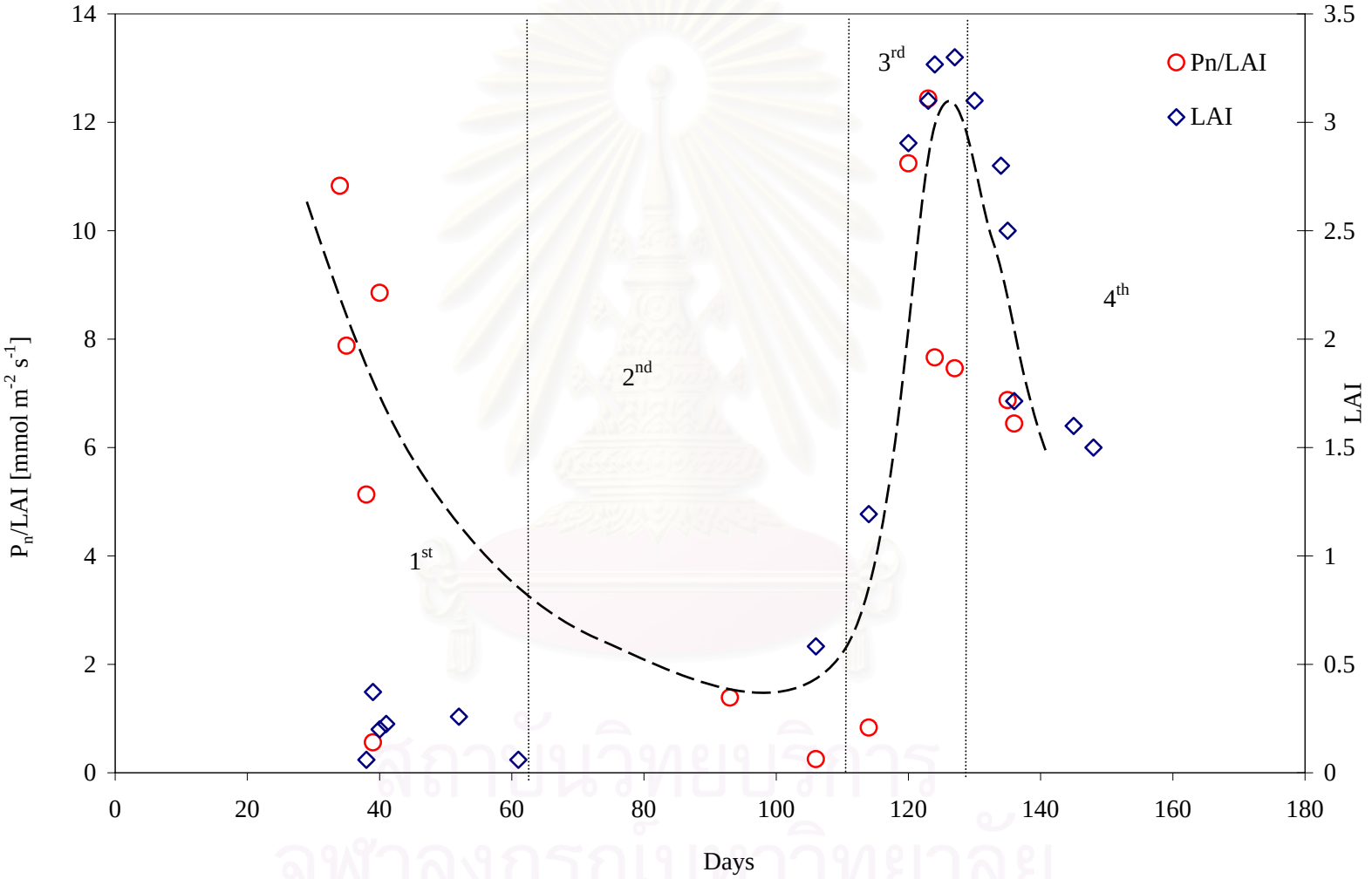

Figure 4.1.7 Net apparent specific photosynthetic activity of Wheat

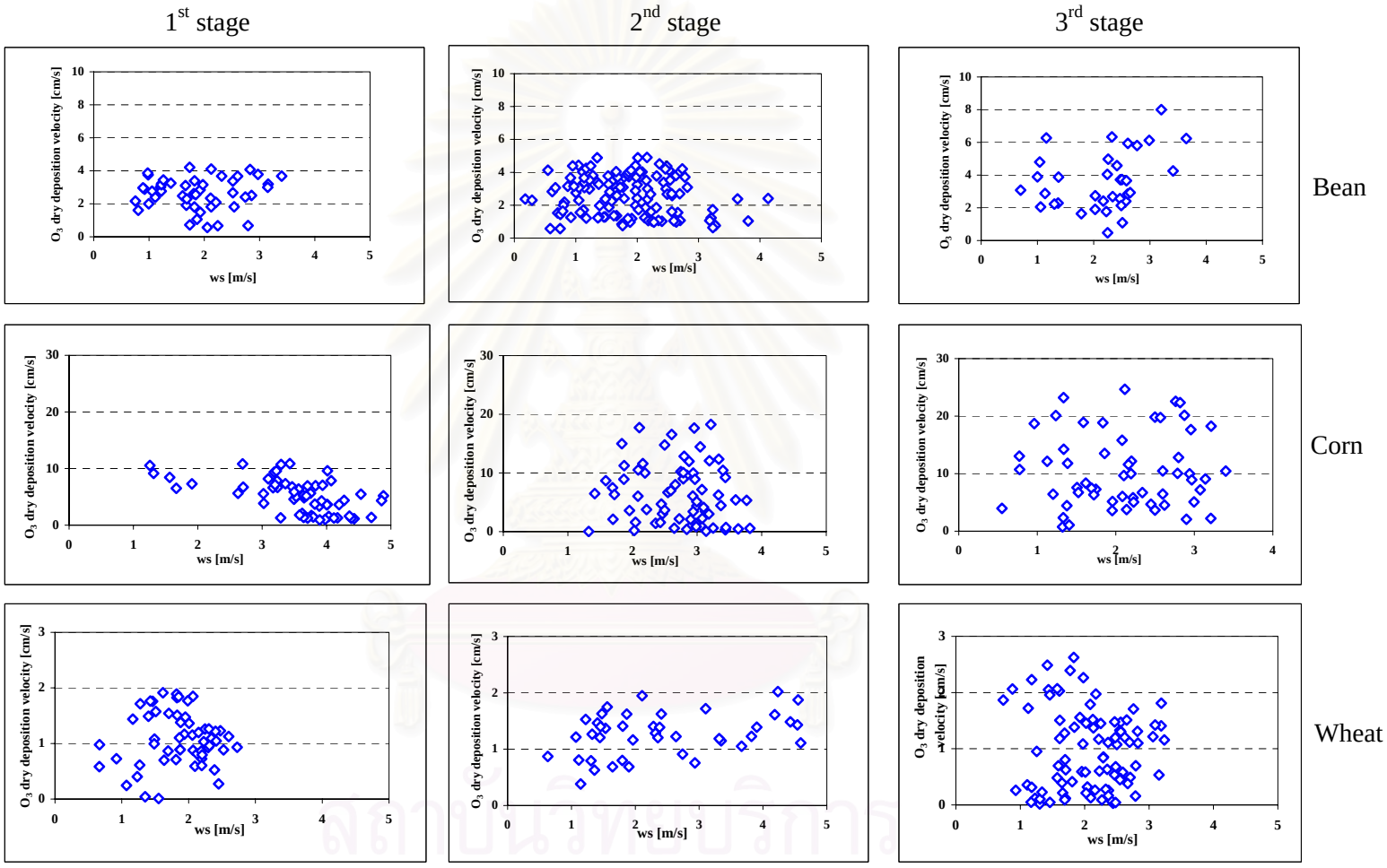

Figure 4.1.8a Effect of wind speed on O_3 dry deposition velocity at various growth stages of bean, corn and wheat

1st stage 2nd stage 3rd stage

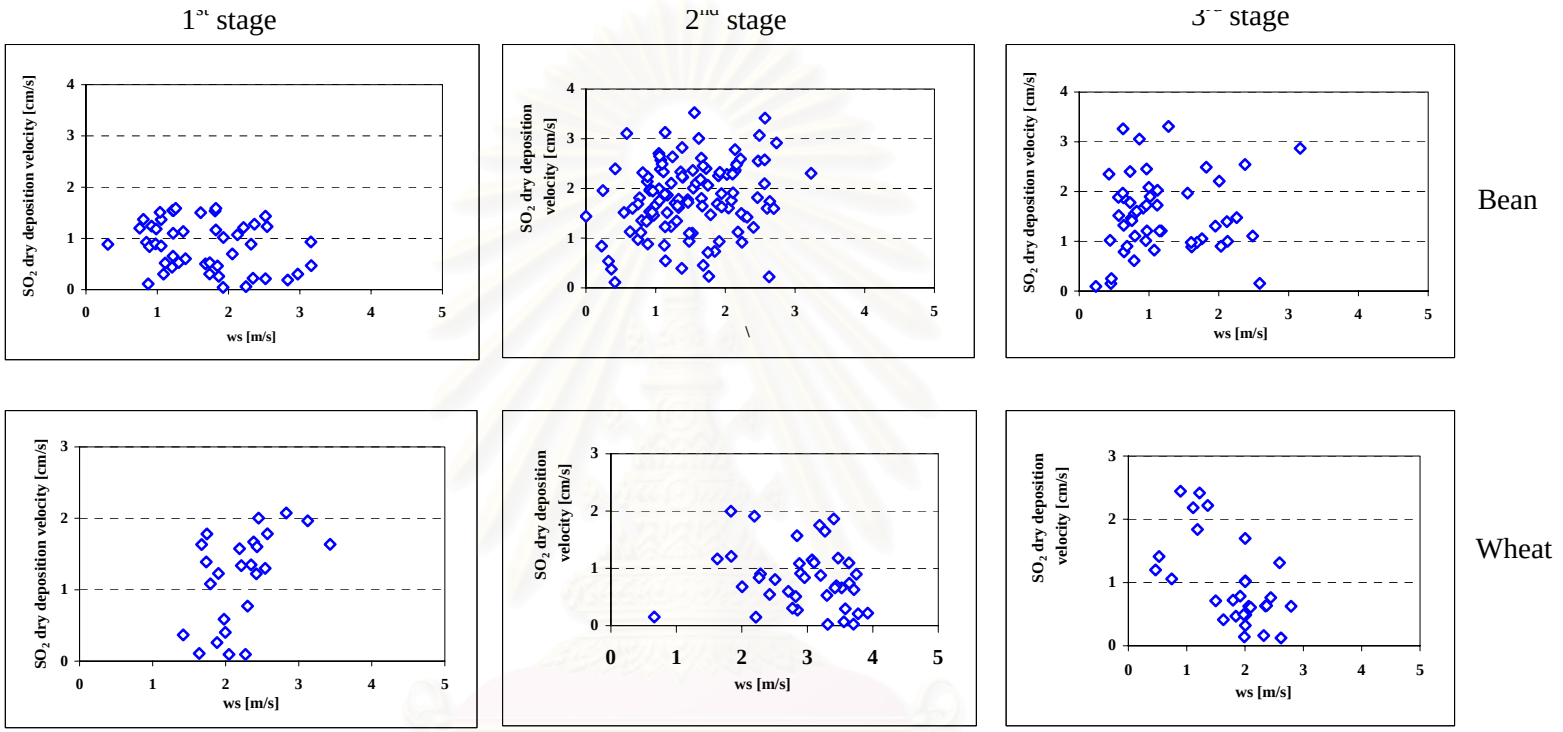

Figure 4.1.8b Effect of wind speed on SO_2 dry deposition velocity at various growth stages of bean and wheat

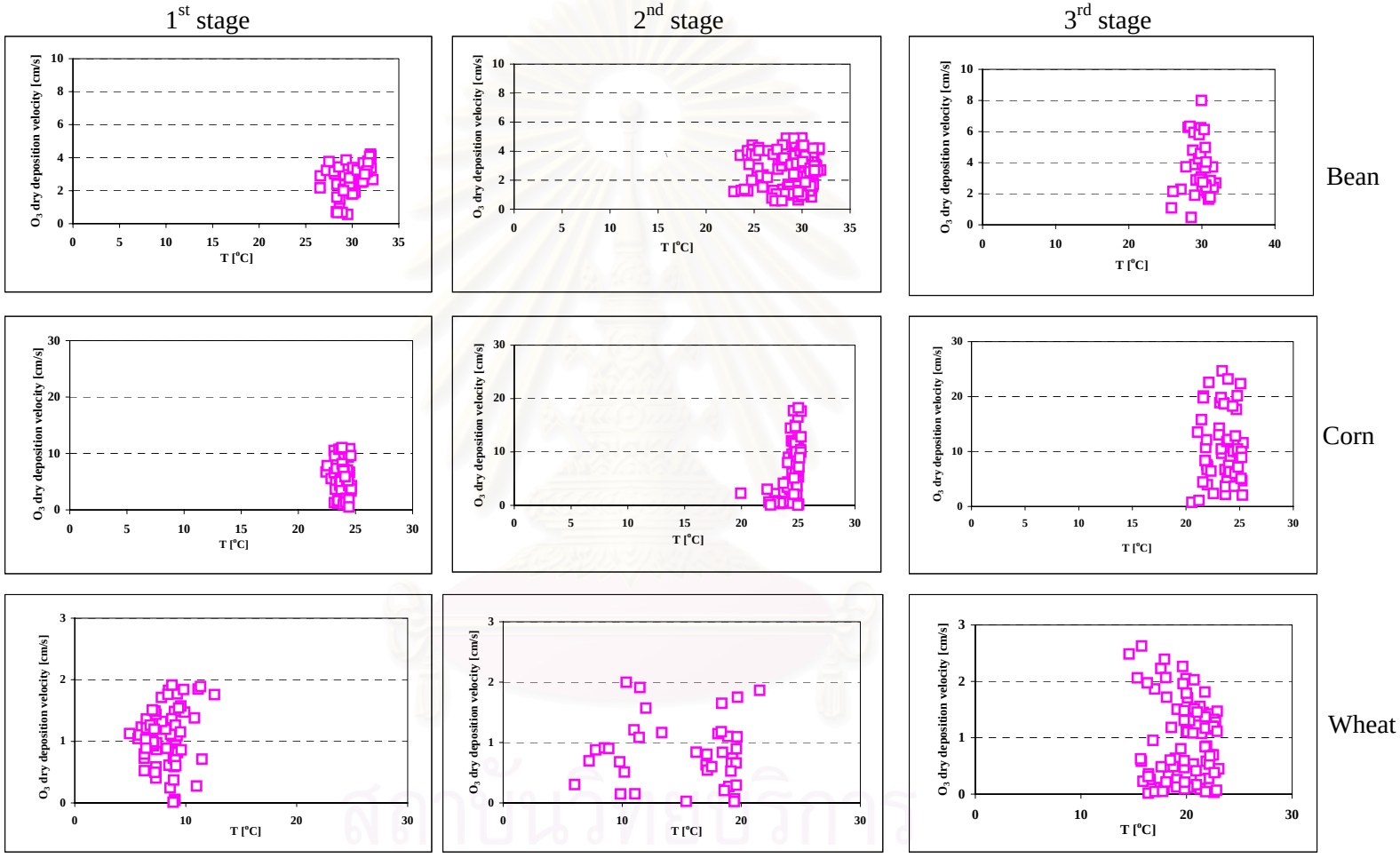

Figure 4.1.9a Effect of temperature on O_3 dry deposition velocity at various growth stages of bean, corn and wheat

1st stage 2nd stage 3rd stage

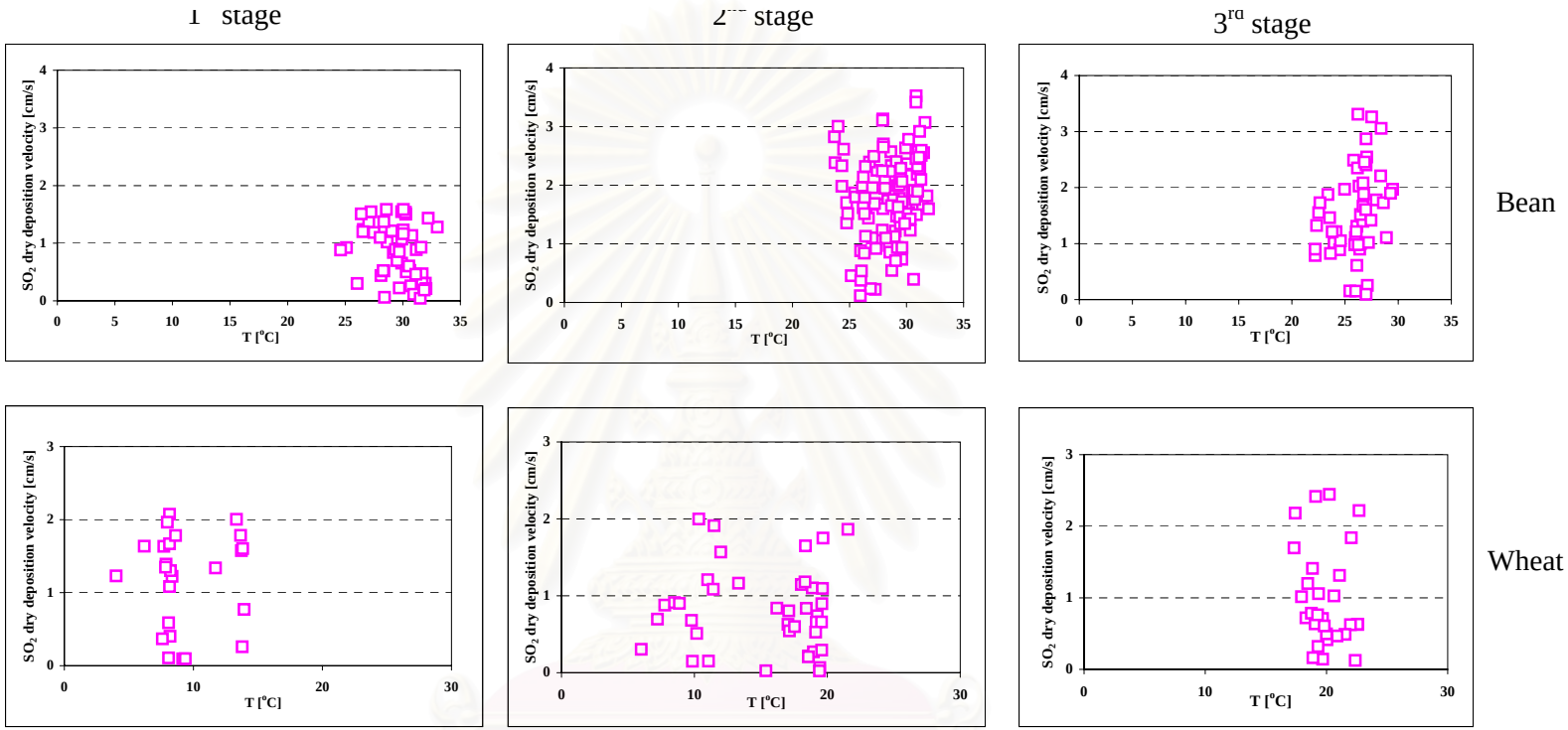

Figure 4.1.9b Effect of temperature on SO_2 dry deposition velocity at various growth stages of bean and wheat

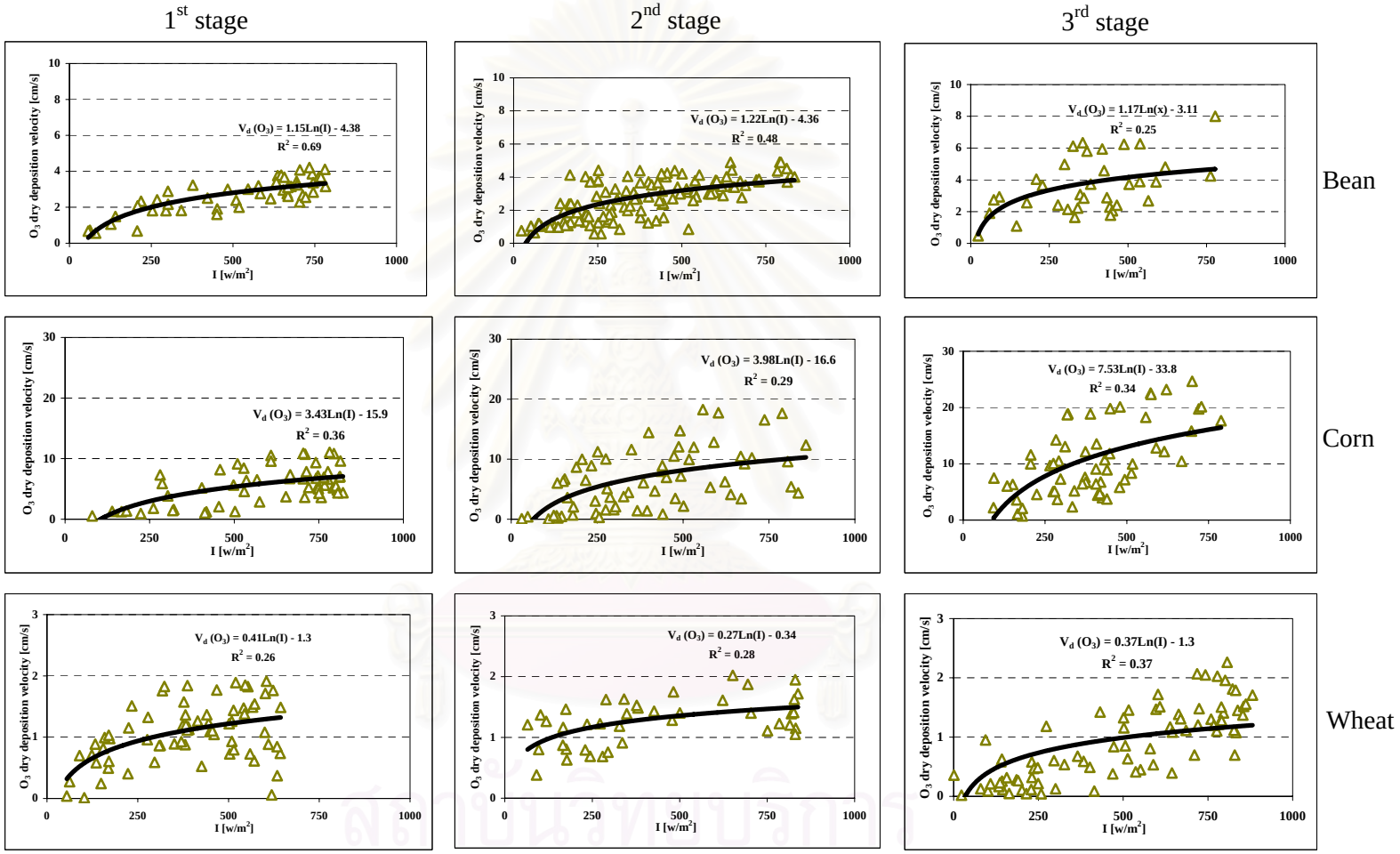

Figure 4.1.10a Effect of solar radiation on O_3 dry deposition velocity at various growth stages of bean, corn and wheat

1st stage 2nd stage 3rd stage

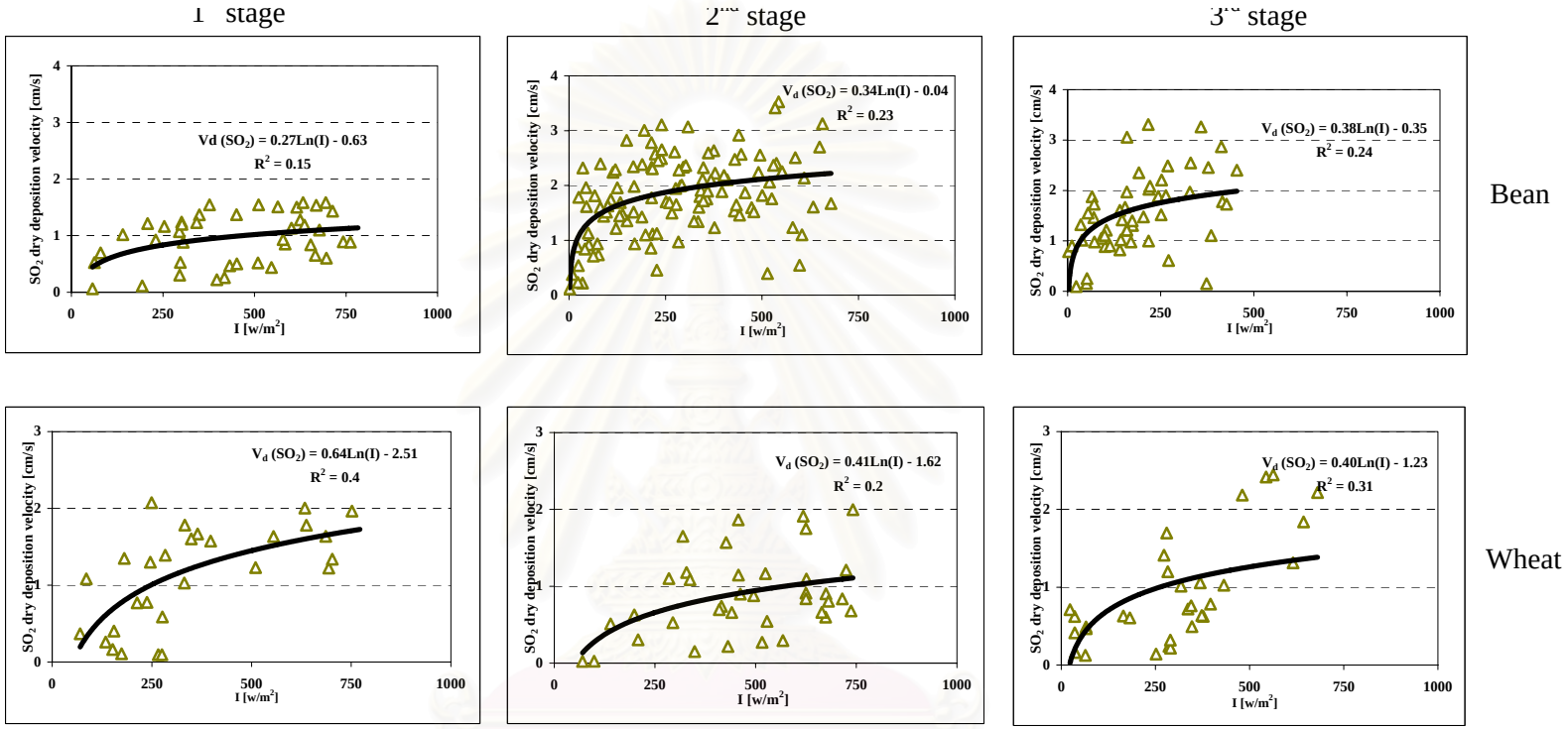

Figure 4.1.10b Effect of solar radiation on SO_2 dry deposition velocity at various growth stages of bean and wheat

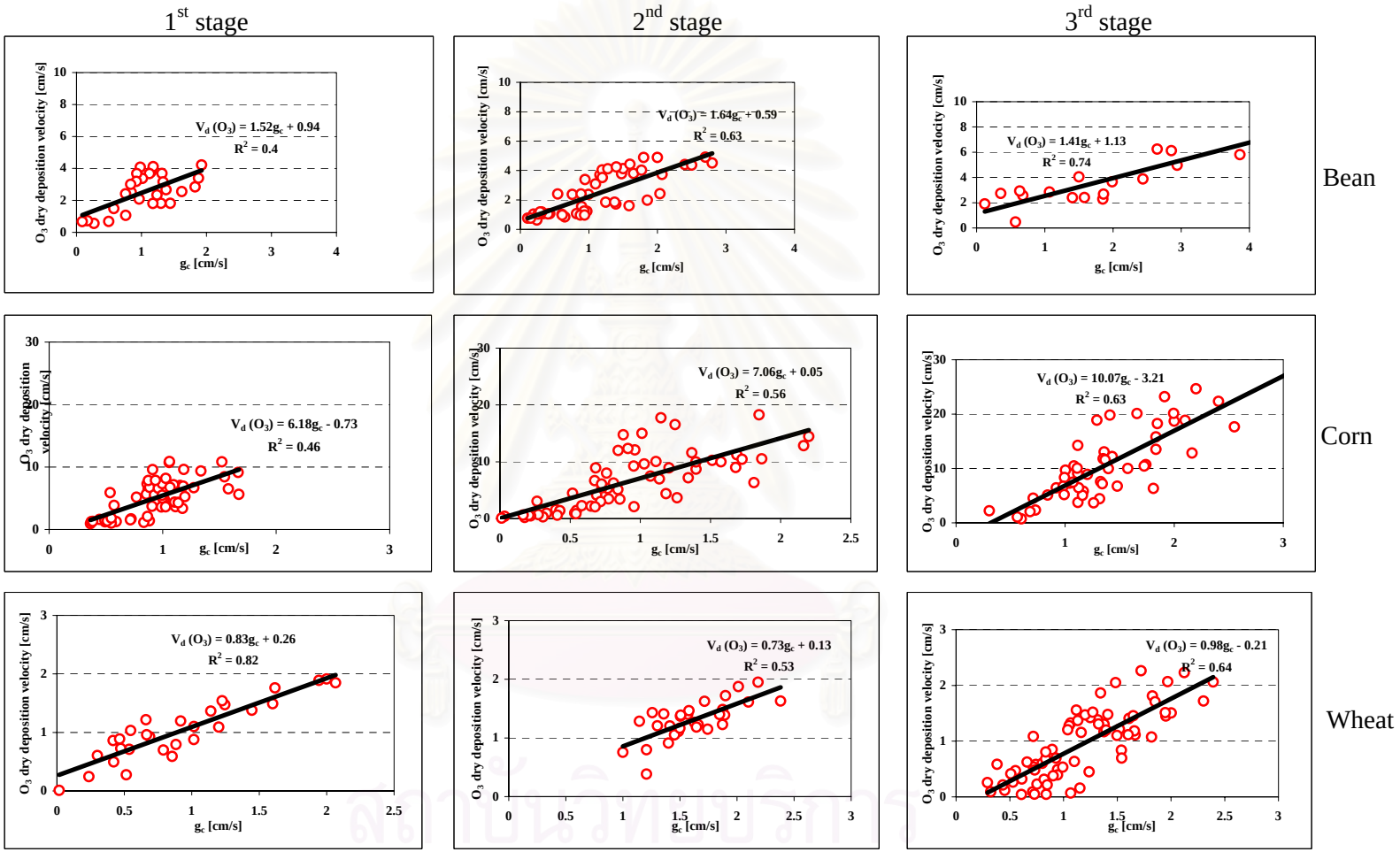

Figure 4.1.11a Effect of canopy conductance on O_3 dry deposition velocity at various growth stages of bean, corn and wheat

1st stage 2nd stage 3rd stage

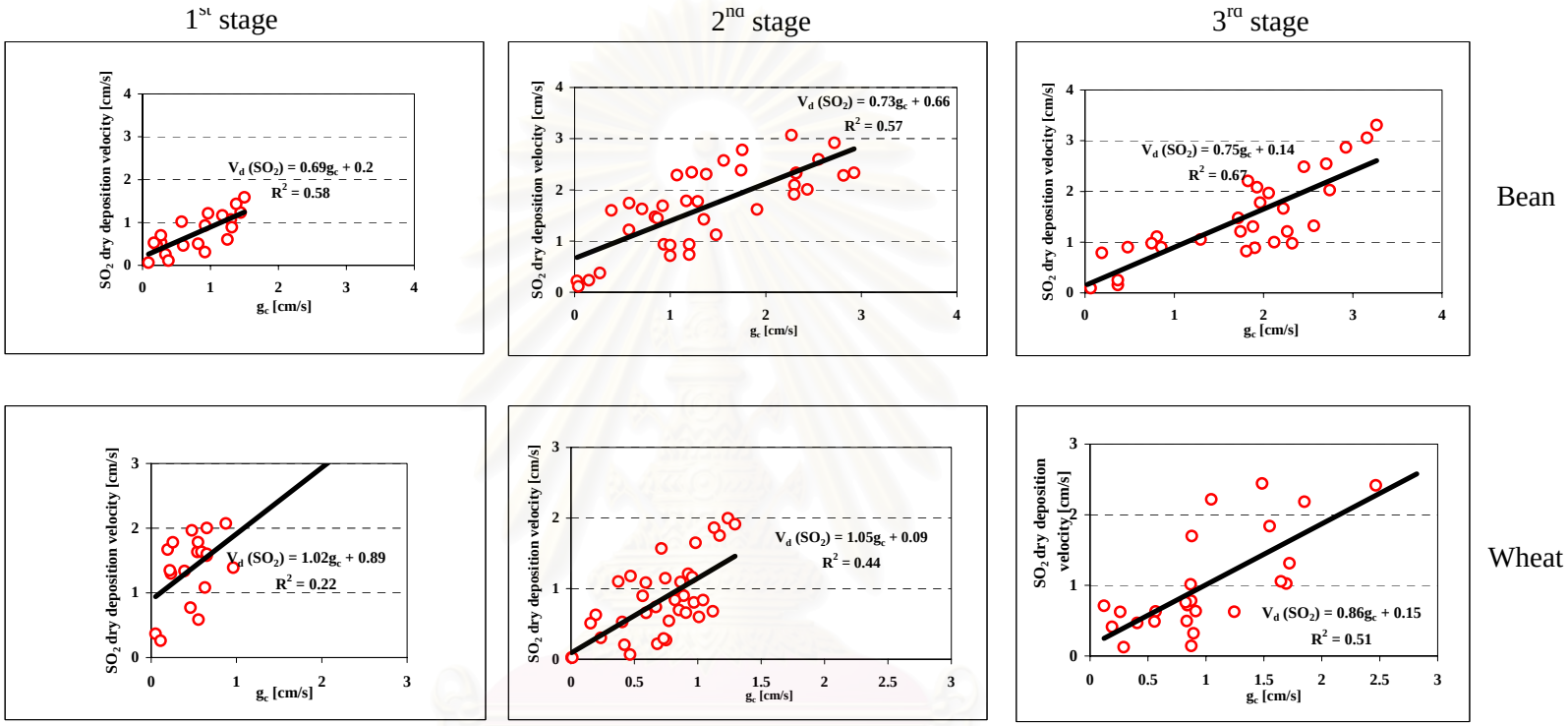

Figure 4.1.11b Effect of canopy conductance on SO_2 dry deposition velocity at various growth stages of bean and wheat

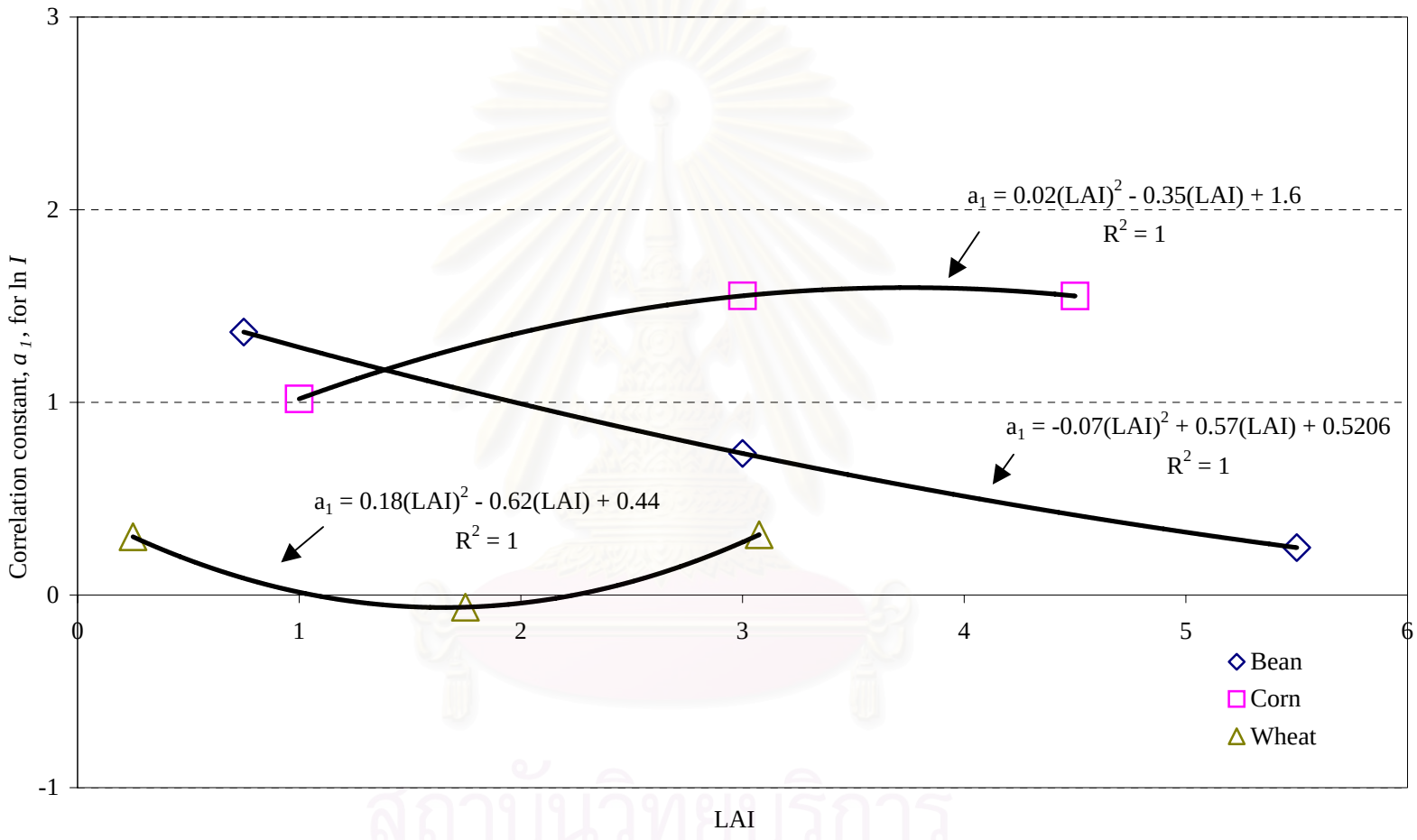

Figure 4.1.12 Relations between correlation constants, a_1, and LAI for the development of V_d for O_3

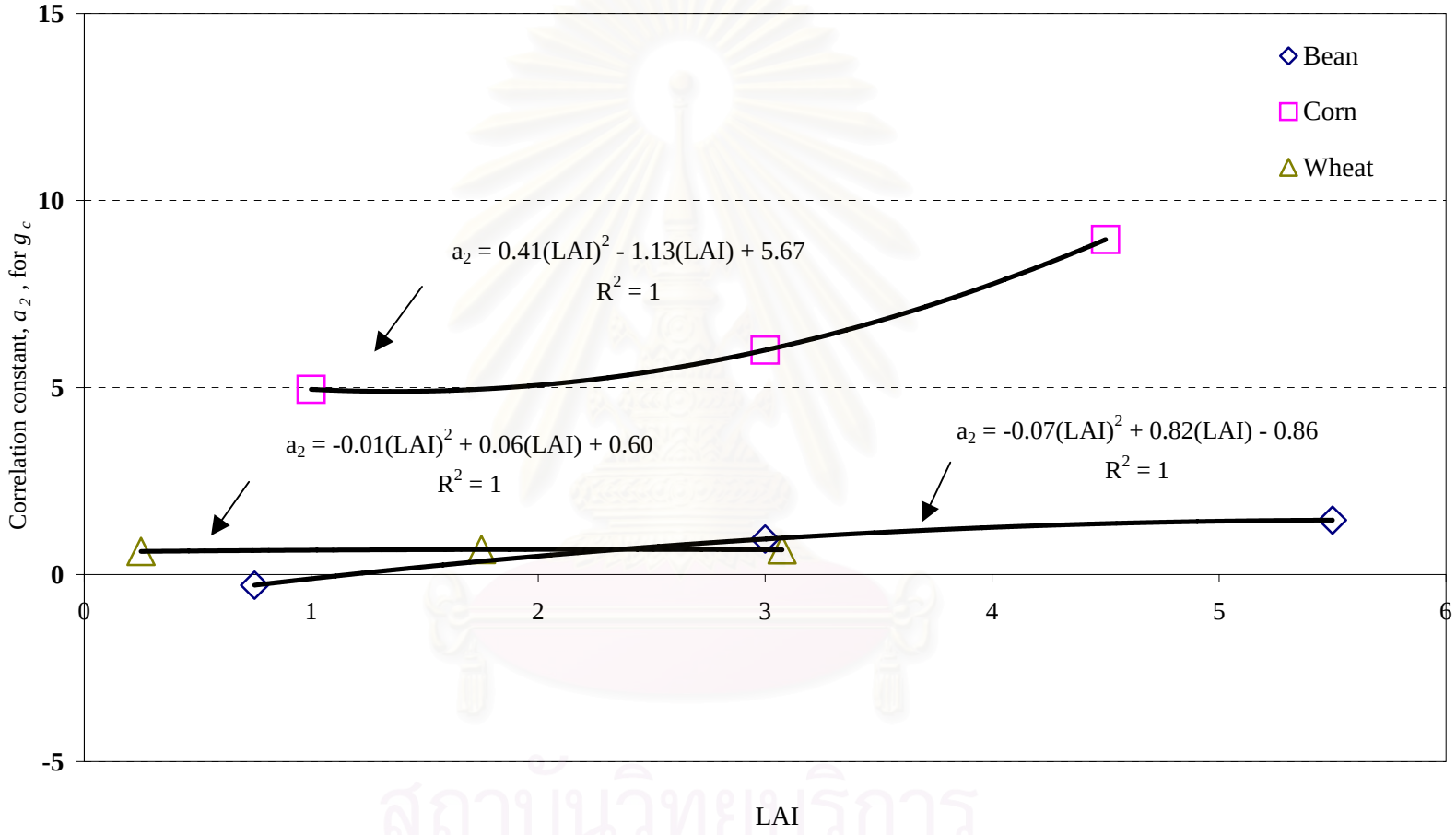

Figure 4.1.13 Relations between correlation constants, a_2, and LAI for the development of V_d for O_3

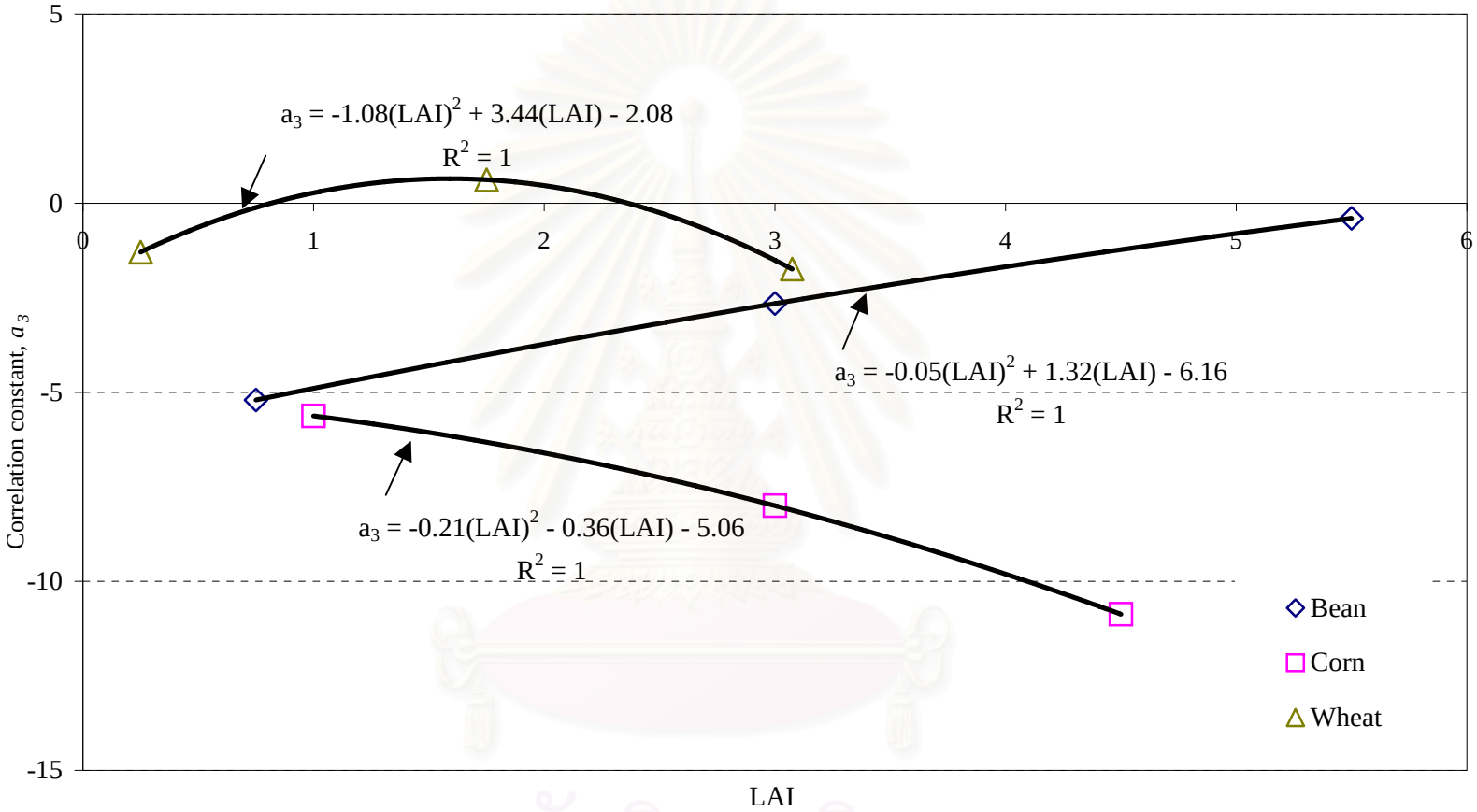

Figure 4.1.14 Relation between correlation constants, a_3, and LAI for the development of V_d for O_3

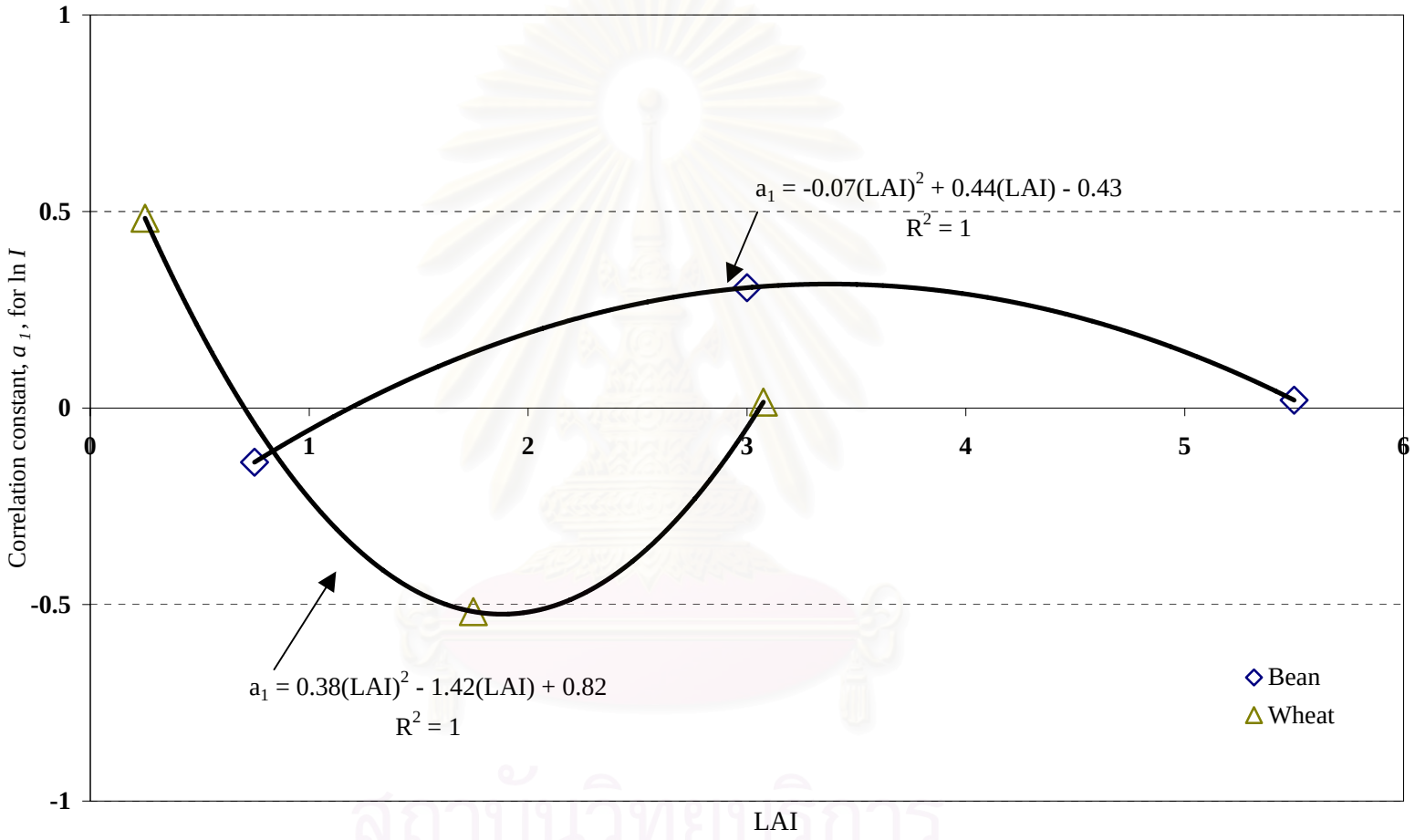

Figure 4.1.15 Relations between correlation constants, a_1, and LAI for the development of V_d for SO_2

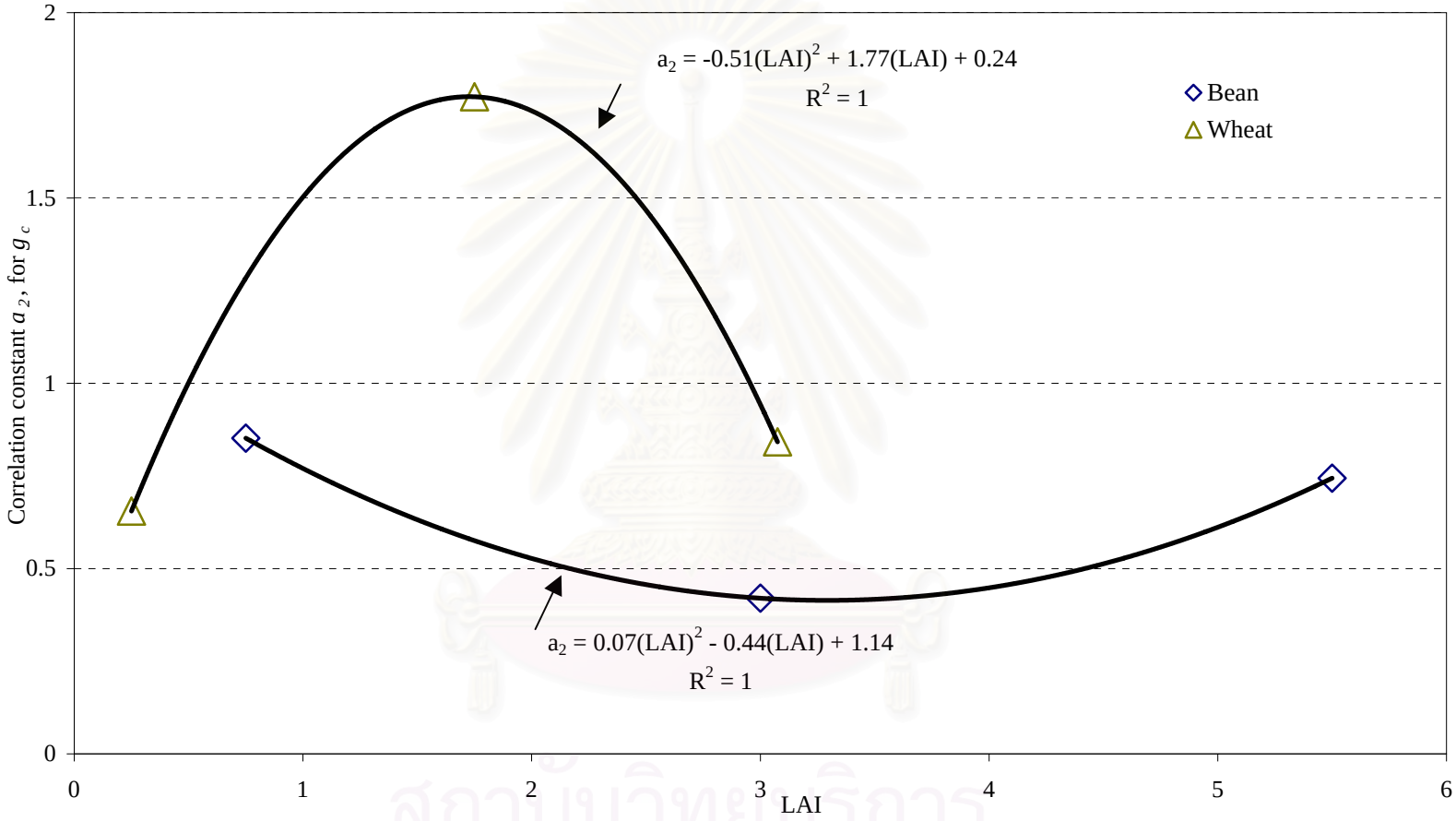

Figure 4.1.16 Relations between correlation constants, a_2, and LAI for the development of V_d for SO_2

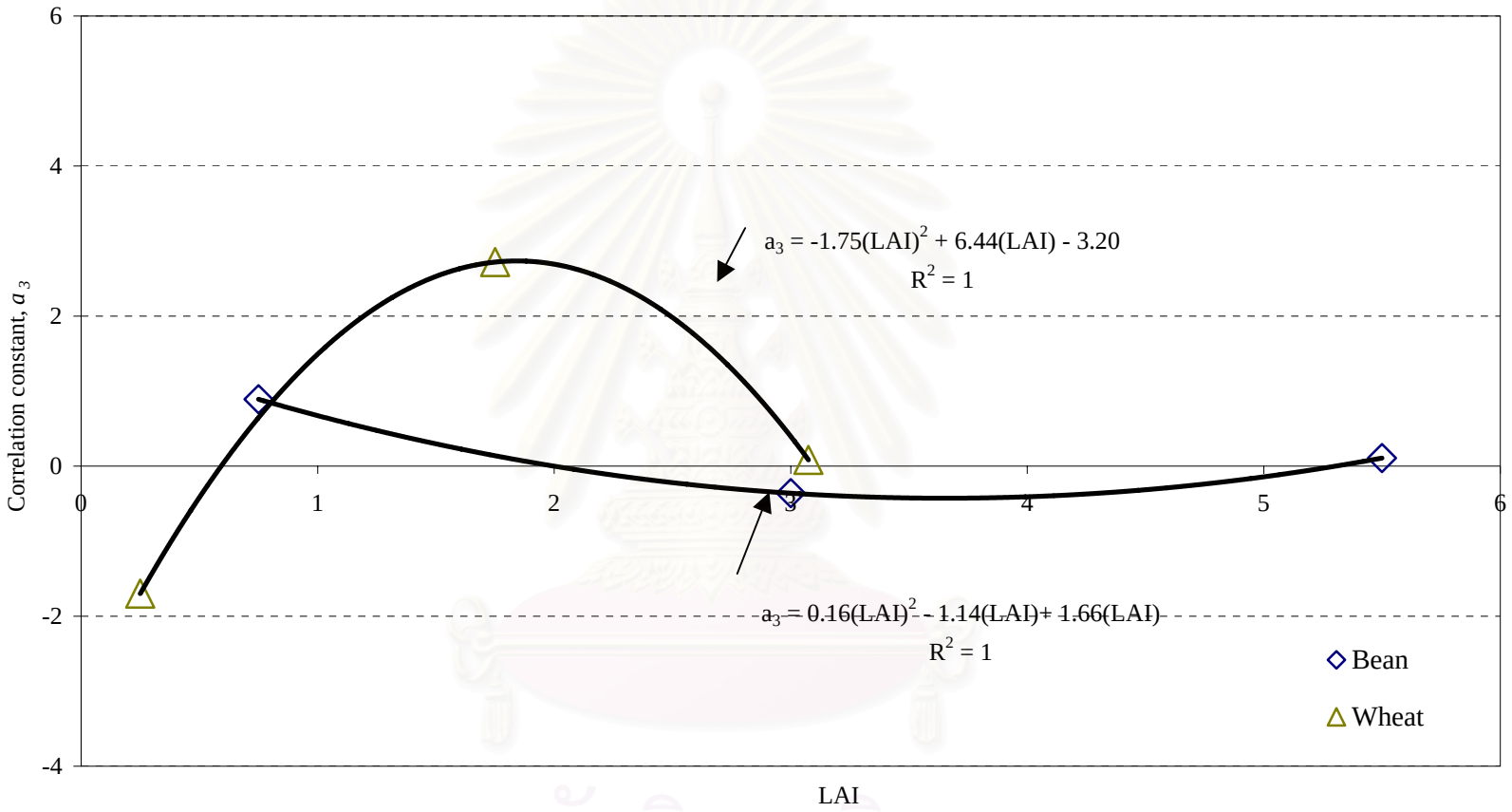

Figure 4.1.17 Relations between correlation constants, a_3, and LAI for the development of V_d for SO_2

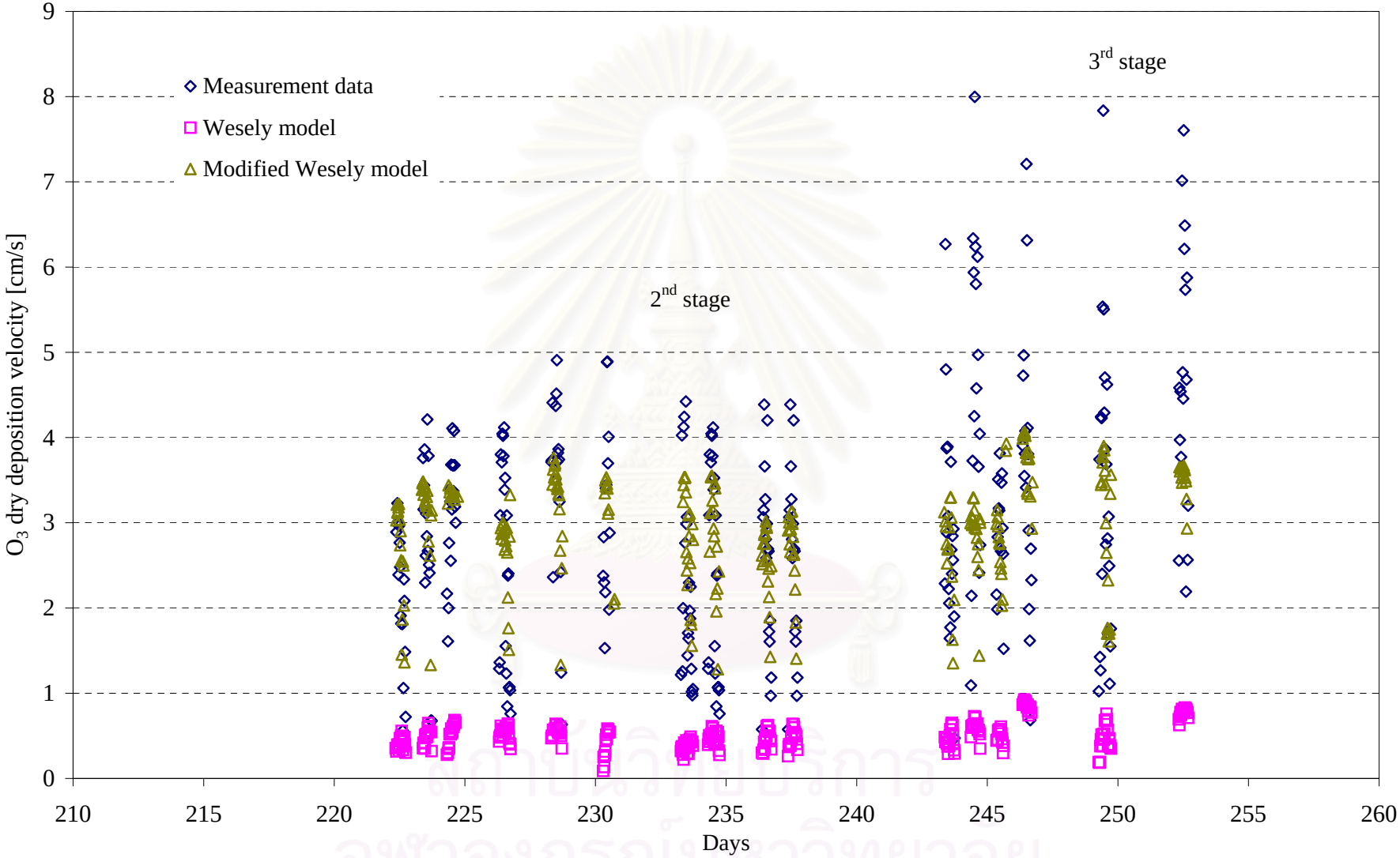

Figure 4.1.18 Dry deposition velocity of O_3 : Measurement and model results at various time periods in bean field

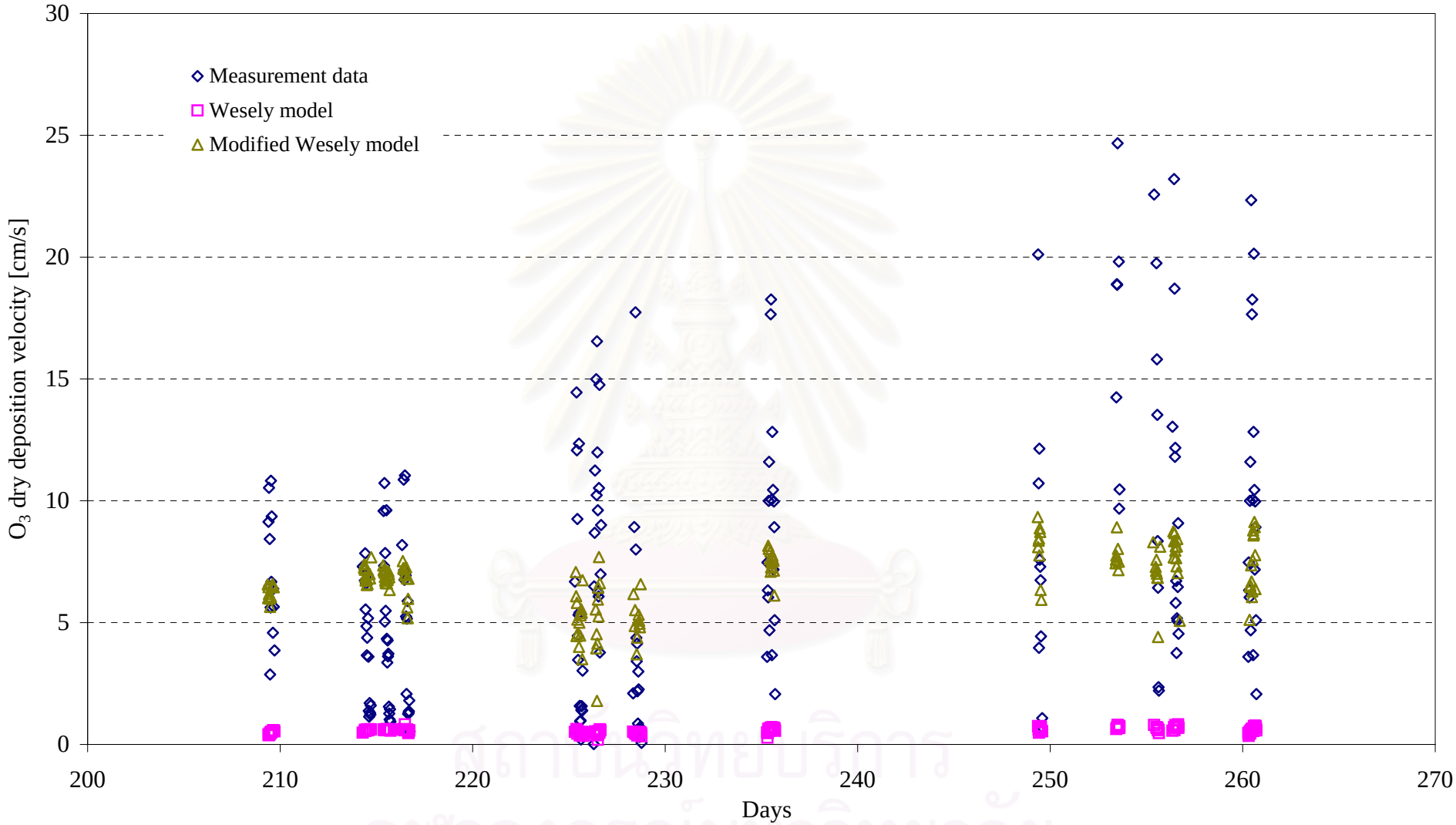

Figure 4.1.19 Dry deposition velocity of O_3 : Measurement and model results at various time periods in corn field

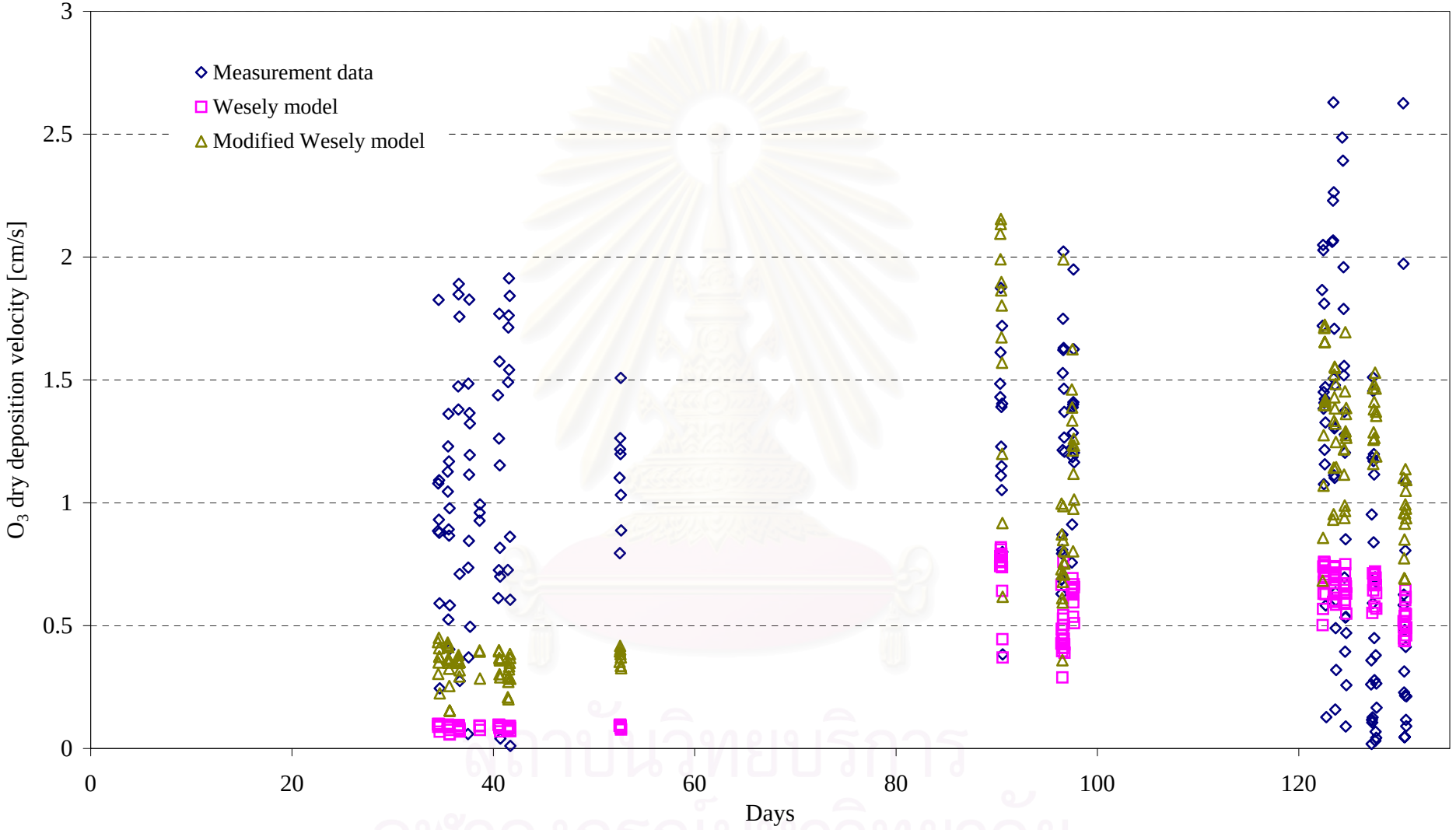

Figure 4.1.20 Dry deposition velocity of O_3 : Measurement and model results at various time periods in wheat field

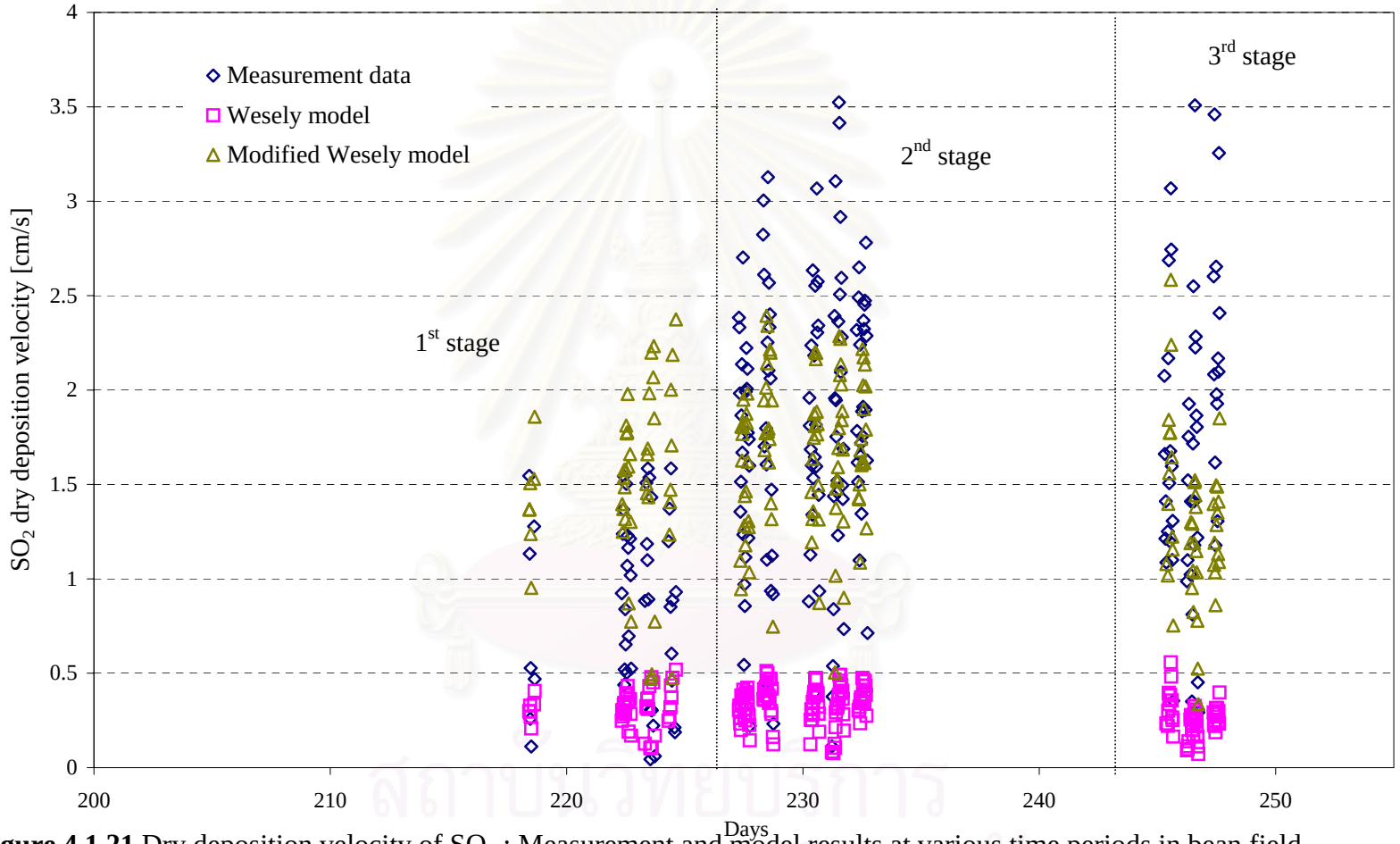

Figure 4.1.21 Dry deposition velocity of SO_2 : Measurement and model results at various time periods in bean field

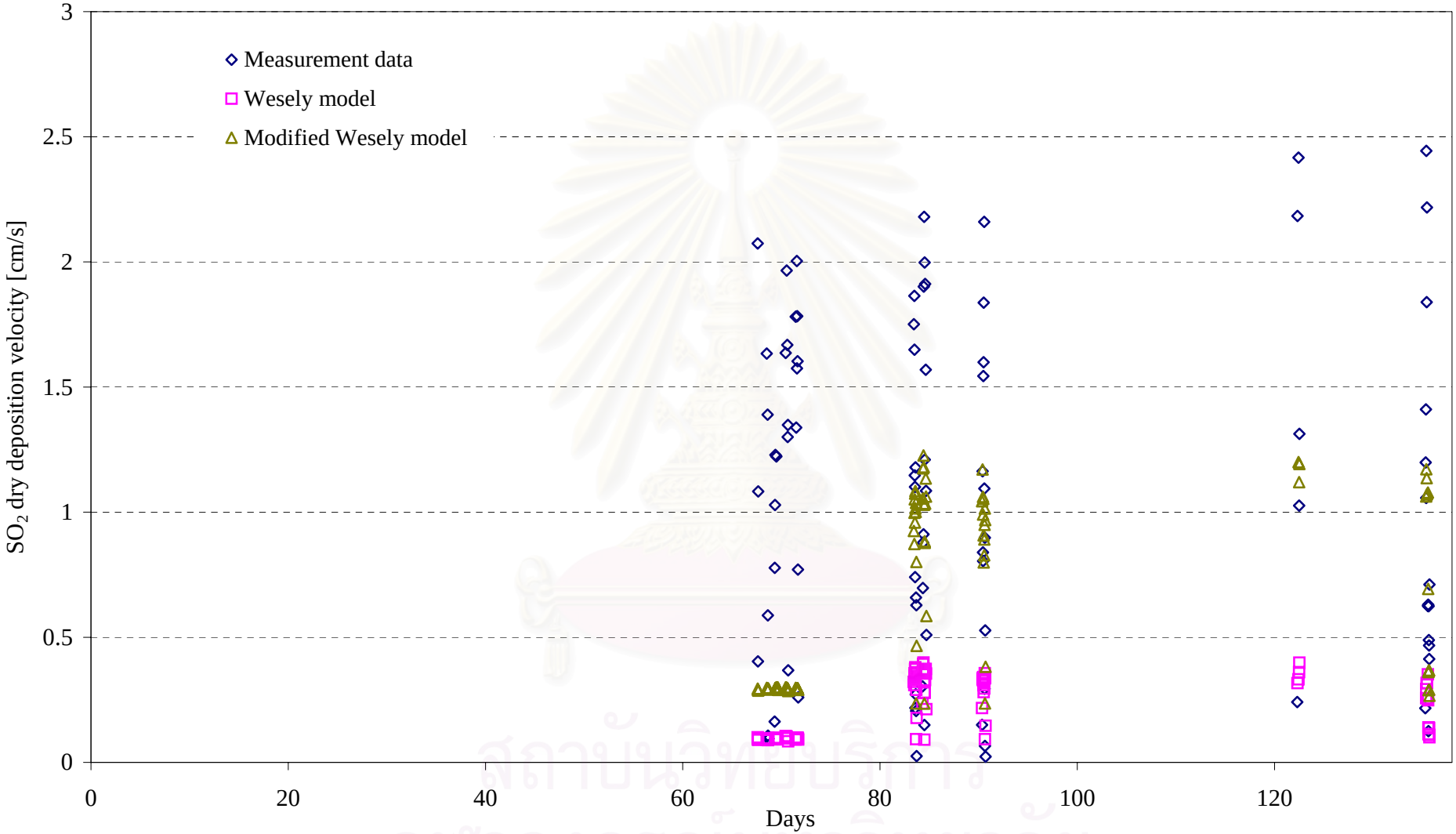

Figure 4.1.22 Dry deposition velocity of SO_2 : Measurement and model results at various time periods in wheat field

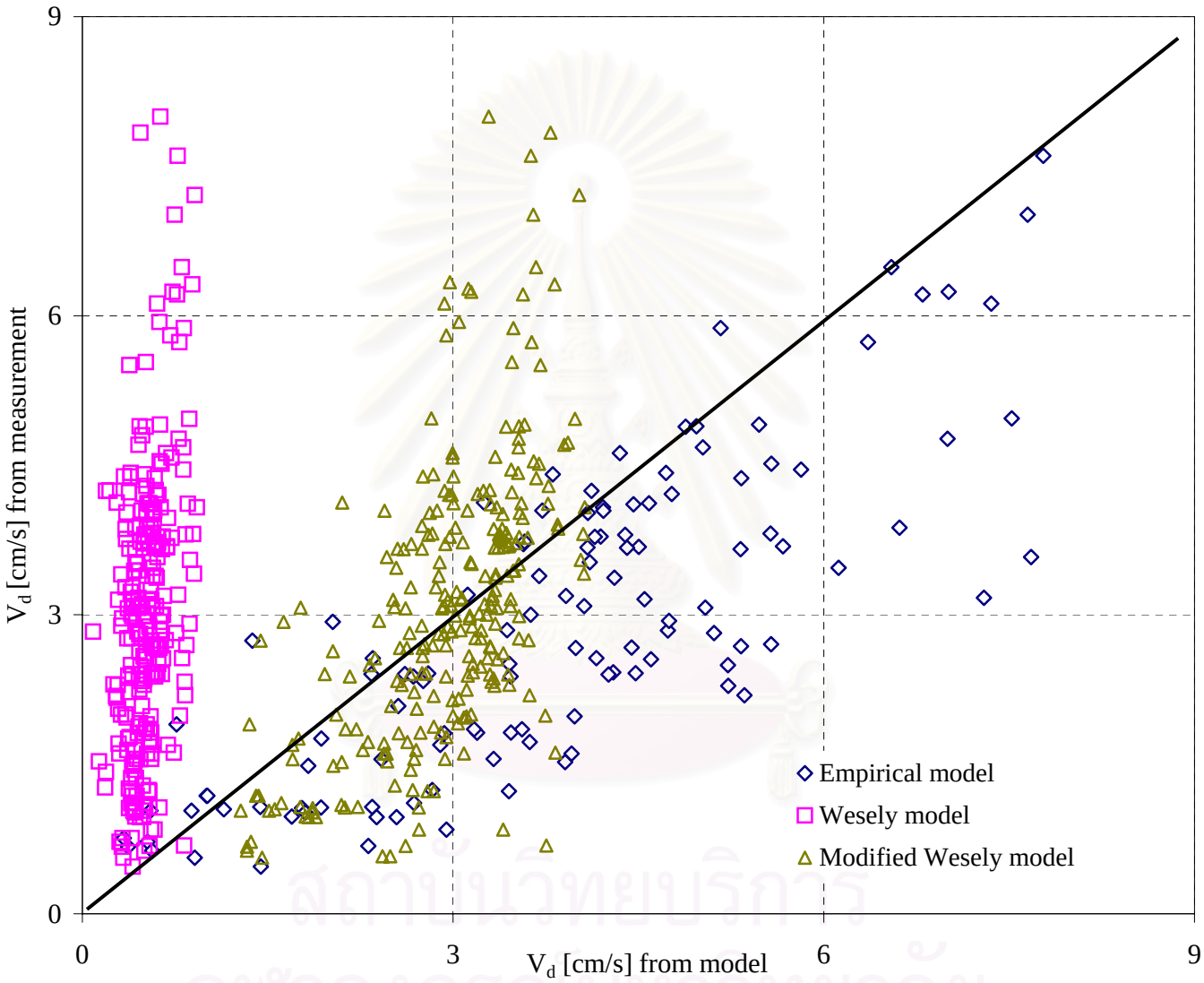

Figure 4.1.23 Comparison between V_d of O_3 from measurement and simulation at all growth stages of bean

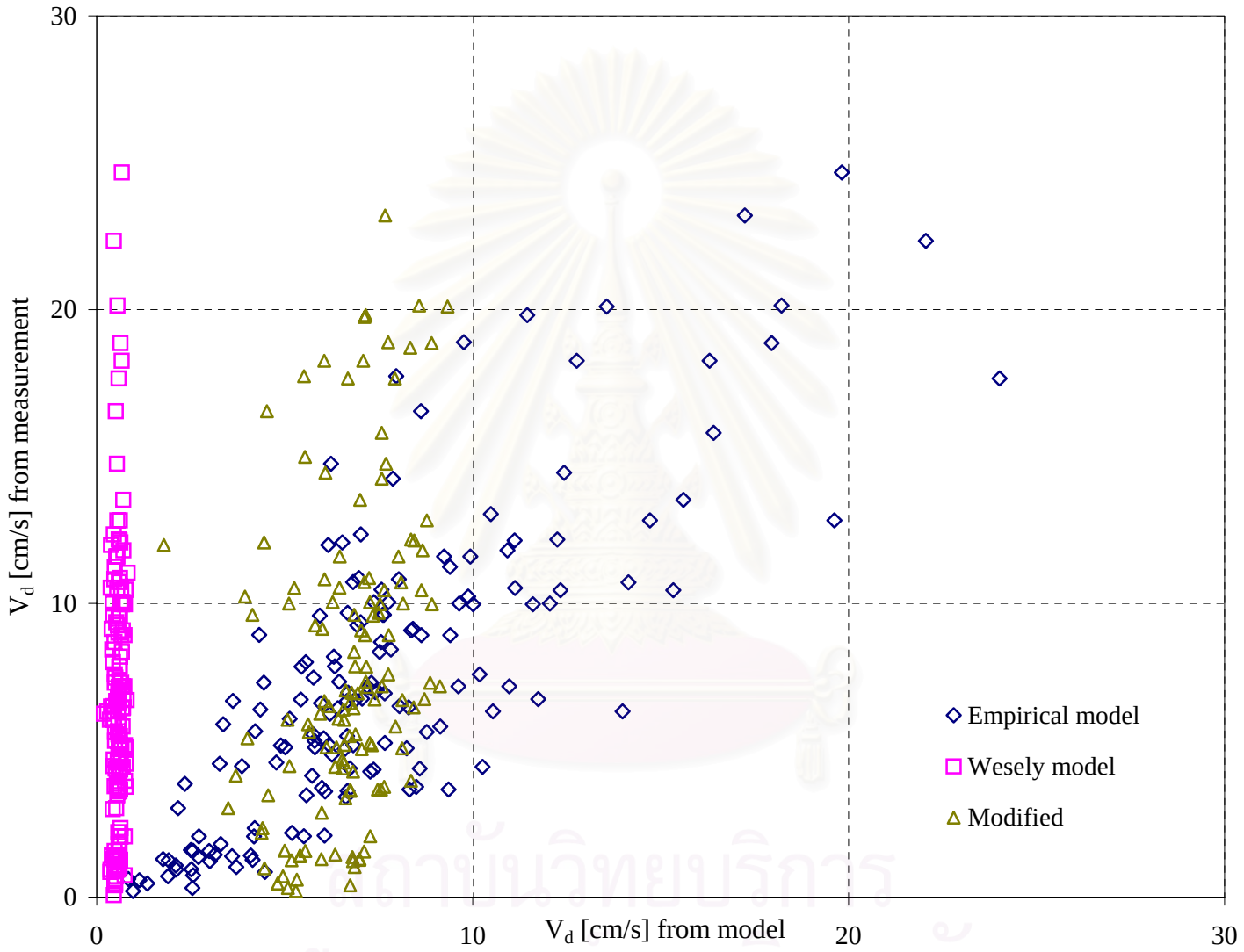

Figure 4.1.24 Comparison between V_d of O_3 from measurement and simulation at all growth stages of corn

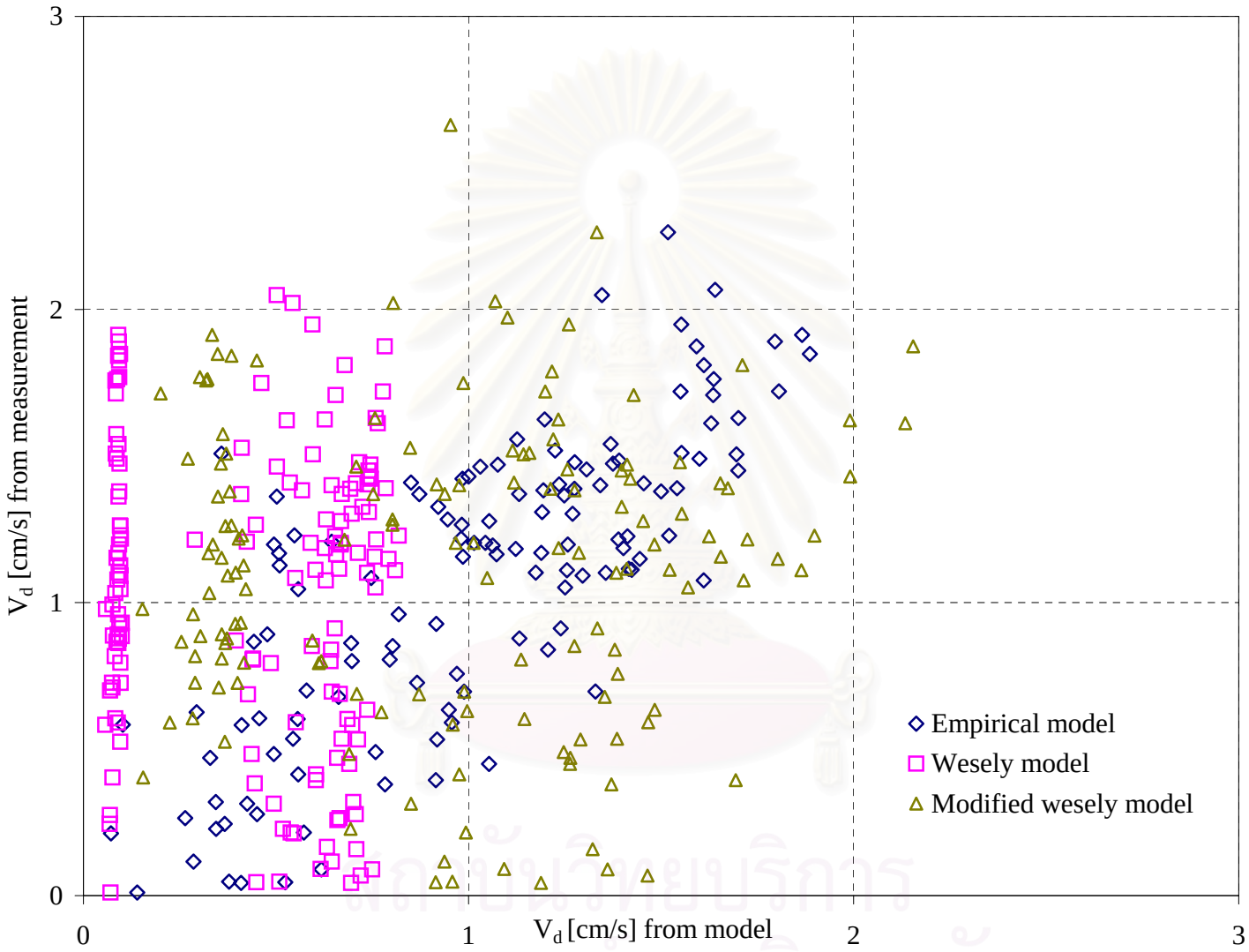

Figure 4.1.25 Comparison between V_d of O_3 from measurement and simulation at all growth stages of wheat

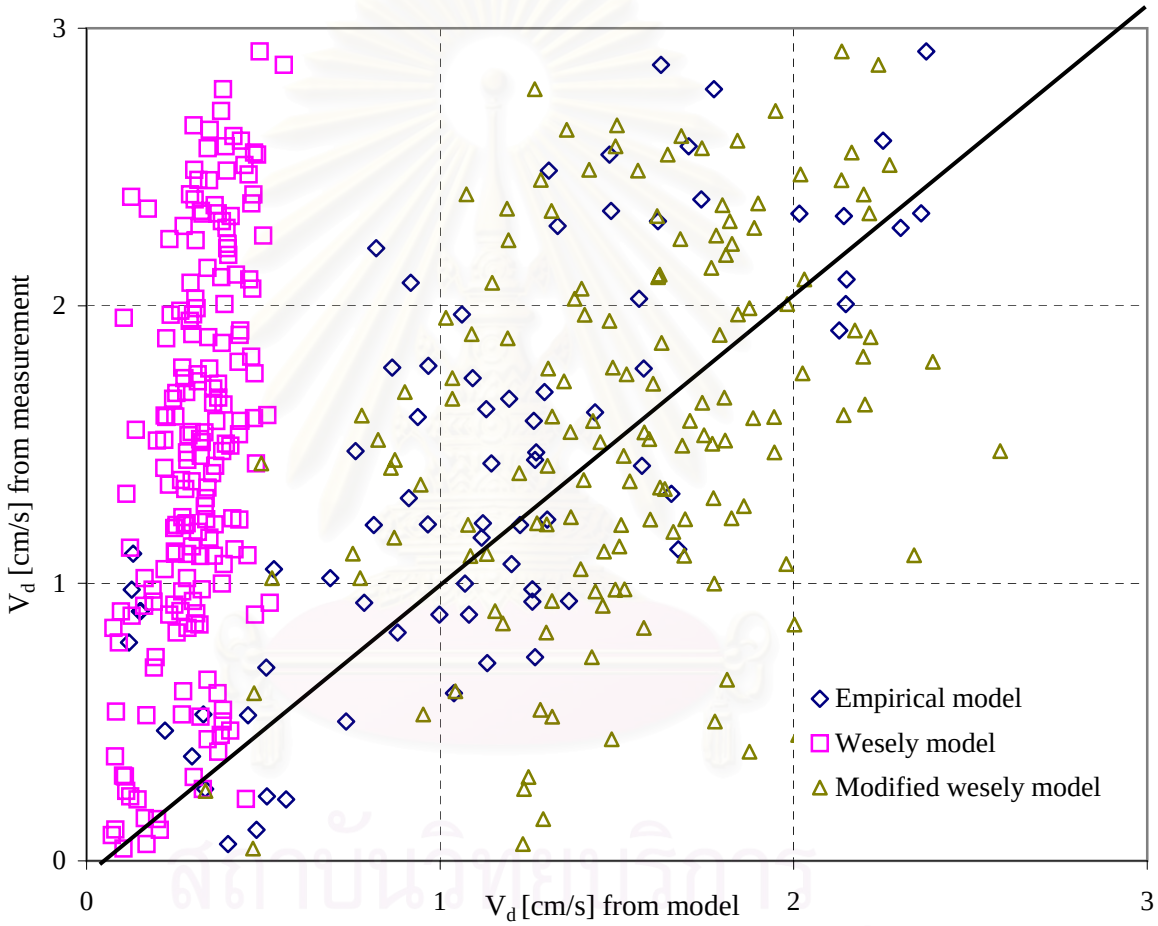

Figure 4.1.26 Comparison between V_d of SO_2 from measurement and simulation at all growth stages of bean

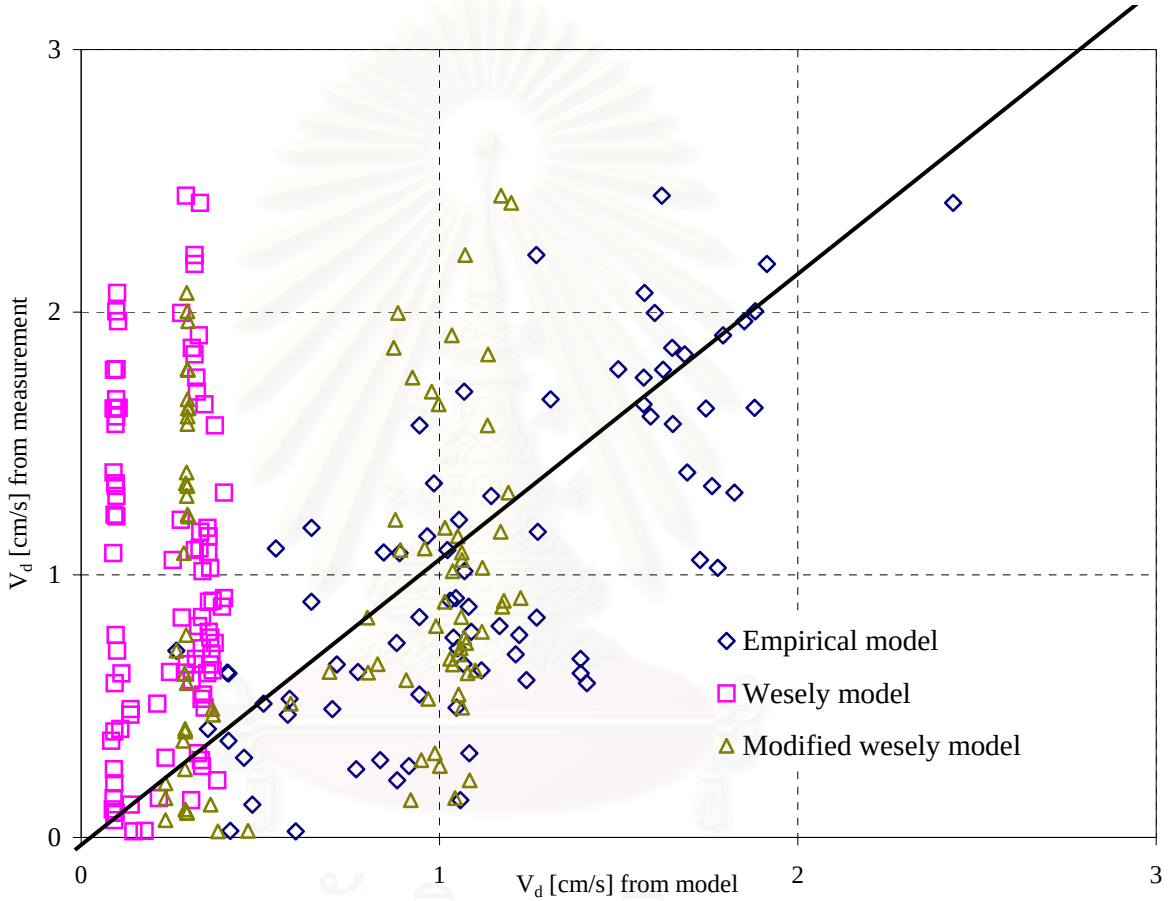

Figure 4.1.27 Comparison between V_d of SO_2 from measurment and simulation at all growth stages of wheat

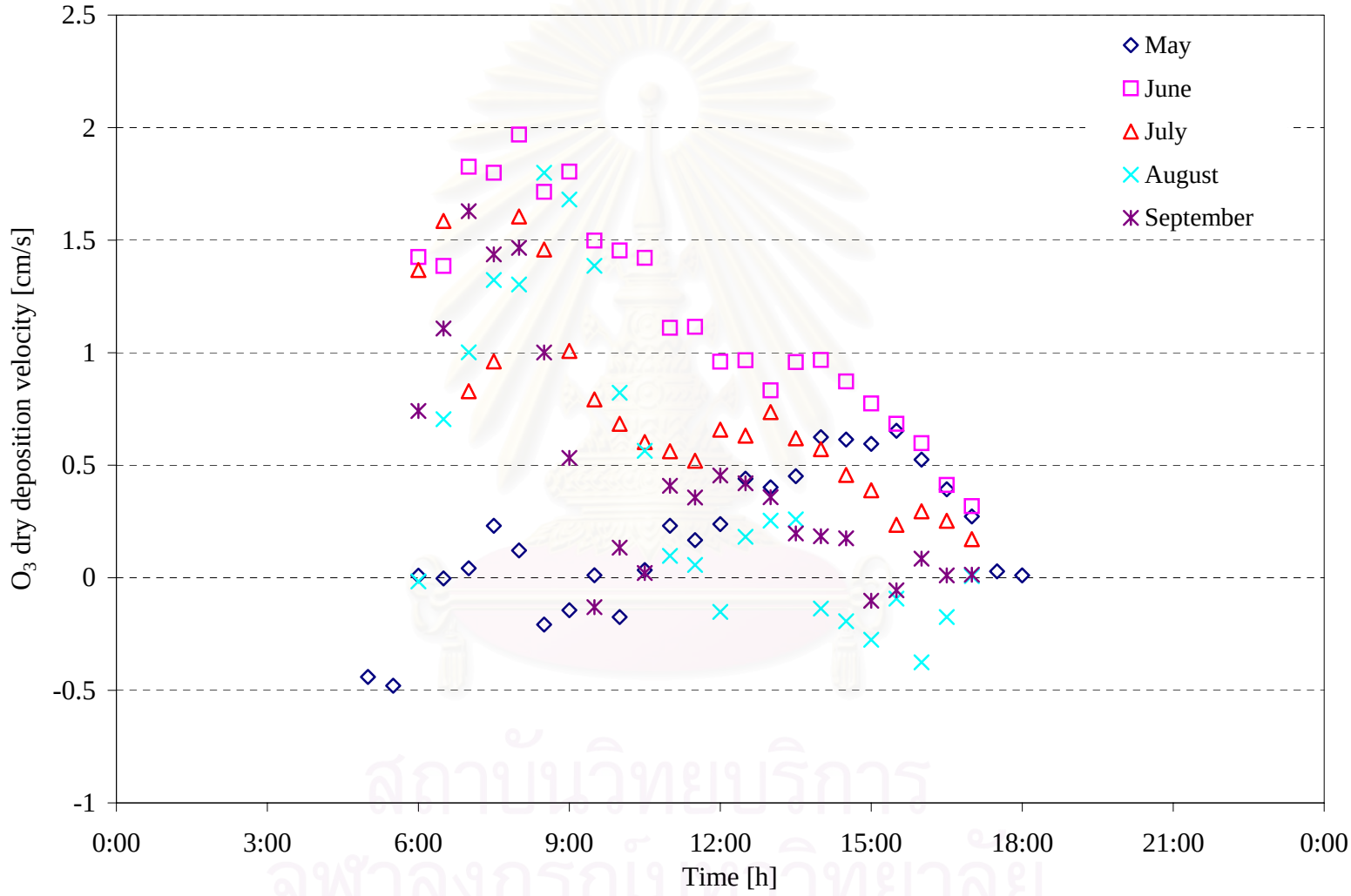

Figure 4.2.1 Dry deposition velocity of O_3 over pine forest at various time periods

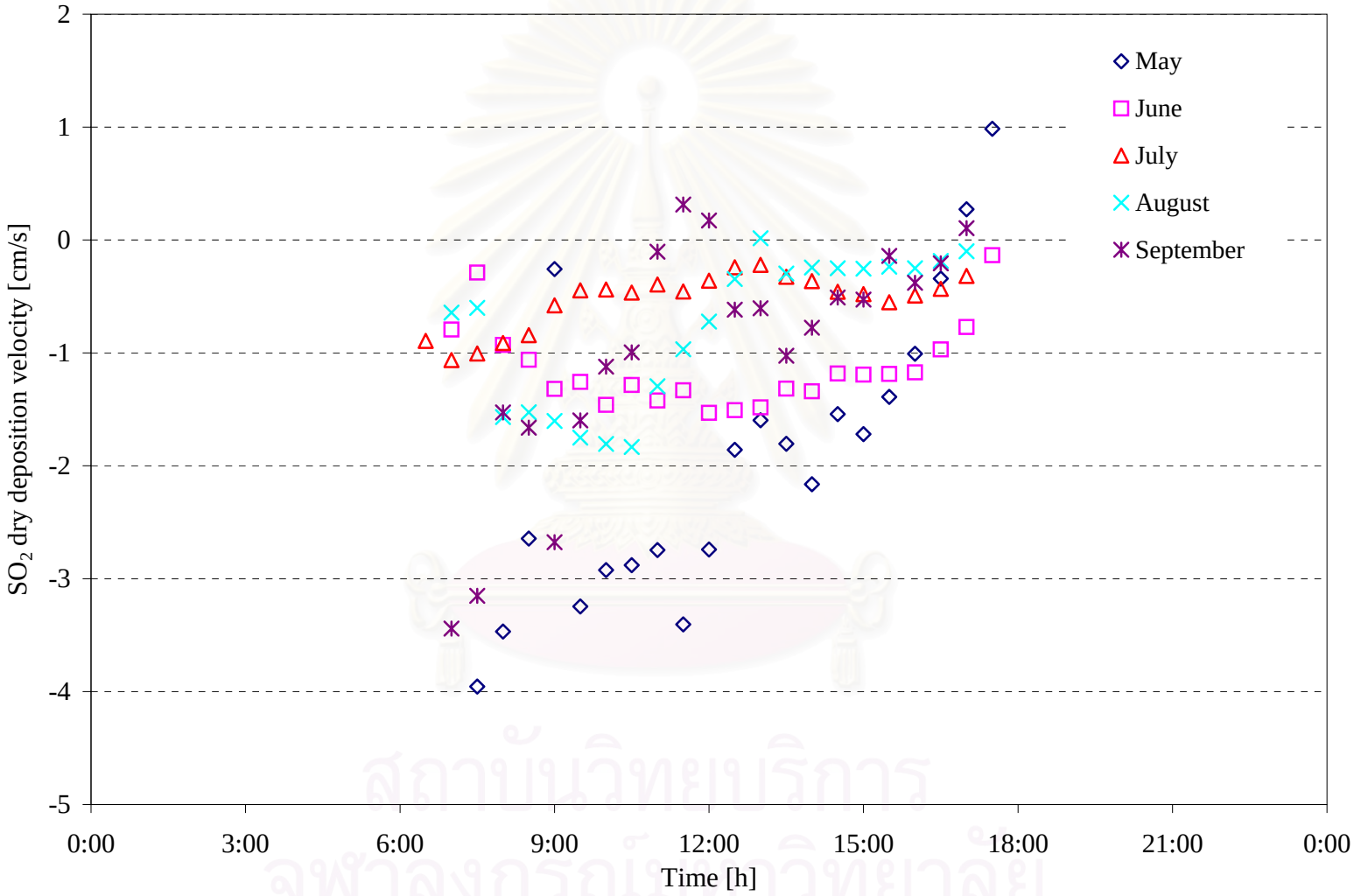

Figure 4.2.2 Dry deposition velocity of SO_2 over pine forest at various time periods

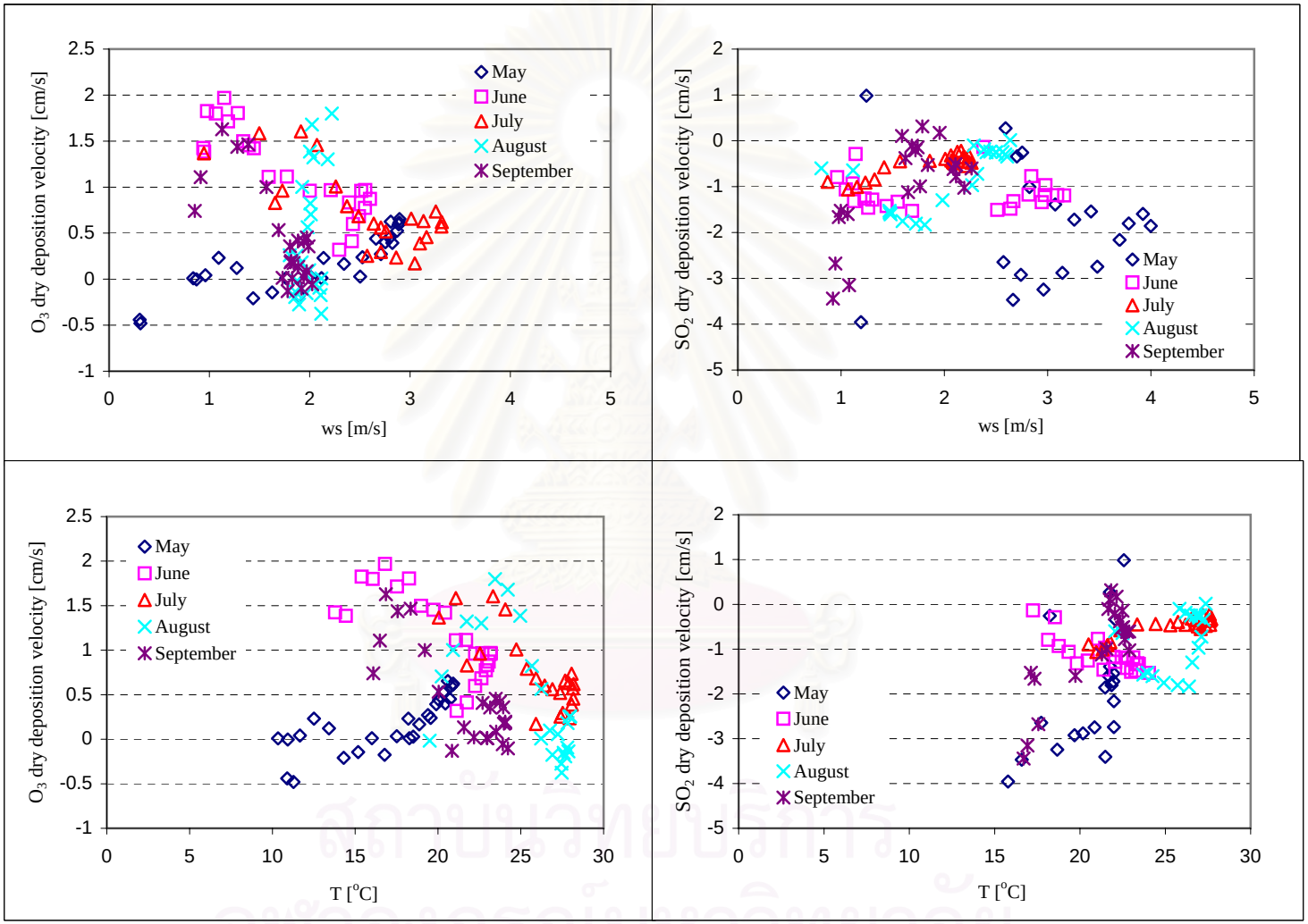

Figure 4.2.3 Effect of wind speed and temperature on O_3 and SO_2 dry deposition velocities

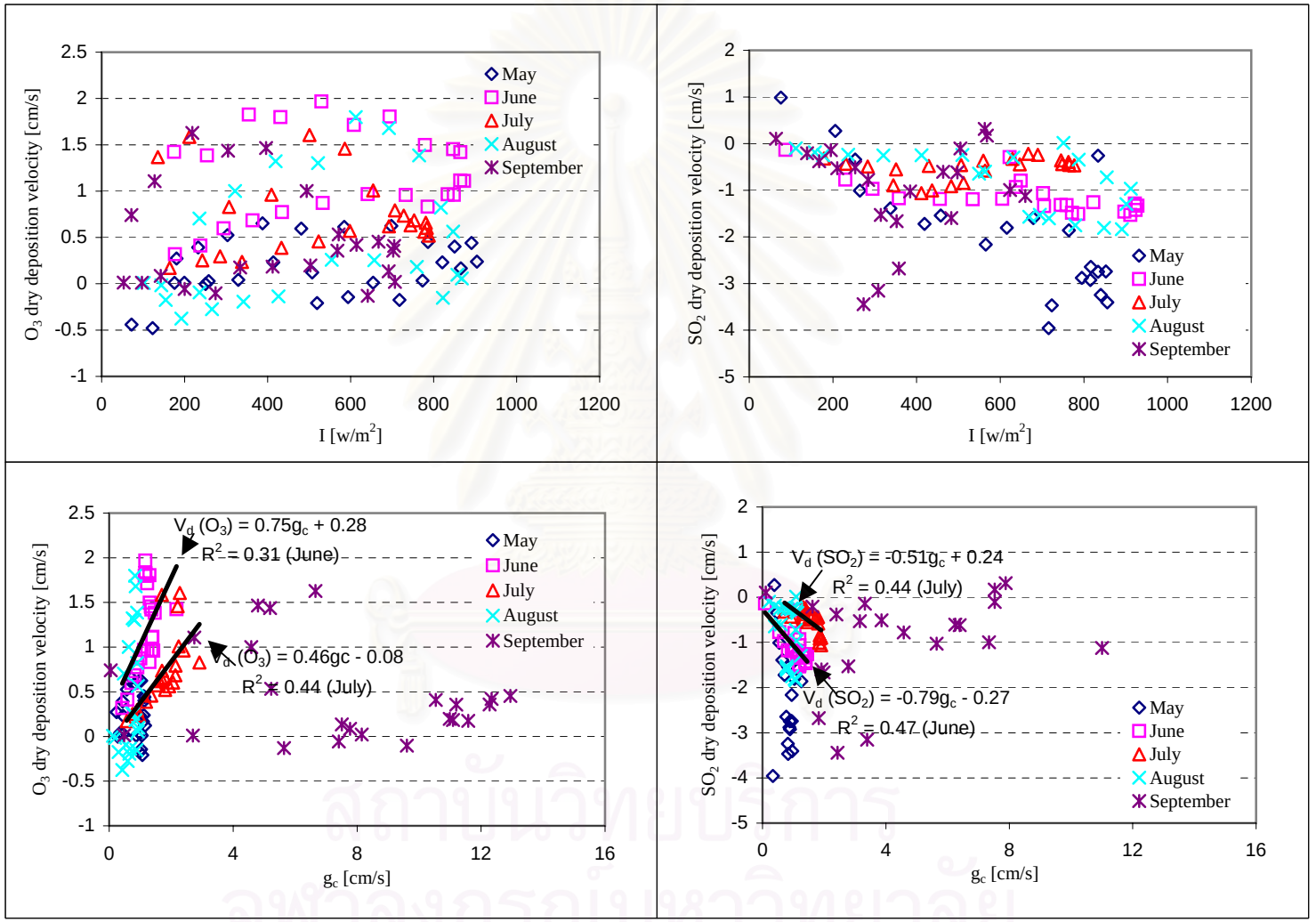

Figure 4.2.4 Effect of solar radiation and canopy conductance on O_3 and SO_2 dry deposition velocities

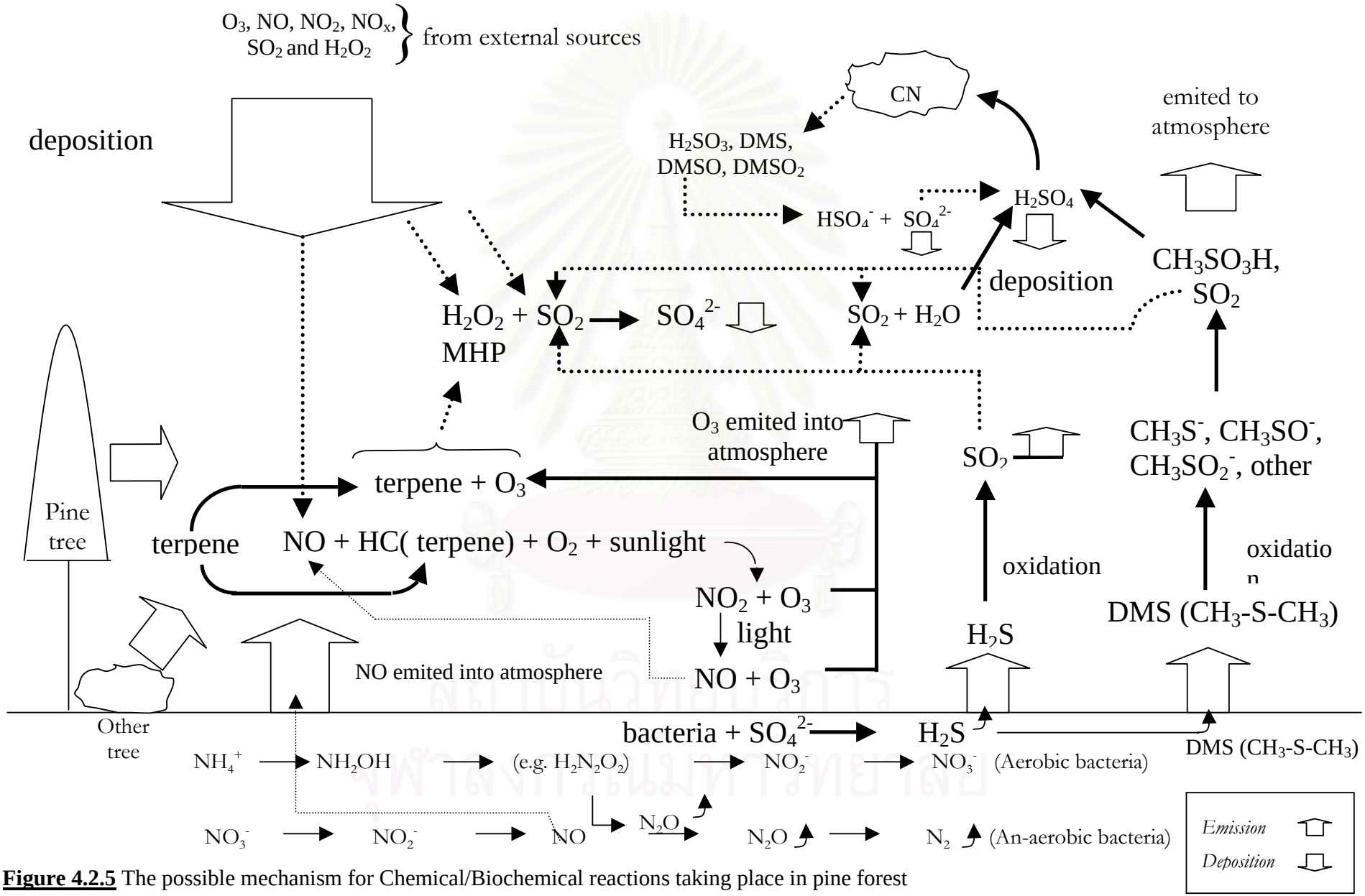

Figure 4.2.5 The possible mechanism for Chemical/Biochemical reactions taking place in pine forest

(by courtesy of Prof. Masatoshi Aoki; Tokyo University of Agriculture & Technology, unpublished information)

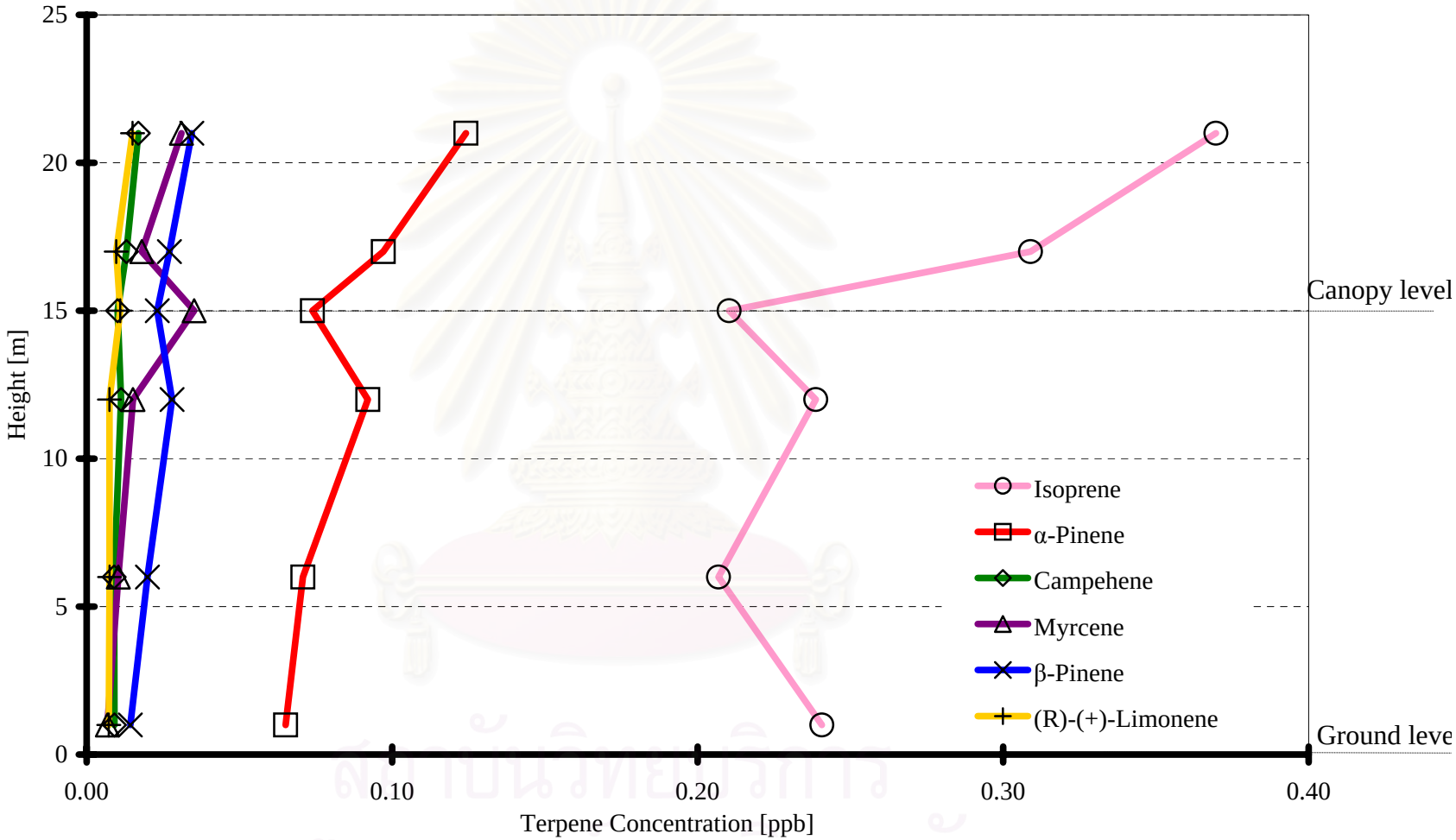

Figure 4.2.6 Concentrations and compositions of terpene at various heights in the pine forest at 8 am., Sep, 7 2001

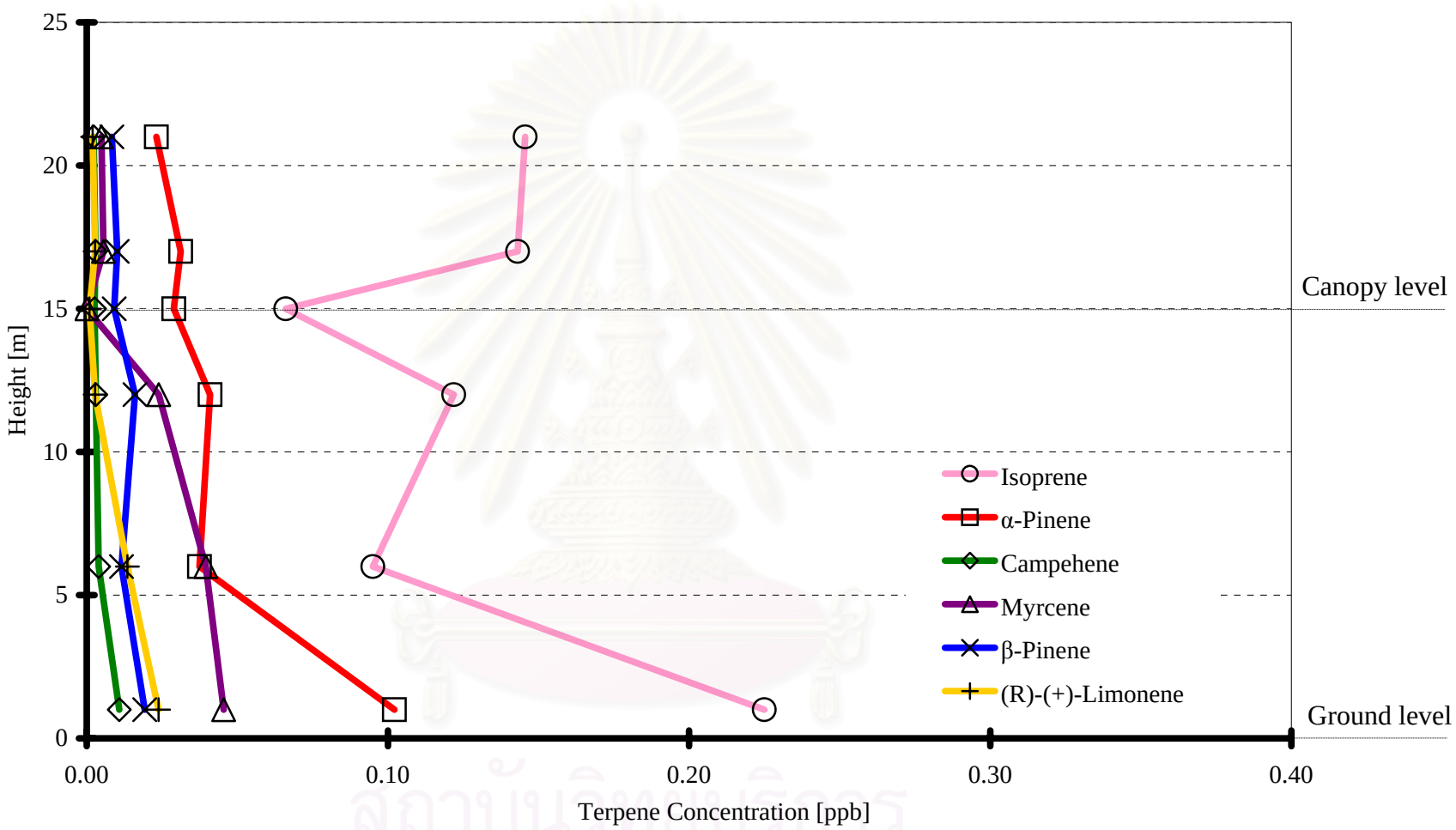

Figure 4.2.7 Concentrations and compositions of terpene at various heights in the pine forest at 3 p.m., Sep, 7 2001

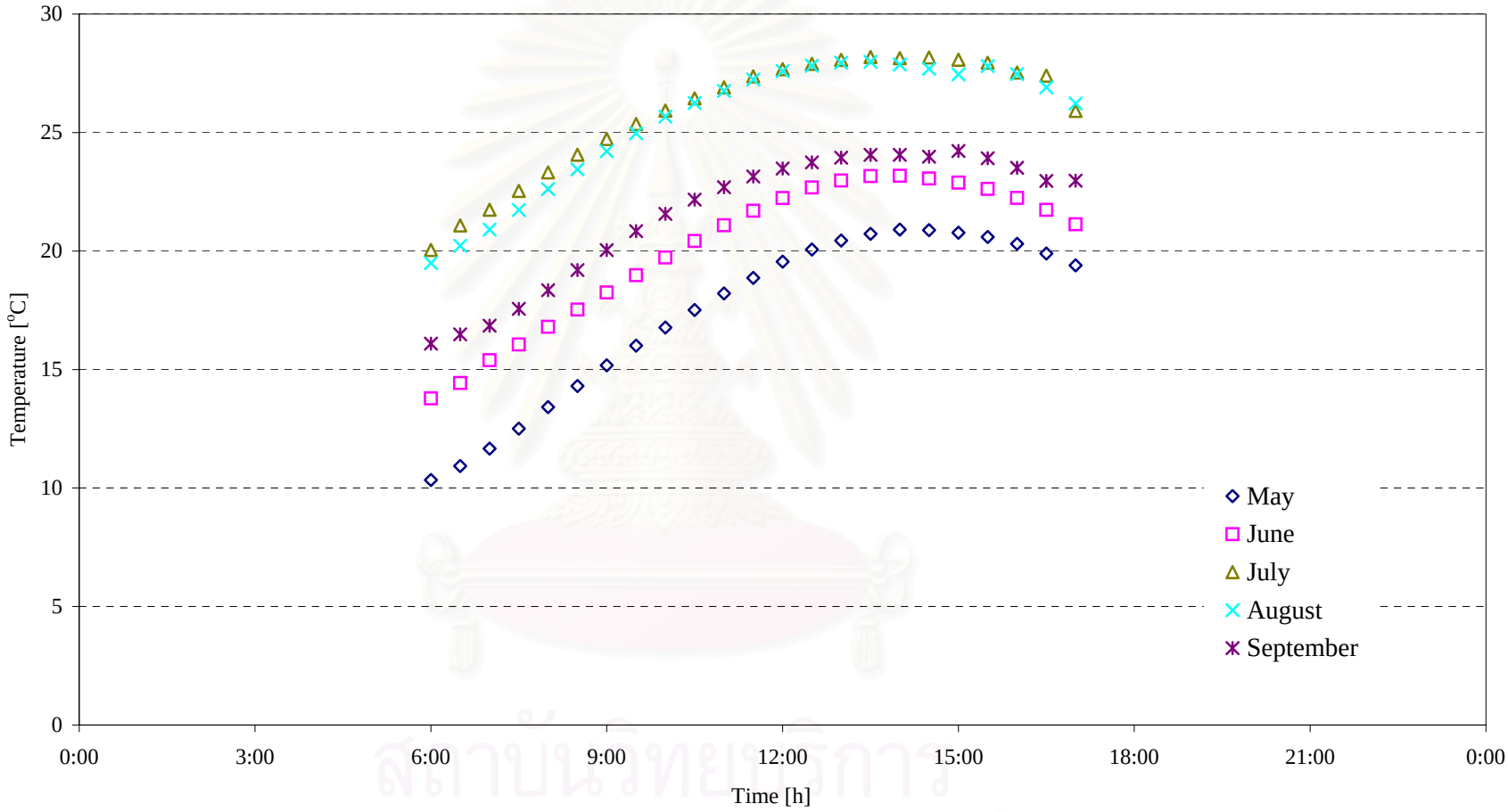

Figure 4.2.8 Dry air temperature on canopy surface in the pine forest at various time periods

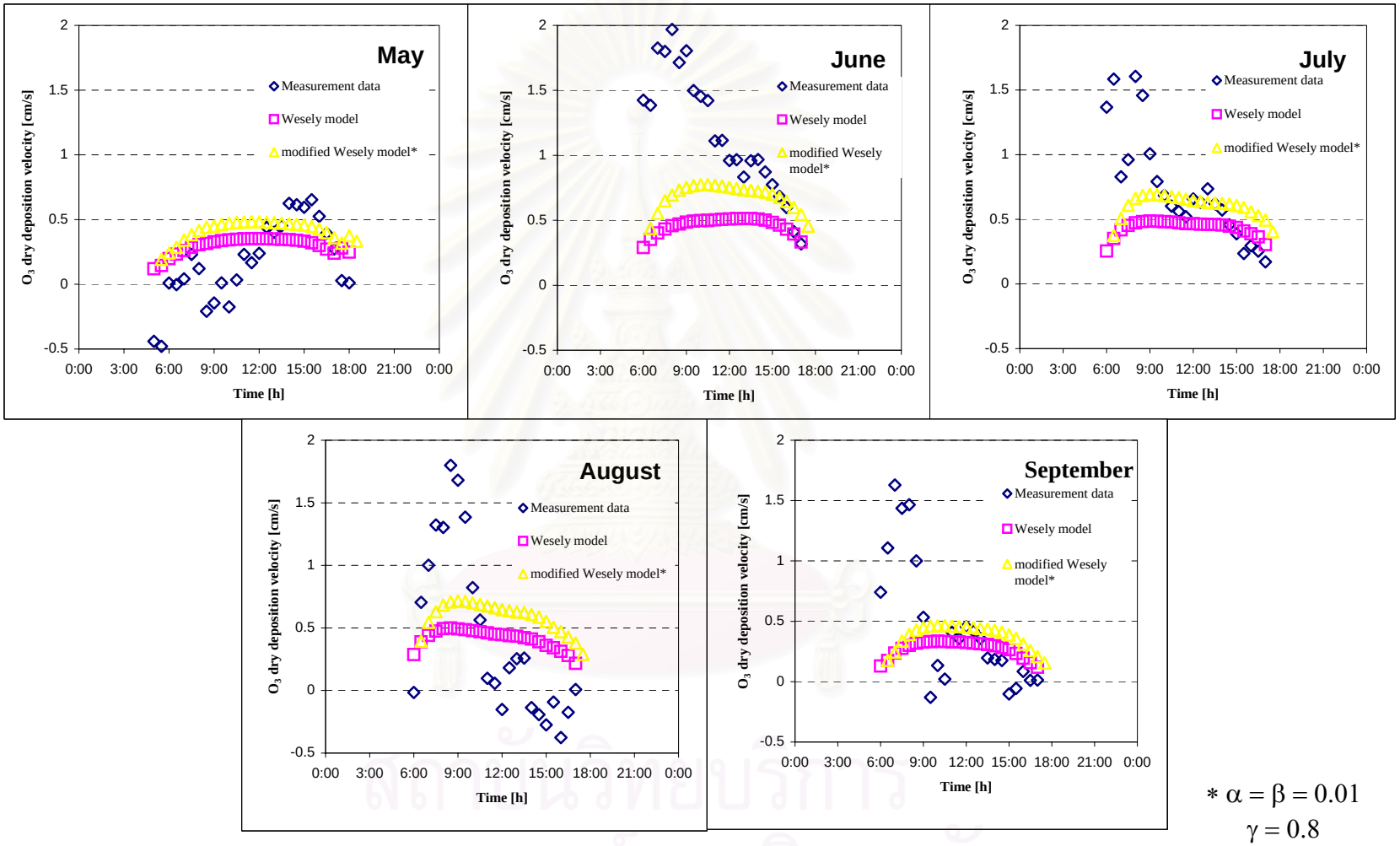

* $\alpha = \beta = 0.01$
$\gamma = 0.8$

Figure 4.2.9 Dry deposition velocity of O_3 : Measurement and Model Results at various time periods in the pine forest

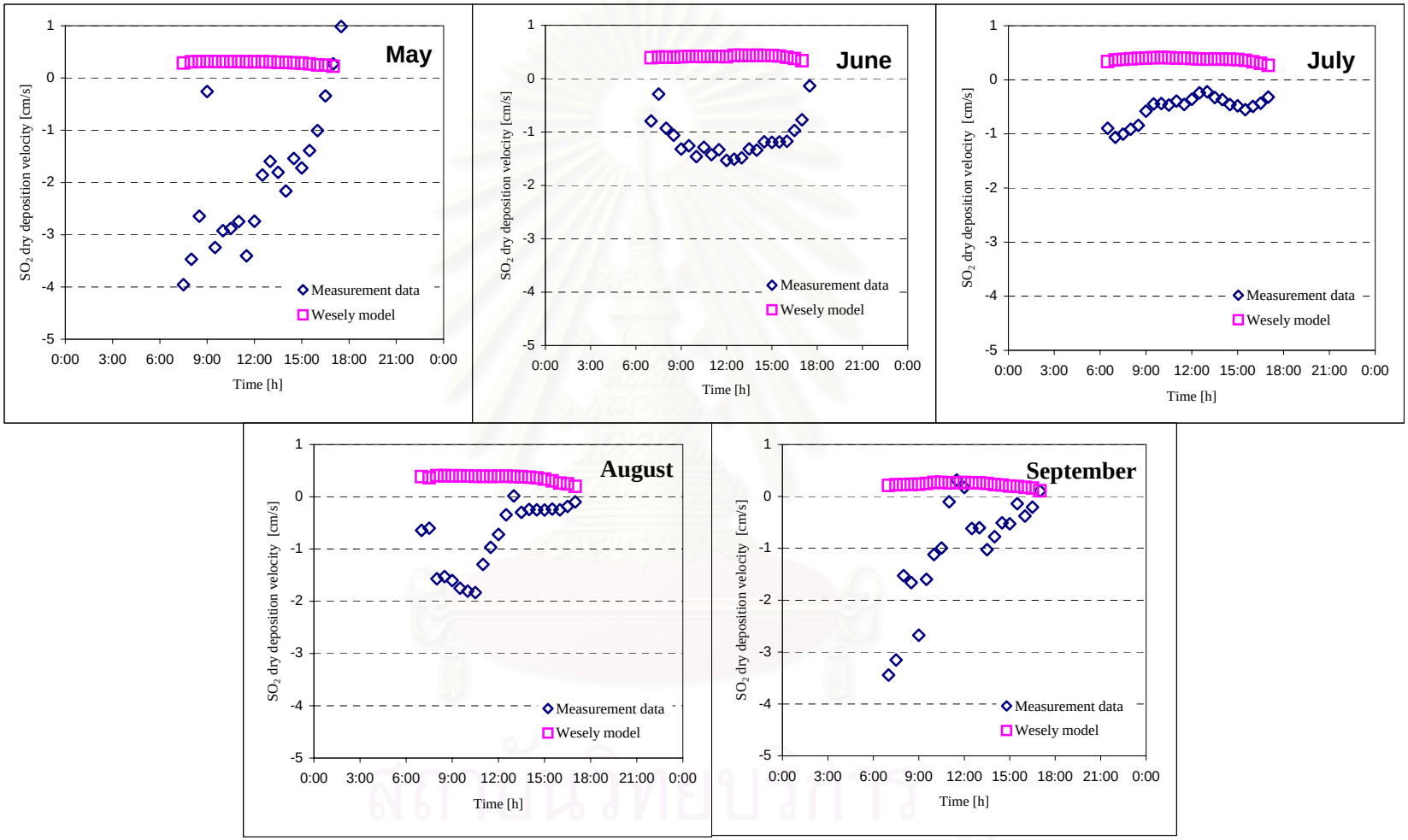

Figure 4.2.10 Dry deposition velocity of SO_2 : Measurement and Model Results at various time periods in the pine forest

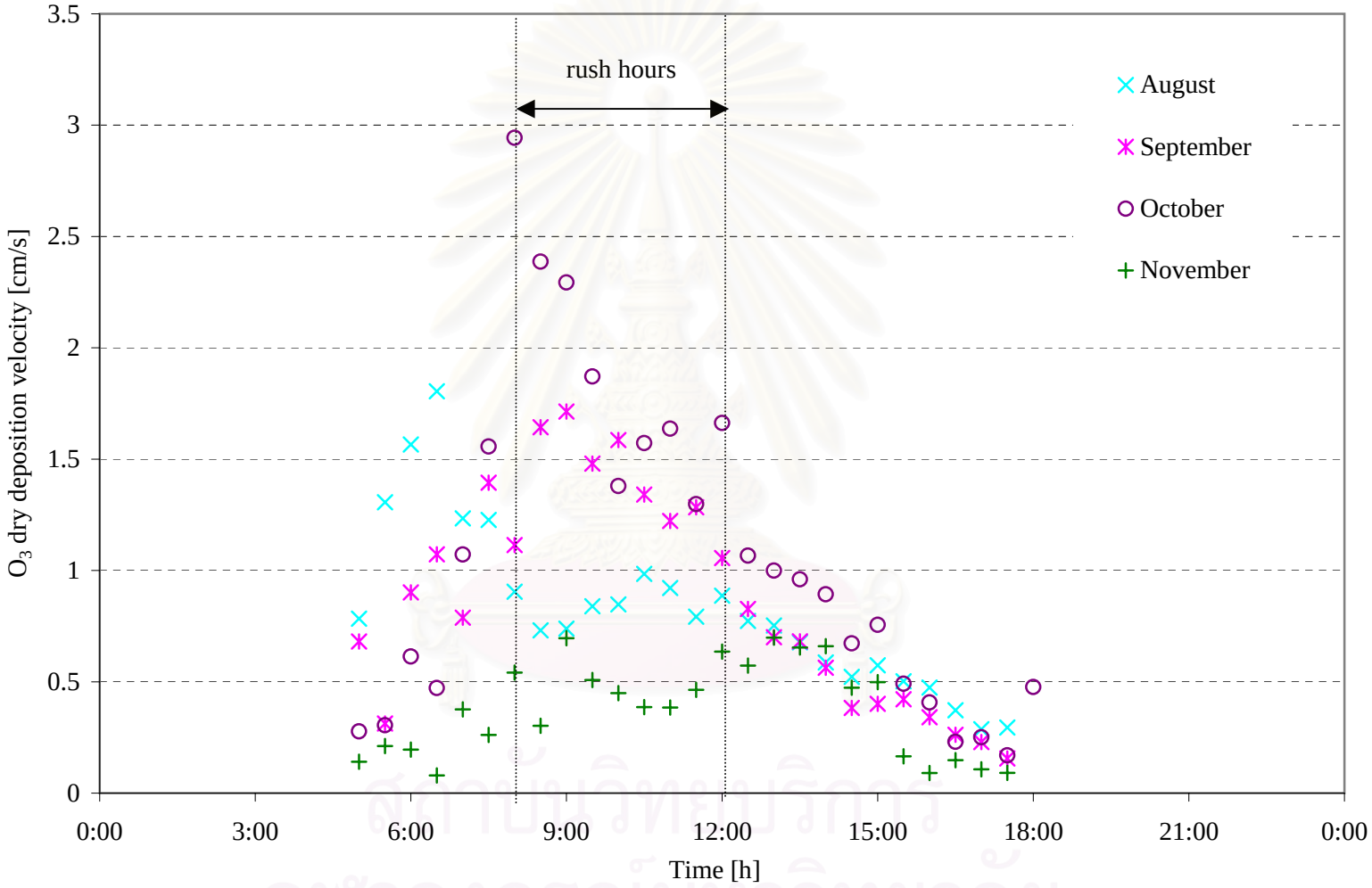

Figure 4.3.1 Dry deposition velocity of O_3 at various time periods in the city area

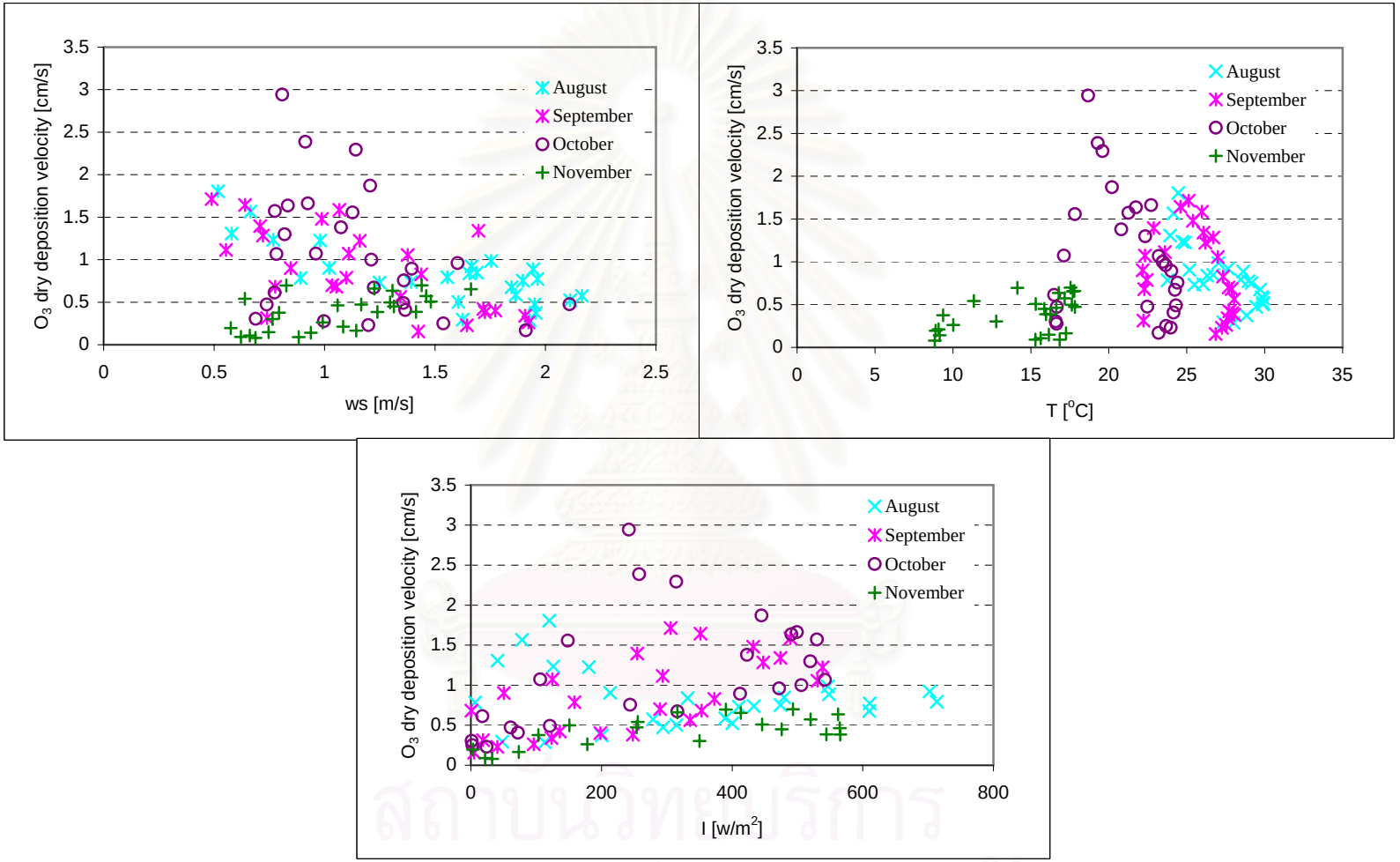

Figure 4.3.2 Effect of meteorological factors on O_3 dry deposition velocity in the city area

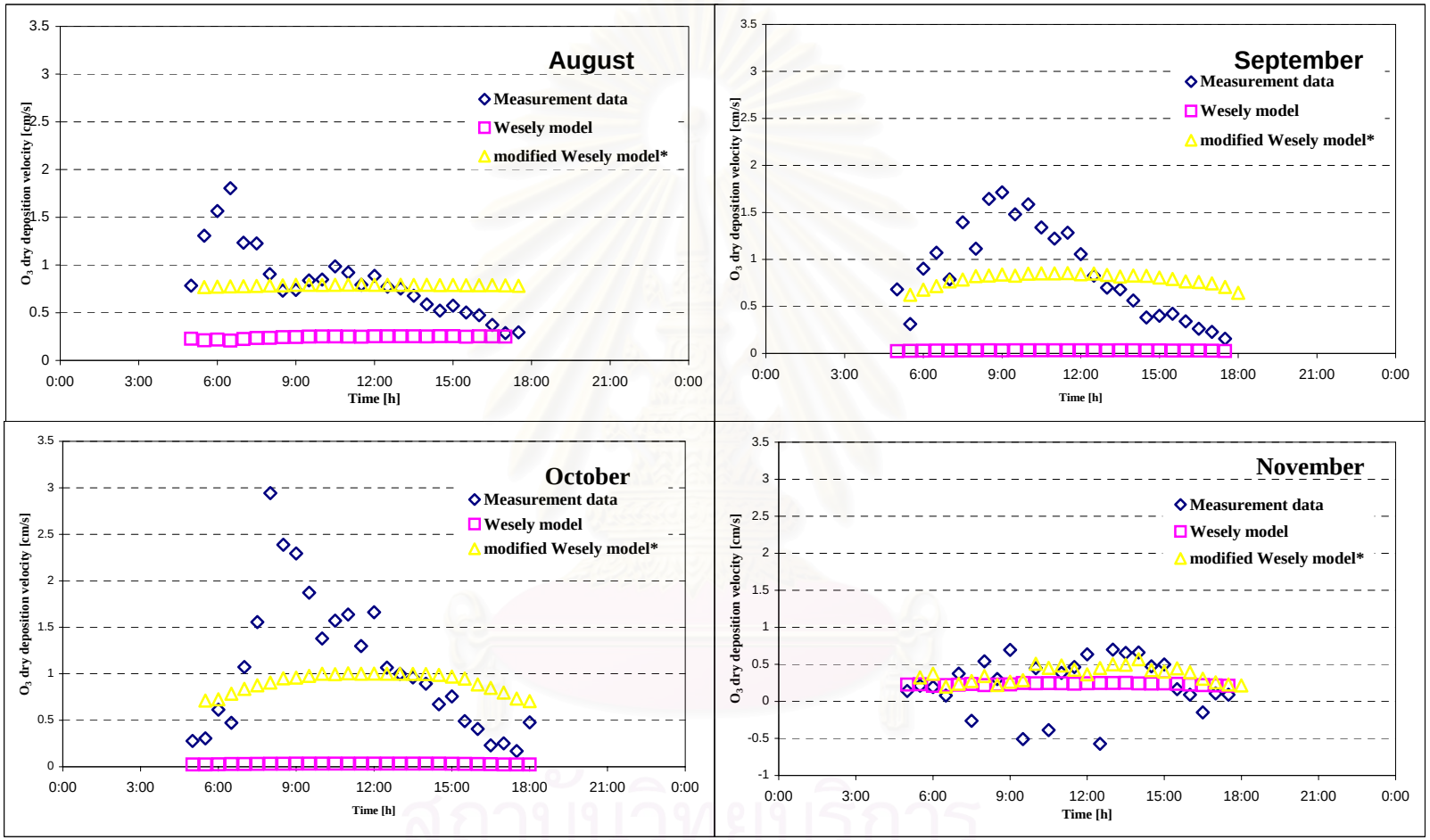

* $\alpha = \beta = 0.01$
$\gamma = 0.34$

Figure 4.3.3 Dry deposition velocity of O_3 : Measurement and Model Results at various time periods in the city area

			a_1	a_2	a_3	R^2	averaged LAI
O_3	Bean						
		stage1	1.37	-0.29	-5.20	0.83	0.75
		stage2	0.74	0.95	-2.65	0.71	3.00
		stage3	0.25	1.45	-0.40	0.62	5.50
	Corn						
		stage1	1.02	4.95	-5.63	0.50	1.00
		stage2	1.55	6.00	-8.00	0.61	3.00
		stage3	1.55	8.96	-10.87	0.66	4.50
	Wheat						
		stage1	0.30	0.62	-1.29	0.90	0.25
		stage2	-0.06	0.67	0.62	0.56	1.75
		stage3	0.31	0.66	-1.74	0.69	3.08
SO_2	Bean						
		stage1	-0.14	0.85	0.89	0.68	0.75
		stage2	0.31	0.42	-0.36	0.67	3.00
		stage3	0.02	0.74	0.11	0.67	5.50
	Wheat						
		stage1	0.48	0.66	-1.70	0.60	0.25
		stage2	-0.52	1.77	2.72	0.51	1.75
		stage3	0.02	0.84	0.08	0.50	3.08

$$V_d = a_1 \ln I + a_2 gc + const;\ a_1,\ a_2 \text{ and } a_3$$

Table 4.1 Summary of coefficients, $a_{1\text{-}3}$, in Eq.4.1 for the prediction of the depositions of O_3 and SO_2

	a_1			a_2			a_3		
	b_1	b_2	b_3	b_1	b_2	b_3	b_1	b_2	b_3
Bean	**0.1**	**-0.2**	**2**	**-0.1**	**0.8**	**-0.86**	**-0.05**	**1.3**	**-6.2**
Corn	**0.7**	**-3**	**8.5**	**0.4**	**1.1**	**5.7**	**-0.2**	**-0.36**	**-5.06**
Wheat	**0.2**	**-0.7**	**1**	**-0.01**	**0.1**	**0.6**	**-1.1**	**3.44**	**-2.08**

$$\mathbf{V_d = a_1 ln\ I + a_2 g_c + a_3;\ a_1, a_2 \text{ and } a_3 = f(LAI)}$$

$$(a = b_1\ LAI^{\,2} + b_2\ LAI + b_3)$$

Table 4.2 Summary of coefficients, $b_{1\text{-}3}$, in Eq.4.2 for the prediction of the depositions of O_3

	a_1			a_2			a_3		
	b_1	b_2	b_3	b_1	b_2	b_3	b_1	b_2	b_3
Bean	**-0.06**	**0.44**	**-0.43**	**0.06**	**-0.45**	**1.15**	**0.15**	**-1.14**	**1.66**
Wheat	**0.38**	**-1.4**	**0.82**	**-0.51**	**1.77**	**0.24**	**-1.75**	**6.44**	**-3.2**

$$\mathbf{V_d = a_1 ln\ I + a_2 g_c + a_3;\ a_1, a_2 \text{ and } a_3 = f(LAI)}$$

$$(a = b_1\ LAI^{\,2} + b_2\ LAI + b_3)$$

Table 4.3 Summary of coefficients, $b_{1\text{-}3}$, in Eq.4.2 for the prediction of the depositions of SO_2

		Error (%)		
		Empirical model	Wesely Model	Modified Wesely Model
O_3				
	Bean	37.4	124.37	33.6
	Corn	38.9	142.2	59.81
	Wheat	29.7	98.71	64.24
SO_2				
	Bean	35.9	120.43	44.07
	Wheat	37	115.5	80.91

Table 4.4 Averaged error from Empirical and wesely models

Chapter 5

Conclusions and Recommendations

This research emphasized that the agriculture could significantly affect the mechanisms for which gaseous pollutants deposited onto the earth surface and it was shown how the rate of dry deposition was influenced by physical and meteorological factors. A simple mathematical model was proposed as a means to describe the dry deposition velocity of ozone and sulfur dioxide in agricultural area. Although the mechanisms of dry deposition of gaseous pollutants in the pine forest could not be examined thoroughly, this work proposed a potential mechanism, which might have taken place for future investigation. The Wesely model was found to adequately describe the dry deposition in the pine forest during the time where no extreme atmospheric variations existed. The Wesely model, in addition, was found to give satisfactory predictions for the dry deposition velocity in the city area. It will be interesting to further investigate the effect of changes of the atmospheric conditions, especially the weather changes, on the dry deposition velocity as this factor was always found to cause a high fluctuation in the deposition velocity data obtained during this work.

This work contributed mainly as a part of the air pollution modeling network, or more particularly on the dry deposition model. The network of air pollution modeling involves the dispersion model that describes how air pollutants travel in the various atmospheric layers and the deposition models which characterizes how the pollutants are transformed back to the earth surface. The later includes wet and dry deposition mechanisms. At present, most of the air transportation/deposition models are subject to a high level of inaccuracy and the verification of these models are rather cumbersome. In this viewpoint, this work proposed a rather simpler empirical model for estimating dry deposition rate of pollutants which, on the one hand, might not be effective for general purposes, but on the other hand, was believed to give higher

accurate quantitative prediction of dry deposition rates. The principal analytical approach employed for the development of the model was the main merit of this work which can be applied to the future work that might be carried out in Thailand. At the present time that this work was written, similar works was being conducted in Lampang (teak forests).

References

Baldocchi, D.D., Hicks, B.B. and Camara, P. 1987. A Canopy Stomatal Resistance Model for Gaseous Deposition to Vegetated Surfaces. Atmospheric Environment. 21: 91-101

Baldocchi, D.D. 1988. A Multi-Layer Model for Estimating Sulfur Dioxide Deposition to a Deciduous Oak Forest Canopy. Atmospheric Environment. 22: 869-884

Brook, J.R., Zhang, L., Di-Giovanni, F. and Padro, J. 1999. Description and Valuation of a Model of Deposition Velocities for Rountine Estimates of Air Pollutant Dry Deposition Over North America. Part I: Model Development. Atmospheric Environment. 33: 5037-5051

Calvert, S. and Harold, M.E. 1984. Handbook of Air Pollution Technology. United States of America. John Wiley & Sons, Inc.

Chapra, S.C. and Canale, R.P. 1998. Numerical Methods for Engineers with Programming and Software Applications. Singapore. McGraw-Hill.

EPA, 2000. National Ambient Air Quality Standards (NAAQS), http://www.epa.gov/reg3artd/airquality/NAAQS.html

Erisman, J.W.and Draaijers, G. P.J. 1995. Atmospheric Deposition in Relation to Acidification and Eutrophication. United States of America . Elsevier Science.

Freyney, J.R. 1997. Emission of nitrous oxide from soils used for agriculture. Nutrient cycling in Agroecosystems 46, 1-6.

Gao, W., and Wesely, M.L. 1995. Modeling Gaseous Dry Deposition Over Regional Scales with Satellite Observations-I. Model Development. Atmospheric Environment. 29: 727-737

Henk M., Stef A., and Hans G. 2000. Microbial production and consumption of dimethyl sulfide (DMS) in a sea grass (Zostera noltii)-dominated marine intertidal sediment ecosystem. Microbiology. 31, 163-172.

Hicks, B.B., Baldocchi, D.D., Meyers, T.P., Hosker, R.P., Matt, Jr. and D.R. 1987. A Preliminary Multiple Resistance Routine for Deriving Dry Dposition Velocities From Measured Quantities. Water, Air, and Soil Pollution. 36:311-330.

Hill, A.C., 1971. Vegetation: A Sink for Atmospheric Pollution. Journal of the Air Pollution Control Association. 21: 341-346.

Isidorov, V., Zenkevich, I. and ioffe, B. 1985. Volatile Organic Compound in the Atmosphere of forests. Atmospheric Environment. 19: 1-8

Janzen, H.H. et al. 2001. Estimates of Emissions. http://res2.agr.ca/research-researche/science/Healthy_Air/toc.html

Jones, H.G., 1996. Plants and microclimate: a quantitative approach to environmental plant physiology. Malta. Interprint Limited.

Lamb, B., Westerberg, H., Allwine, G. and Quarles, T. 1985. Biogenic Hydrocarbon Emission from Deciduous and Coniferous trees in the United States. Journal of Geophysical Research. 90: 2380-2390.

Lindskog, A. and Potter. 1993. A Terpene Emission and Ozone Stress. Chemosphere. (30): 1171-1181.

Monteith, J.L. and Unsworth, M.H. 1995. Principles of Environmental Physics. United States of America. Arnold, a member of the Hodder Heading Group.

Nevers, N.D. 1995. Air pollution Control Engineering. Singapore. McGraw-Hill.

Oden, S. 1976. The Acidity Problem An Outline of Concept. Water, Air, and Soil Pollution. 6:137-145.

Padro, J., Hartog, G.D. and Neumann, H.H. 1991. An Investigation of the ADOM Dry Deposition Module Using Summertime O_3 Measurements Above a Deciduous Forest. Atmospheric Environment. 25A: 1689-1704

Padro, J. 1996. Summary of Ozone Dry Deposition Velocity Measurements and Model Estimates Over Vineyard, Cotton, Grass and Deciduous Forest in Summer. Atmospheric Environment. 13: 2363-2369

Patrick, D. 1994. Toxic Air Pollution Handbook. United States of America. Van Nostand Reinhold.

PCD 2002. Pollution Control Department: Ministry of Science, Technology and Environment, Thailand.
http://www.pcd.go.th/AirQuality/bangkok/

Peñuelas, J., Llusià, J. and Gimeno, B.S. 1999. Effects of ozone concentrations on biogenic volitle organic compounds emission in the Mediterranean region. Environmental Pollution. 105: 17-23.

Sienfeld, J. H. and Pandis, S. N. 1996. Atmospheric Chemistry and Physics. United States of America, A Wiley-Interscience Publication.

Smith, W.H. 1981. Air Pollution and Forests. Spring-Verlag New York Inc.

Venkatram, A., Karamchani, P.K. and Misra, P.K. 1988. Testing A Comprehensive Acid Deposition Model. Atmospheric Environment. 22: 737-747

Wesely, M.L., and Hicks, B.B. 1977. Some Factors that Affect the Deposition Rates of Sulfur Dioxide and Similar Gases on Vegetation. Journal of the Air Pollution Control Association. 27: 1110-1116

Wesely, M.L. 1989. Parameterization of Surface Resistances to Gaseous Dry Deposition in Regional-Scale Numerical Models. Atmospheric Environment. 23: 1293-1304

William, H.S. 1981. Air Pollution and Forests: Interactions between Air Contaminants and Forest Ecosystems. United States of America. Springer-Verlag New York Inc.

Williams, E.J., Guenther, A and Fehsenfeld, F.C. 1991. An Inventory of Nitric Oxide Emission from Soils in the United States. Journal of Geophysical Research. 97: 7511-7519.

Zhang, L., Padro, J. and Walmsley, J.L. 1996. A Multi-Layer Model vs. Single-Layers Models and Observed O_3 Dry Deposition Velocities. Atmospheric Environment. 30: 339-345

APPENDICES

Appendix A

Wesely model (1989)

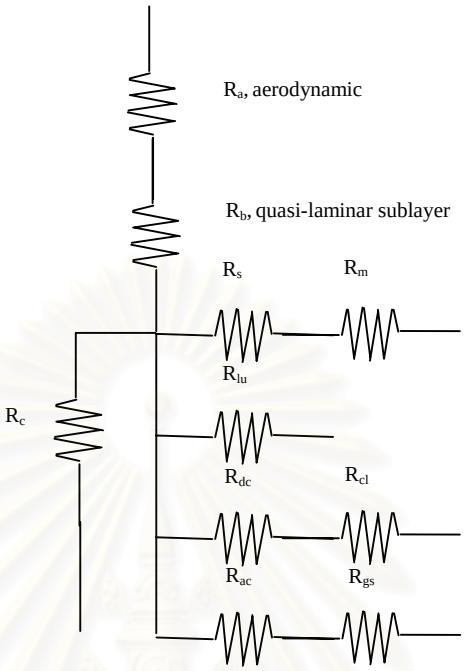

Figure A1 Schematic pathway resistance of Wesely (1989)

$$r_c = \left(\frac{1}{r_{st} + r_m} + \frac{1}{r_{lu}} + \frac{1}{r_{dc} + r_{cl}} + \frac{1}{r_{ac} + r_{gs}} \right)^{-1} \quad \text{(a1)}$$

where

r_{st} = leaf stomatal resistance

$$r_{st} = r_j \left[1 + \left(\frac{200}{G+0.1} \right)^2 \left(\frac{400}{T_s (40-T_s)} \right) \right] \quad \text{(a2)}$$

T_s= surface temperature (0-40 ^{0}C)

G = solar radiation (w/m^2)

r_j = the minimum bulk canopy stomatal resistance for water vapor lower canopy

For outside this range, the stomata are assumed to be closed and r_{st} is set to be large value. The combined minimum stomatal and mephyll resistance is calculated from

$$r^i_{sm} = r^i_{st} + r^i_m = r_{st} \times (D_{H2O}/D_i) + 1/(3.3 \times 10^{-4} H^*_i + 100 f^i_0) \qquad (a3)$$

where

D_{H2O}/D_i = the ratio of the molecular diffusivity of water to that of the specific gas

H^*_i = the effective Henry's Law constant (M atm^{-1}) for the gas

f^i_0 = a normalized(0 to 1) reactivity factor for the dissolved gas

r^i_{lu} = the leaf cuticular resistance in healthy vegetation and the other outer surface resistances

$$r^i_{lu} = r_{lu} (1/(10^{-5} H^*_i + f^i_0) \qquad (a4)$$

r_{dc} = resistance to transfer by bouyant convection

$$r_{dc} = 100\{1+1000/ (G+10)\}\{1/(1+1000\theta)\} \qquad (a5)$$

θ is slope of the local terain in radians

r^i_{cl} = resistance to uptake by leaves, twigs and other exposed surfaces

$$r^i_{cl} = (10^{-5} H^*_i / r_{clS} + f^i_0 / r_{clO}) \qquad (a6)$$

r^i_{ac} = transfer resistance for processes that depend only on canopy height and resistance for uptake by the soil, leaf litter

$$r^i_{gs} = (10^{-5} H^*_i / r_{gsS} + f^i_0 / r_{clO}) \qquad (a7)$$

r_{gs} = ground surface resistance

Note 1. r_j, r_{lu}, r_{clS}, r_{clO}, r_{gsS}, r_{clO} and r_{gs} are given for each season and land-use category in Table A1

2. the value of D_{H2O}/D_i, H^*_i, f^i_0 were shown in table A2

Table A1 Input resistance (s m^{-1}) for computations of surface resistance (r_c)

	Land Use Type										
Resistance Component	1	2	3	4	5	6	7	8	9	10	11
	Seasonal Category 1 : Midsummer with Lush Vegetation										
r_j	9999	60	120	70	130	100	9999	9999	80	100	150
r_{lu}	9999	2000	2000	2000	2000	2000	9999	9999	2500	2000	4000
r_{ac}	100	200	100	2000	2000	2000	0	0	300	150	200
r_{gsS}	400	150	350	500	500	100	0	1000	0	220	400
r_{gsO}	300	150	200	200	200	300	2000	400	1000	180	200
r_{clS}	9999	2000	2000	2000	2000	2000	9999	9999	2500	2000	4000
r_{clO}	9999	1000	1000	1000	1000	1000	9999	9999	1000	1000	1000
	Seasonal Category 2 : Autumn with Unharvested Cropland										
r_j	9999	9999	9999	9999	250	500	9999	9999	9999	9999	9999
r_{lu}	9999	9000	9000	9000	4000	8000	9999	9999	9000	9000	9000
r_{ac}	100	150	100	1500	2000	1700	0	0	200	120	140
r_{gsS}	400	200	350	500	500	100	0	1000	0	300	400
r_{gsO}	300	150	200	200	200	300	2000	400	800	180	200
r_{clS}	9999	9000	9000	9000	2000	4000	9999	9999	9000	9000	9000
r_{clO}	9999	400	400	400	1000	600	9999	9999	400	400	400
	Seasonal Category 3 : Late Autumn After Frost Snow										
r_j	9999	9999	9999	9999	250	500	9999	9999	9999	9999	9999
r_{lu}	9999	9999	9000	9000	4000	8000	9999	9999	9000	9000	9000
r_{ac}	100	10	100	1000	2000	1500	0	0	100	50	120
r_{gsS}	400	150	350	500	500	200	0	1000	0	200	400
r_{gsO}	300	150	200	200	200	300	2000	400	1000	180	200
r_{clS}	9999	9999	9000	9000	3000	6000	9999	9999	9000	9000	9000
r_{clO}	9999	1000	400	400	1000	600	9999	9999	800	600	600
	Seasonal Category 4 : Winter, Snow on Ground and Subfreezing										
r_j	9999	9999	9999	9999	400	800	9999	9999	9999	9999	9999
r_{lu}	9999	9999	9999	9999	6000	9000	9999	9999	9000	9000	9000
r_{ac}	100	10	10	1000	2000	1500	0	0	50	10	50
r_{gsS}	100	100	100	100	100	100	0	1000	100	100	50
r_{gsO}	600	3500	3500	350	3500	3500	2000	400	3500	3500	3500
r_{clS}	9999	9999	9999	9000	200	400	9999	9999	9000	9999	9000
r_{clO}	9999	1000	1000	400	1500	600	9999	9999	800	1000	800

Seasonal Category 5 : Transitional Spring with Partially Green Short Annuals

r_j	9999	120	240	140	250	190	9999	9999	160	200	300
r_{lu}	9999	4000	4000	4000	2000	3000	9999	9999	4000	4000	800
r_{ac}	100	50	80	1200	2000	1500	0	0	200	60	120
r_{gsS}	500	150	350	500	500	200	0	1000	0	250	400
r_{gsO}	300	150	200	200	200	300	2000	400	1000	180	200
r_{clS}	9999	4000	4000	4000	2000	3000	9999	9999	4000	4000	8000
r_{clO}	9999	1000	500	500	1500	700	9999	9999	600	800	800

(1) Urban land, (2) agriculture land, (3) range land, (4) deciduous forest, (5) coniferous forest, (6) mixed forest including wetland, (7) water, both salt and fresh, (8) barren land, mostly desert, (9) nonforest wetland, (10) mixed griculture land and range land, and (11) rocky open areas with low-growing shrubs.

Table A2 Relevant properties of gases for dry deposition calculation

Species	Ratio of Molecular Diffusivities ($D_{h2o}/D_{species}$)	Henry's Law Constant[b] (H^*) ($M\ atm^{-1}$)	Henry's Law Exponent[a] (A)	Noemalized Reactivity (f_o)
Sulfur dioxide	1.89	1×10^5	-3020	0
Ozone	1.63	1×10^{-2}	+2300	1
Nitrogen dioxide	1.6	1×10^{-2}	-2500	0.1
Nitric oxide	1.29	2×10^{-3}	-1480	0
Nitric acid	1.87	1×10^{14}	-8650	0
Hydrogen peroxide	1.37	1×10^5	-6800	1
Acetaldehyde	1.56	15	-6500	0
Propionaldehyde	1.8	15	-6500	0
Formaldehyde	1.29	6×10^3	-6500	0
Methyl hydroperoxide	1.6	220	-5600	0.3
Formic acid	1.6	4×10^6	-5740	0
Acetic acid	1.83	4×10^6	-5740	0
Ammonia	0.97	2×10^4	-3400	0
Petroxyacetyl nitrate	2.59	3.6	-5910	0.1
Nitrous acid	1.62	1×10^5	-4800	0.1
Pernitric acid	2.09	2×10^4	-1500	0
Hydrochloric acid	1.42	2.05×10^6	-2020	0

[a]The exponent A is used in the expression $H(T) = H \exp\{A[1/298 - 1/T]\}$ to calculate H at the surface temperature

[b]Effective Henry's law constant assuming a pH of about 6.5.

Appendix B

Diagrams of the experiment setups

1) Agriculture area

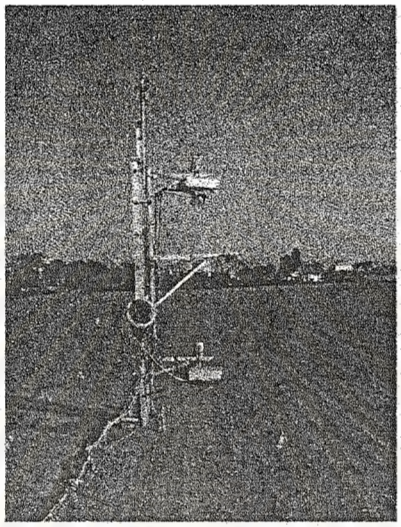

2) Pine forest

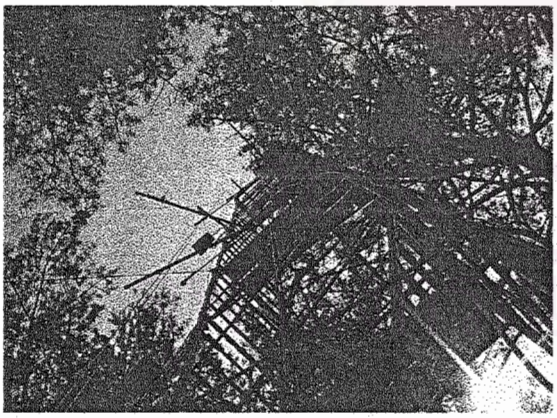

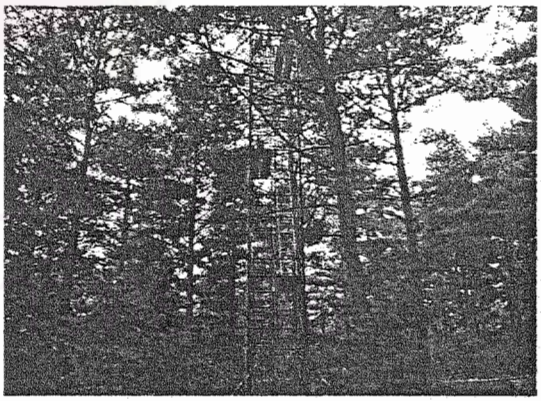

3) City area

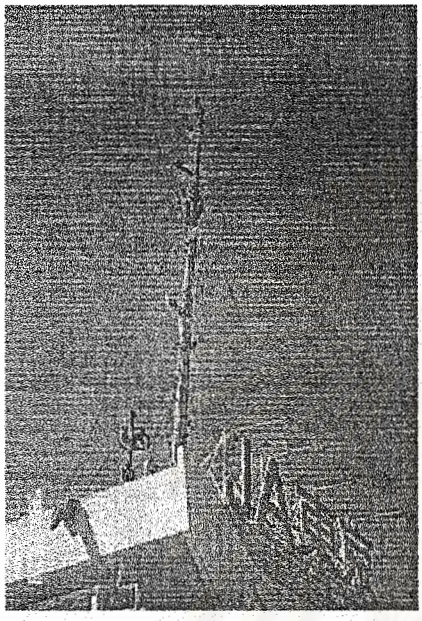

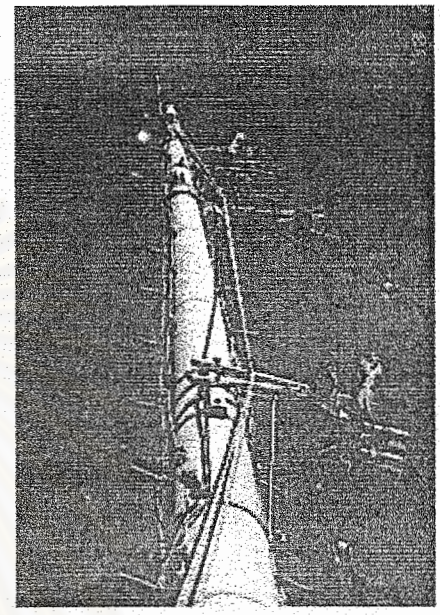

Experimental apparatus

1) Anemometer

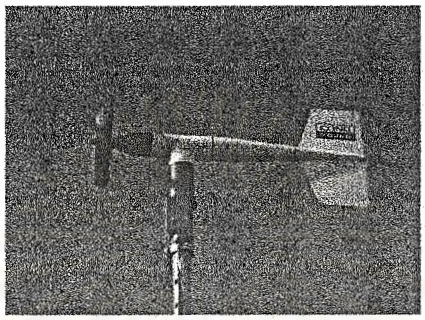

2) Dry-wet bulb thermometers

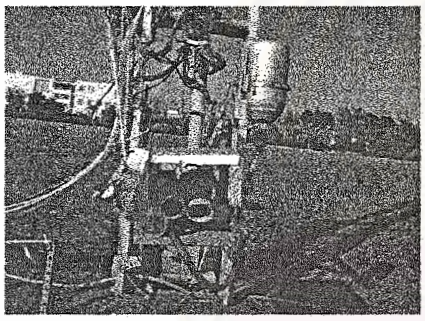

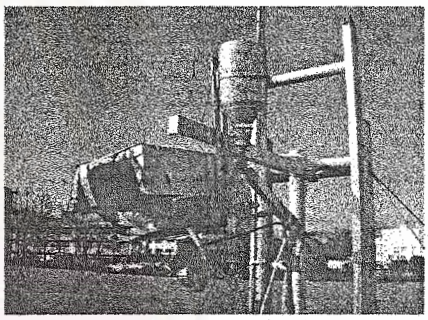

3) Net radiometer

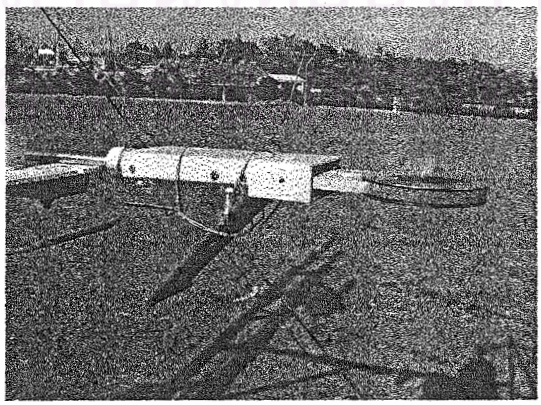

4) Soil heat flux plates

5) O_3 analyzer

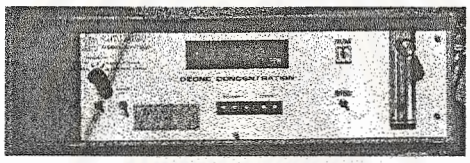

6) SO_2 analyzer

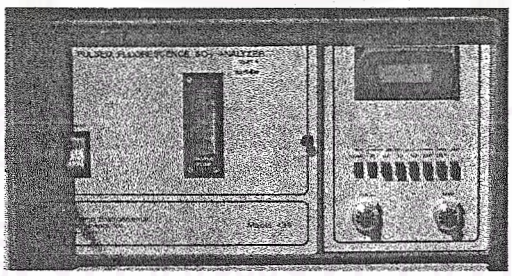

7) Air Sampling & Computing System

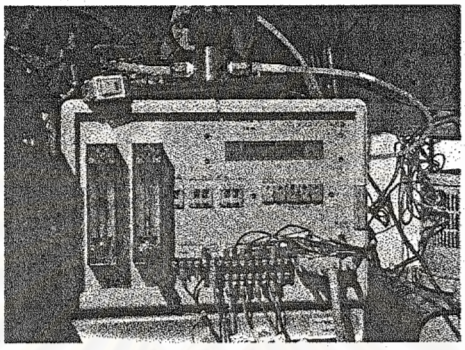

8) Recorder

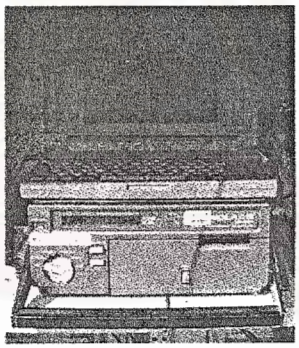

BIOGRAPHY

Mr. Sarit Chotchakornpant was born on 9th February , 1977 in Nakhonratchasima. He finished his higher secondary course from Saint Gabriel College in March, 1995. After that, he studied in the major of Chemical Engineering in Faculty of Engineering at Chulalongkorn University. He continued his further study for Master's degree in Chemical Engineering at Chulalongkorn University. He participated in the Environmental Engineering research group and achieved his bachelor's degree in April, 1999.